# Earliest bison dispersal in Western Palearctic: insights from the *Eobison* record from Pietrafitta (Early Pleistocene, Central Italy)

Leonardo Sorbelli[a,*], Marco Cherin[b,*], Dimitris S. Kostopoulos[c], Raffaele Sardella[d], Beniamino Mecozzi[d], Valerii Plotnikov[e], Maria Prat-Vericat[a], Beatrice Azzarà[b], Saverio Bartolini-Lucenti[a,f], Joan Madurell-Malapeira [a,f]

[a]*Institut Català de Paleontologia Miquel Crusafont,Universitat Autònoma de Barcelona, Edifici ICTA-ICP, c/ Columnes s/n, Campus de la UAB, 08193, Cerdanyola del Vallès, Barcelona, Spain.*
[b] *Dipartimento di Fisica e Geologia, Università degli Studi di Perugia, Via A. Pascoli, 06123 Perugia, Italy*
[c]*Laboratory of Geology and Paleontology, School of Geology, Aristotle University of Thessaloniki, 54124, Thessaloniki, Greece.*
[d]*Dipartimento di Scienze della Terra (PaleoFactory), Sapienza Università di Roma, Piazzale A. Moro 5, 00185 Roma, Italy.*
[e] *Academy of Sciences of the Republic of Sakha (Yakutia), 677007 Yakutsk, Lenin ave. 33, Russia.*
[f] *Dipartimento di Scienze della Terra, Universitá di Firenze, 50121 Firenze, Italy*

[*] Corresponding author.

*E-mail address:* leonardo.sorbelli@icp.cat

**Abstract:** The late Villafranchian is one of the pivotal time-spans in the succession of Pleistocene European faunal assemblages, setting the bases for the major faunal renewal that characterized the continent during the Epivillafranchian. *Bison* is one of the most important and successful large mammals to spread in Europe at the latest stages of the Early Pleistocene. Here we describe the remains of a large bovid from the late Villafranchian site of Pietrafitta (ca. 1.5 Ma), previously attributed to *Leptobos*. Our analyses allow to refer this sample to the genus *Bison*. The primitive characters featured by this sample suggest the attribution to the subgenus *Eobison*, a long-debated taxon which includes all the earliest forms of *Bison*. At Pietrafitta, thus, one of the largest and most complete record of primitive *Bison* is recorded. The vague diagnosis and confused taxonomic history of *Eobison* called for a reappraisal of its status. We present a re-definition of the diagnostic characters and a review of the Eurasian record of *Eobison* with a focus on the late Villafranchian samples from the Mediterranean area. We recognize at least three valid species of *Eobison* remarking, however, the extreme morphological variability of this group. The comparative analysis of *Eobison* and its closest relatives (i.e., *Leptobos* and *Bison* s.s.), confirms that both the leptobovine and bisontine clades

underwent to an increase of stoutness of the appendicular skeleton in response to the shrinking of forested habitats and the onset of colder, arid climate during the Pleistocene.

**Keywords:** *Bison*, Bovidae, Europe, Quaternary, Villafranchian

## 1 Introduction

### 1.1. *The genus* Leptobos *and its historical and taxonomic background*

According to most scholars the origin of *Bison* probably lies within the extinct genus *Leptobos* (McDonald, 1981; Duvernois and Guérin, 1989; Masini, 1989; Geraads, 1992; Martínez-Navarro et al., 2007; Tong et al., 2013; Cherin et al., 2019 among others). This group of mid- to large-sized and slender bovines is a constant faunal element during the whole Villafranchian European Land Mammal Age (ELMA; about 3.3–1.2 Ma; Cherin et al., 2019). Fossils of these ungulates have been found in all the Palearctic of Eurasia, from the Iberian Peninsula to China (Dong, 2008; Garrido, 2008), and from northern India to, possibly, the British Isles (Pilgrim, 1937; Breda et al., 2010). Since the establishment of the genus by Rütimeyer (1877-1878), a large number of remains was attributed to *Leptobos* and several species were erected. According to the most recent review, *Leptobos* includes the species: *Leptobos brevicornis* (Asia), *Leptobos crassus* (Asia), *Leptobos falconeri* (Asia), *Leptobos stenometopon* (Europe), *Leptobos elatus* (Europe), *Leptobos merlai* (Europe), *Leptobos furtivus* (Europe), *Leptobos etruscus* (Europe), and *Leptobos vallisarni* (Eurasia) (Cherin et al., 2019).

Masini (1989) and Masini et al. (2013) divided the European species of *Leptobo*s into two groups or lineages, the first including *L. stenometopon*, *L. elatus*, *L. merlai*, and *L. furtivus*; the second *L. etruscus* and *L. vallisarni*. Duvernois (1990, 1992), on the basis of horn and tooth morphologies established two subgenera for the aforementioned groups: *Leptobos* (*Leptobos*) *and Leptobos* (*Smertiobos*), respectively, adding to the latter the species *Leptobos bravardi*. These two subgenera, however, suffer from nomenclatural inconsistencies (see Croitor and Popescu, 2011; Cherin et al., 2019), thus this subdivision is not commonly used in literature (Masini et al., 2013). The Asian group includes the species *L. falconeri* (type species), *L. brevicornis* (which embraces also *L. amplifrontalis and L. laochihensis*), and *L. crassus* (Mead et al., 2014). Over the years, several authors tried to find relationships between the Asian and European forms (Dong, 2008). However, up to date, it is still not clear if these groups are actually related or if, for instance, the Asian taxa are part of a third, distinct, clade (Mead et al., 2014). This incapability of linking the European and Asian groups might find a solution in the species *L. vallisarni*, which is the only occurring in both continents (Zheng et al., 1985; Tong et al., 2016). The existence of advanced *Leptobos* forms in the Early Pleistocene of eastern Asia, along with the fact that the earliest *Bison sensu lato* (s.l.) species are known from

India and China roughly in the same time span, led most authors to suggest that *Bison* could have originated in Asia, emerging from a derivate stock of *Leptobos* (Sala, 1986; Masini, 1989; Duvernois, 1990; Martinez-Navarro et al., 2007; Sorbelli et al., 2021a among others).

### 1.2 *Earliest Eurasian bison in the paleontological literature, a review*

The earliest forms of *Bison* most probably emerged in the eastern Palearctic and, as soon as they reached Europe at the end of the Early Pleistocene, started to replace *Leptobos* in all the large herbivore guilds. Indeed, a possible co-existence between *Bison* and *Leptobos* is reported only in few late Villafranchian European localities of south-eastern Europe (Duvernois, 1990; Agadzhanyan et al., 2017; Kostopoulos et al., 2018; Lopatin et al., 2019). In Asia, on the contrary, *Bison* and *Leptobos* seem to have shared the same geographic areas for a prolonged time, possibly for almost two million years (Tong et at., 2016). This long overlap could be explained (i) by the large size of suitable habitats in Asia, which may have triggered niche partitioning among these bovines in a context of wide trophic availability, and/or (ii) by bias in the taxonomic identification and/or stratigraphic range of fossils.

The first occurrence of *Bison* s.l. is represented by the scanty remains of *Bison* (*Eobison*) *sivalensis* and *B.* (*Eobison*) *palaeosinensis* from India and China, respectively. Flerov (1979) referred to the newly erected subgenus *Eobison* these two Asian species, as well as *B.* (*Eobison*) *tamanensis* from Eastern Europe. The author, however, did not deepen the diagnosis of the subgenus, which is currently flawed by several issues. *Bison* (*Eobison*) *georgicus* from Dmanisi (Georgia) is putatively the earliest *Bison* s.l. approaching Europe at ca. 1.77 Ma (Burchak-Abramovich and Vekua, 1992; Bukshianidze, 2005). From the late Villafranchian on, a large number of localities in Mediterranean and Eastern Europe are characterized by the presence of these mid-sized bison-like bovids (Fig. 1), still commonly grouped in the subgenus *Eobison* (Masini et al., 2013; Sorbelli et al., 2021a). After 1.2 Ma (i.e., at the beginning of the Epivillafranchian stage), with the onset of new climatic conditions in the context of the Early-Middle Pleistocene Transition (EMPT; Head and Gibbard, 2005; Clark et al., 2006), *Eobison* was replaced by the larger-sized *Bison sensu stricto* (s.s.) (i.e., *B. schoetensacki*, *B. menneri*, and *B. priscus*, in chronological order of appearance), which rapidly colonize most of the Holarctic (Kahlke, 1999; Sorbelli et al., 2021a).

In the time interval between the age of the Dmanisi fauna and the beginning of the Epivillafranchian, crucial information on the evolution of early bison can be sought, but, unfortunately, paleontological records are scarce. Here, we describe the rich sample from Pietrafitta (central Italy), which can shed new light on this intriguing topic. In a preliminary analysis, this sample was attributed to *Leptobos* aff. *vallisarni* based on cranial similarities with the holotype of *L. vallisarni* from the Upper Valdarno (Italy; Masini, 1989). Later on, this attribution was confirmed by Masini and Gentili (2005), although not supported by quantitative comparative analysis. Nevertheless, the authors noticed that the material from Pietrafitta was characterized by some features more advanced than in *L. vallisarni*, hence the choice of open nomenclature. Building on that insight, this paper presents the first detailed description of the Pietrafitta record, in the context of the arrival of the first bison in Europe and their replacement of *Leptobos*.

## 2. Geological setting

The Tavernelle-Pietrafitta Basin is located in the upper valley of the Nestore River. During the early stages of the Pleistocene, after an intense phase of tectonic activity, the Tavernelle-Pietrafitta Basin became part of a lateral branch of the main Tiberino Basin and started to be characterized, alternatively, by lacustrine/palustrine and alluvial plain conditions (Conti and Esu, 1981; Cherin et al., 2012; Pazzaglia et al., 2013). The lignite deposition was a result of the elevation of the delta of the Nestore paleo-river causing the formation of several small basins filled with stagnant water (Gentili et al., 1996). At the end of the Pleistocene, new tectonic events occurred causing an uplift of the area and the desiccation of the basin, which subsequently underwent an erosive phase (Ambrosetti et al., 1989). The site of Pietrafitta (42°59′33″N 12°12′42″E) is located close to the homonymous village in the municipality of Piegaro. The lignite seam had a thickness comprised between 5 and 8.5 m and was exploited industrially for almost half a century. Lignite was intercalated with thin layers of organic clay yielding freshwater mollusks and oligohaline ostracods (Gliozzi et al., 1997). Facies analysis suggests that the lignite was deposited in a swampy area located on the edge of a lake (Conti and Girotti, 1977; Ambrosetti et al., 1992; 1995; Martinetto et al., 2014). This hypothesis is furtherly confirmed by paleobotanical studies, which report the presence of a large water body surrounded by broad-leaved deciduous forests in a humid climatic context. The plant assemblage of Pietrafitta is dominated by aquatic genera such as *Azolla*, *Najas*, *Nymphaea*, and

*Potamogeton* (Martinetto et al., 2014). Palynological data show a variation in the forest composition surrounding the swamp, due to a progressive harshening of the climatic conditions. In particular, moving along the stratigraphic succession from bottom to top, the disappearance of *Taxodium*-type and its replacement by "Quercetum" taxa is observed, followed by the spread of herbaceous plants and *Pinus* in the upper layers (Lona and Bertoldi, 1972; Kottek et al., 2006; Martinetto et al., 2017). The depositional and environmental conditions of the swamp allowed the preservation of one of the richest continental vertebrate samples in the Italian Early Pleistocene, including some thousand specimens belonging to almost 40 taxa of freshwater fishes, anurans, reptiles, birds, and mammals (see revised faunal lists in Martinetto et al., 2014 and Sorbelli et al., 2021b). The vertebrate assemblage is referred to the Farneta Faunal Unit (FU; approx. 1.6–1.4 Ma) of the late Villafranchian ELMA, corresponding to late MNQ 18 in the French mammal biochronology scheme (Guérin, 1982; Torre et al., 1992; Gliozzi et al., 1997; Gentili et al., 2000; Rook and Martínez-Navarro, 2010). The taphonomic evidence and the presence of numerous skeletons of large mammals found in their original anatomical position or slightly scattered, suggest a low degree of post-mortem movement (Ambrosetti et al. 1992).

## 3. Materials and Methods

More than 400 remains of a large bovid have been recovered from the lignite deposits of Pietrafitta (Table S1). Most of the material come from the "Miniera Vecchia" and few from "Poderetto" and "Poderone" excavations (Gentili et al., 1996). The studied sample is stored in the "Museo Paleontologico Luigi Boldrini" at Pietrafitta except for a metacarpal (IGF 1011), a cast of the original fossil which is lost, housed in the IGF (see abbreviations below). The fossils present different state of preservation and colours, suggesting that the bones undergone to different taphonomic processes. Most of the specimens share the same kind of preservation with dark grey to dark brown colour, mildly to strongly deformed volumes, and slightly to strongly cracked surfaces testifying a certain degree of subaerial exposure before final burial. Few of the cranial and postcranial remains are characterized by dark greyish colour and are less deformed or cracked.

In this review of the primitive forms of *Bison* we attempt to use the largest comparative sample available, including both the putative ancestors and descendants of this group (i.e., *Leptobos* and *Bison* s.s.). However, due to the difficulties in studying the original material, lack of data in the literature, debated taxonomy, or

scanty fossil record, we kept out from the discussion some samples, e.g., *Leptobos* spp. from China and *L. furtivus* and *L. bravardi* from Europe. The two *Leptobos* groups considered in this work are thus, the one including *L. stenometopon, L. elatus*, and *L. merlai* (gr. LSEM hereinafter) and the one including *L. etruscus* and *L. vallisarni* (gr. LEV hereinafter). A large number of *Leptobos* specimens reported by Masini (1989) from unknown localities of the Upper Valdarno and referred to *L. etruscus*, *L.* cf. *etruscus*, or *L.* cf. *vallisarni* were not considered due to their undefined stratigraphic provenience and uncertain taxonomy. The genera *Bos, Bison, Poephagus* (as well as other bovines) are often grouped within *Bos* based on molecular evidence (Groves and Grubb, 2011; Hassanin, 2014; Castelló, 2016). In order to keep consistency with decades of paleontological studies, we follow the nomenclature by Kostopoulos et al. (2018) which retain *Bison* (including both extinct and extant species) as a separate genus. In this context, *Bison* s.l. is used to indicate members of the three subgenera *Bison* (*Bison*), *Bison* (*Poephagus*), and *Bison* (*Eobison*).

The fossil material directly studied by us includes the following records (for the institutional abbreviations see below): *Leptobos* spp. from Villarroya (Spain), Upper Valdarno, Pantalla, and Umbria undetermined locality (Italy), housed in the ICP, IGF, NHMB, and SABAP_UMB; *B.* (*E.*) *degiulii* from Pirro Nord (Italy), housed in the DST and PF; *B.* (*E.*) *degiulii* from Mygdonia Basin (Greece) housed in the LGPUT and NHCK; *B.* (*E.*) cf. *degiulii* from Capena (Italy) and *B.* (*B.*) cf. *schoetensacki* from Cava Redicicoli (Italy) housed in the MUST; *B.* (*E.*) sp. from Mugello (Italy) housed in the MGCB; *B.* (*E.*) cf. *georgicus* from Salita di Oriolo (Italy) housed in the MCSNF; *B.* (*B.*) *schoetensacki* from Isernia La Pineta (Italy), Cesi (Italy), and Vallparadís Section (Spain) housed in the MPPPL, MuPA, and ICP, respectively*; B.* (*B.*) *priscus* from Siberia (Russia), housed in the Yakutia AS. The digital material studied by us includes the 3D models of *B.* (*E.*) *georgicus* from Dmanisi (Georgia) housed in the MG; *B.* (*B.*) *bonasus* from Białowieża (Poland) housed in the MRI PAS; *B.* (*B.*) *latifrons* from several North American sites housed in the IMNH. Other comparative data were retrieved from the literature. Juvenile specimens are not included in the study. The measurements of the fossils were taken with digital and analogic callipers and recorded at the nearest 0.1 mm. The measurements on the digital 3D models were taken with the aid of the software MeshLab (Cignoni et al., 2008). Statistical analyses were performed with PAST v.4 (Hammer et al., 2001). The anatomical terminology used in this paper are from Heintz (1970), Sala (1986), Masini (1989), Kostopoulos et al.

(2018), and Sorbelli et al. (2021a) with minor changes. Linear measurements follow Masini (1989) and Sorbelli et al. (2021a) with minor changes, and are explained in Table S2 and shown in Fig. S1.

The shape and size of horn-core bases were defined by bivariate plot comparing the anteroposterior and dorsoventral diameters (HDV *vs* HAP). The shape and size of the intertemporal bridge and frontal bones were analysed with bivariate plots featuring IBH *vs* IBW and FWmin *vs* FLmin, respectively. $Log_{10}$ diagrams of teeth (Simpson, 1941) were constructed based on the average values of eight selected variables of *Leptobos* and *Bison* samples from various Eurasian sites. The record of *B.* (*B.*) *priscus* from Krasny Yar, R–W was used as a standard of comparison (y=0; data taken from Vasiliev, 2008). To assess the stoutness of limb bones, we used bivariate plots featuring Lmax *vs* DEW/Lmax % for the metapodials and astragali and Lmax *vs* PEW/Lmax % for the radii. Principal component analyses (PCAs) were performed based on metapodials and cranial remains to estimate the differences between *Leptobos* and *Bison* species. These analyses rely on seven Mosimann Log-Shape variables for the metapodials and six for the crania (Table 1), obtained by log-transforming the ratio between each measurement and the geometric mean of the measurements for each specimen (Jungers et al., 1995). Histograms were employed to determine the length of metatarsals and radii relatively to the metacarpals, featuring the average values of LmaxMT/LmaxMC-100 and LmaxRAD/LmaxMC%-100, respectively. The robusticity index of metacarpals was defined by the ratio DEW/Lmax %. Body mass estimations were obtained as average of three estimations based on metatarsal linear measurements (PEW, PET, and DEW) following Scott (1983), taken in consideration only complete specimens.

*Institutional abbreviations*—DGPU, Department of Geology, Panjab University, Chandigarh, (India); DST, Dipartimento di Scienze della Terra, Università di Firenze (Italy); GIN RAS, Geological Institute of Russian Academy of Sciences, Moscow (Russia); ICP, Institut Català de Paleontologia Miquel Crusafont, Sabadell (Spain); IGF, Museo di Storia Naturale, Sezione di Geologia e Paleontologia, Università di Firenze (Italy); IGPB, Istituto di Geologia di Bari; IMNH, Idaho Museum of Natural History, Pocatello (USA); LGPUT, Museum of Geology, Palaeontology and Palaeoanthropology of the Aristotle University of Thessaloniki (Greece); MAEGR, Museo Arqueológico y Etnológico de Granada (Spain); MCSNF, Museo Civico delle Scienze Naturali di Faenza (Italy); MG, S. Janashia Georgian National Museum, Tblisi (Georgia); MPLB, Museo Paleontologico “Luigi Boldrini” di Pietrafitta, Piegaro (Italy); MPPPL, Museo di

Paleontologia e Preistoria Piero Leonardi, Università di Ferrara (Italy); MGCB, Museo di Geologia e Paleontologia "Giovanni Capellini", Università di Bologna (Italy); MR PAR, Mammal Research Institute, Polish Academy of Sciences (Poland); MuPA, Museo Paleontologico Archeologico di Serravalle di Chienti (Italy); MUST, Museo Universitario di Scienze della Terra, Sapienza Università di Roma (Italy); NHCK, Natural History Collection of Kalamoto, Kalindoia (Greece); NHMB, Natural History Museum of Basel (Switzerland); PF, PaleoFactory Lab, Dipartimento di Scienze della Terra, Sapienza Università di Roma (Italy); PIN, Orlov Paleontological Museum, Moscow (Russia); SABAP UMB, Soprintendenza Archeologia Belle Arti e Paesaggio dell'Umbria, Perugia (Italy); Yakutia AS, Academy of Sciences Republik of Sakha, Yakutsk (Russia); ZIN RAS, Zoological Institute of Russian Academy of Sciences, St. Petersburg (Russia);

## 4. Results

Class Mammalia Linnaeus, 1758

Order Artiodactyla Owen, 1848

Family Bovidae Gray, 1821

Subfamily Bovinae Gray, 1821

Genus *Bison* Hamilton Smith, 1827

Subgenus *Eobison* Flerov, 1972

*Emended diagnosis*—Small to mid-sized *Bison* with small horns (present in both males and females) and slender limbs. Cranium with relatively deep and high temporal fossae; lower than in *Leptobos* but higher than in *Bison* (*Bison*). The fossae extend far behind the horn-cores, along the lateral sides of the postcornual part of the cranium (not so much as in *Leptobos*). As a result, the occipital squama is separated from the frontal by an abrupt constriction, giving to it a trapezoidal to semi-circular or bell shape with a wide base and a narrow top. Nuchal crest outline, in dorsal view, undulated or semicircular, never squared or straight. Supraoccipital portion of the cranium quite reduced; intertemporal bridge almost completely fused with the nuchal crest. Orbits protruding anterolaterally, weakly tubular, without thickened edges. Postorbital notch variable depending on the sex but, generally, stronger than in *Leptobos* and weaker than in *Bison* (*Bison*). Frontals short; their length (distance from the edge of nuchal crest to nasion) is shorter than the width of frontals between postorbital notch. Frontals concave and pneumatized at the horn-core bases; elevated above the occipital area. Horn-core pedicles shorter than in *Leptobos*. Horn-cores short and stout, emerging

posterolaterally (the angle between the sagittal axis and the midline of the horn-core is comprised between 50° and 75°); horn-cores bending posteriorly and ventrally at the base, then laterally and markedly dorsally at the tip; in some cases, there can be a small anticlockwise torsion; horn-cores dorsoventrally compressed at the base; section oval in the first two third, tending to get circular toward the tips; absence of keels; posteroventral surface strongly furrowed. Premaxillary bone ends before the nasals. Nasals elongated, ending at the level of the anterior margin of the orbit or slightly behind. Mandible with relatively straight corpus and short symphysis. Angle between ramus and corpus around 90° or slightly obtuse. Coronoid process projects backwards, often exceeding the level of processus condyloideus. Teeth are generally smaller than in *Bison* (*Bison*). Neural processes of the thoracic vertebrae well developed but less than in *Bison* (*Bison*). Limbs relatively slender and short. Metapodials stouter than in *Leptobos* but slenderer than in *Bison* (*Bison*). Metatarsal less than 20% longer than metacarpal. Radius generally shorter than in *Bison* (*Bison*) but longer than in *Leptobos*; more than 30% but less than 50% longer than the metacarpal.

*Bison* (*Eobison*) *degiulii* Masini, Palombo and Rozzi, 2013

(Figs 2–5; Figs S2–S6)

*Diagnosis*—Mid- to large-sized *B.* (*Eobison*). Frontals concave between the horn-cores with a small crest running along the suture line in the posterior portion. Very short and stout horn-cores. Postcornual portion of the cranium moderately developed. Temporal fossae wide and stretched posteriorly. Nuchal crest outline in dorsal view, arched, feebly undulated. Occipital squama trapezoidal or bell shaped.

*Referred specimens*—The Pietrafitta record includes 93 cranial (Figs 2–4) and 337 postcranial remains (Fig. 5 and Figs S2–S6). See Table S2 for the complete list.

4.1. *Description*

4.1.1. *Cranial material*

Five incomplete crania were unearthed from Pietrafitta, all affected by taphonomic deformation. The most complete crania are SABAP UMB 19. 2.1178 and SABAP UMB 19. 2.1179, both flattened in dorsoventral direction. The former preserves most of the frontals, nasals, and the left horn-core whereas the latter is represented by the occipital and basioccipital areas and the horn-cores. In both specimens four of the upper

molars (left and right M2s and M3s) and three not identified upper premolars are still embedded in the cranium or matrix. SABAP UMB 19. 2.1178 is associated with its two hemimandibles. The ossified sutures and the stage of wear of teeth (were present) suggest that all the five crania belong to adult individuals. The small size of the horn-cores and the reduced tuberosities of the basioccipital indicate that SABAP UMB 19. 2.1178 was probably a female whereas SABAP UMB 19. 2.1179 is characterized by larger horn-cores and a massive basioccipital, indicating it is a male. The horn-cores are located rather close to the orbits but far from each other and emerge posterolaterally (i.e., the angle between the sagittal axis and the midline of the horn-core is around 65°). Compared to the overall cranium size, the horn-cores are small and stout whereas the pedicles are relatively long. The horn-cores are thicker at the pedicle contact and taper abruptly. Their section at the base is ovoidal with the major axis developing in antero-posterior direction, then it tends to become circular toward the tips. The horn-cores weakly curve ventrally in the first third, then bend laterally and dorsally, then posteriorly and somewhat medially (especially in SABAP UMB 20. 1.6803). The ventral surface is deeply grooved whereas the dorsal one is less furrowed. The grooves tend to disappear toward the apexes. In some specimens (i.e., SABAP UMB 21. 1.1323, SABAP UMB 20. 2.7345) the dorsal side of the tips is marked by deep irregular furrows that run parallel to the major axis of the horn-core. In all the specimens the tips are marked by numerous small nutrient foramina. In the broken specimen SABAP UMB 21. 1.1179 it is possible to observe that the most basal part of the horn-core is strongly pneumatized. The horns and pedicles are elevated above the frontals, even if the compression does not permit to assess the degree of elevation. In SABAP UMB 19. 2.1178 the frontal area is quite wide and, although strongly deformed, it is possible to observe a slight concavity in the central part, between the pedicles. A small crest runs in the middle of this depression, following the interfrontal suture. This suture is very clear as well as the bregma. The supraorbital foramina are far from each other, positioned just behind the orbits, in narrow but elongated grooves. These grooves are anteriorly converging and end at the level of the posterior margin of the orbits. The postorbital constriction is strongly convex. One orbit is preserved in SABAP UMB 19. 2.1178. Although the deformation altered the outline of the orbit, a certain tubular shape can be still recognized. The nasal bone wedges into the frontals with an acute angle, posteriorly to the anterior margin of the orbits. The nasals anterior end is bifurcated. The maxilla thins towards its anterior end expanding below the premaxilla, which prolongs anteriorly with a shovel-like knot in the anterior edge. The contact between

maxilla and premaxilla ends above the alveolar level. The posterior part of the premaxilla tapers rapidly and abruptly ends before the nasals. The postcornual portion of the neurocranium is relatively reduced in both SABAP_UMB 19.2.1178 and SABAP_UMB 19.2.1179. The intertemporal bridge (=chignon, sensu Duvernois, 1990) is fused with the nuchal crest which is characterized by a vaulted dorsal outline, and slightly undulated edges. The occipital squama is preserved in SABAP UMB 19. 2.1179 and SABAP UMB 21. 2.1177; it is large and has a semicircular outline, marked by a narrow top and a wide base. The two temporal fossae indent behind the horns, nonetheless their posterior ends are well separated by the dorsal margin of the squama. The jugular processes are hooked, bending inward and projecting below the ventral margin of the condyles. The bulging and robust mastoid processes are separated from the jugular processes by a shallow groove. The condyles are large and sub-triangular with the pointed end located ventrally. The position and number of the foramina on the occipital squama are variable (e.g., a single foramen is visible dorsally to the right condyle of SABAP UMB 21. 2.1177). The basioccipital has a wedged shape formed by the two pairs of tuberosities. Overall, it is short and broad. The posterior tuberosities are triangular and wide and separated by a shallow depression. A faint, small crest starts between the anterior bases of these tuberosities, follows the median axis of the basioccipital, and reaches the anterior tuberosities. The latter are elongated but much smaller than the posterior ones, and are divided by a deep V-shaped furrow. Anteriorly to the anterior tuberosities there is a secondary crest, which is the prolongation of the one mentioned above. A small foramen is located on the posterior margin of this crest, just at the anterior limit of the tuberosities. SABAP UMB 19. 2.1179, SABAP UMB 21. 2.1177 and SABAP UMB 20. 1.6803 differs for having: larger posterior tuberosities divided by a narrower depression; wider and shorter anterior tuberosities; less developed crest in the valley between the anterior and posterior tuberosities; more developed crest anteriorly to the anterior tuberosities; and an overall larger size. In SABAP_UMB 20.1.6802 the basioccipital still articulates with a portion of the basisphenoid and the pterygoid processes. The basisphenoid is strongly bent upward. A small canal is present on both sides of the basioccipital, just above the posterior tuberosities.

The most complete hemimandibles (SABAP UMB 130074 and SABAP UMB 130075) associated to SABAP UMB 19. 2.1178 are in good state of preservation except for some parts of the rami. The angle formed by the ramus and the corpus is slightly obtuse. The symphysis is relatively short with a bulge on the ventral edge and a rugose surface. In dorsal view, the symphyseal area is slightly inflated as well as the

316 molar portion of the mandibula. SABAP UMB 21. 1. 1298 is the only mandible preserving the processus
317 condyloideus. The condyle is stout and depressed in the middle. The coronoid process is quite elongated and
318 projects backwards, ending posteriorly to the processus condyloideus.
319 4.1.2. *Dentognathic material*
320 The studied specimens include 28 isolated teeth, and 70 associated to mandibles.
321 The upper teeth are quadrangular in occlusal shape (especially the molars) with a wide base and high
322 crown. In the P2, the parastyle and paracone are shifted mesially and the paracone fold is quite deep. The
323 metastyle is poorly separated from the labial wall of the tooth. The enamel central cavity has a complex
324 outline, being divided into three islets in SABAP UMB 20. 1.7361. The P3 is characterized by a well-
325 developed metastyle, protruding distally. The parastyle is relatively reduced. The paracone is shifted toward
326 the metastyle, oblique in labial view. The P4 is the largest and stoutest premolar and has a squared occlusal
327 outline. It shows various degree of molarization. The metastyle is slightly more pronounced than the
328 parastyle, the former protrudes distolabially whereas the latter mesiolabially. The paracone is not particularly
329 protruding, its fold is slightly shifted toward the metastyle and it is divided from the styles by two
330 pronounced furrows. The outline of the central cavity is U-shaped with a more complex distal wall, often
331 featuring a small fold. SABAP UMB 20. 1.6804/8 and SABAP UMB 20. 1.6804/7, belonging to the same
332 individual, show the most incipient molarization with a faint hypocone developing distolingually and the
333 presence, in the latter specimen, of a small enamel islet distally to the central cavity. The upper molars show
334 a high degree of hypsodonty with strong pillars and almost parallel margins, slightly diverging occlusally. In
335 all the upper molars the distal lobe is slightly shifted labially. In M1 and M3 the mesial lobe is
336 buccolingually more developed than the distal one whereas, in M2, the two lobes are generally of the same
337 size. The styles are strong and labially projected, marked by a small constriction at the contact with the tooth
338 which forms ribbon-like structures. In M1 and M2 the parastyle is slightly larger than the mesostyle and
339 metastyle which are, more or less, of the same size. The metastyle is strongly projected distally in M3,
340 creating, thus, a vertical, shallow furrow that delimitates its distal contact with the main body of the lobe. In
341 all upper molars the paracone and metacone are less prominent than the styles. In occlusal view, the entostyle
342 shows a subcircular (e.g., SABAP UMB 20. 1.6804/5) to relatively complex outline (e.g., SABAP UMB 20.
343 1.7346/1). The cement is always present in upper molars, especially on the lingual side; in some specimens it

is scarce (e.g., SABAP UMB 20. 1.6806), but in few teeth is present in both the labial and lingual sides (e.g., SABAP UMB 20. 1.7346/1). The cement, in the lingual side, penetrates deeply between the entostyle and the two lobes. The outline of the central cavities has an irregular crescent-moon shape, sometimes characterized by the so-called "bubaline fold" (sensu Merla, 1942). This fold is always present in the distal wall of the distal cavity, in some cases in both the cavities (e.g., SABAP UMB 20. 1.6804/3, SABAP_UMB 20. 1.7348) although is always more complex in the distal one. No enamel islets were found between the two lobes.

The lower teeth are mesiodistally elongated with high crowns. The p3 is quite similar to the p4, differentiating in the less developed paraconid and the more joined entoconid/entostylid, a deeper distal valley developed mesially and a less globular metaconid. The p4 is narrow and, in most of the specimens, relatively shortened. The parastylid is sharp and projects mesiolingually, divided from the paraconid by a shallow and short groove that ends well before the neck (1$^{st}$ valley, sensu Heintz, 1970). In some specimens this groove is quite reduced (e.g., SABAP UMB 20. 1.7342). The paraconid is perpendicular to the mesiodistal axis of the tooth. The 2$^{nd}$ valley separating the paraconid from the metaconid, is deep and wide (but less in some specimens, e.g., SABAP UMB 20. 1.7340/3). The protoconid is quite developed, especially lingually, creating a small stylid-like bulge in the 2$^{nd}$ valley, mesially to the metaconid. The metaconid itself is a robust pillar and projects lingually (e.g., SABAP UMB 20. 1.7342) or distally with a thinner outline (e.g., SABAP UMB 21. 1.1236). Toward the cervix the metaconid is mesiodistally enlarged and shows a flat lingual surface. The 3$^{rd}$ valley, due to the constriction of the metaconid, is quite deep but ends well before the neck of the tooth. The entoconid and entostylid are almost completely fused, separated by a faint 4$^{th}$ valley which is more or less developed depending on the specimen but tends to disappear rapidly with the wear of the tooth. The labial valley separating the protoconid from the hypoconid is deep and short, ending before the base of the tooth. The molars have large and sharp metastyle projecting mesiolabially (especially m2 and m3). The protoconid is more developed mesiodistally than the hypoconid. The ectostylid is narrow and located in the mid-point between the two lobes, slightly shifted toward the mesial one. In m2 and m3 the ectostylid has an elliptical shape in occlusal view whereas it has a more complex outline in m1. Labially the molars are flattened, the protoconid and hypoconid are lingually separated by an open valley. The hypoconulid size varies depending on the specimen from mesiodistally elongated (e.g., SABAP UMB 20.

1.7340/5) to short and robust (e.g., SABAP UMB 20. 1.7341/6). All molars are characterized by a thick layer of cement on both sides.

4.1.3. *Metapodials*

Eight metacarpals are known from the lignite of Pietrafitta. Four specimens (SABAP UMB 20. 1.7324, SABAP UMB 20. 1.7325, SABAP UMB 130038, IGF 1011) are almost complete and little deformed. There are no significant differences in the shape of the proximal facets neither in the trochlear surfaces of the analyzed specimens. Two metacarpals belong to the same individual (SABAP UMB 22. 4.247), being part of an almost complete skeleton. Generally, all specimens are characterized by a relatively slender built; the two epiphyses have roughly the same width and are much wider than the diaphysis. Seen from above, the proximal outline of the bone is D-shaped; the anterior margin has subrounded edge whereas the posterior one is markedly straight. The proximal articular surface is composed by two facets. The lateral one for the unciform is triangular and smaller than the medial for the trapezoid-magnum which is sub-quadrangular with rounded anterior margin. The former is separated from the latter by a small crest perpendicular to the mediolateral axis of the articulation. The lateral facet is anterolaterally marked by a small notch. The proximal foramen is visible only in SABAP UMB 20. 1.7324 and is located in a deep and narrow groove, at the posterior end of the crest that divides the two facets. A foramen is present distally to the proximal end, in the middle of the epiphysis. The anterior margin of the proximal epiphysis is marked by a large, protruding tuberosity. The diaphysis has hourglass-shaped medial and lateral margins, the minimum width of the shaft is located slightly above mid length. The anterior vascular groove is narrow and shallow, deeper in the distal portion. The ovoidal foramen is located just above the distal end of the vascular groove. The contact area between the diaphysis and the distal epiphysis is marked by an evident tubercle (in both medial and lateral sides), so that the maximum distal width between these tubercles is almost the same as that across the trochleae. A slight mediolateral constriction is present between these tubercles and the distal articulation surface of the corresponding trochlea. The intertrochlear margins converge distally. The distal intercondylar crests are generally sub-parallel. Two deep depressions are present proximally to either side of each trochlear crest, on the anterior side of the epiphysis. The two outer depressions are larger and deeper than the inner ones. The same four pits are present on the posterior side of the bone, dorsally to the crests. The lateral and

398 medial trochlear pits are deep and marked by radial rugosities. The lateral abaxial hemicondyle is slightly to
399 strongly anteroposteriorly thinner than the medial one but is laterally more protruding.
400 Twelve metatarsals were recovered from Pietrafitta, of which six are well preserved. These bones are
401 hourglass shaped with a slender and long shaft and a stout distal end. The proximal epiphysis hosts two
402 major articulation surfaces (anterolateral and anteromedial facets for the articulation with the cubonavicular
403 and cuneiform) and two secondary ones (posterolateral and posteromedial facets for the accommodation of
404 the two cubonavicular posterior facets). The two primary facets converge anteriorly, separated by a well-
405 developed ridge, proximally protruding in the anterior portion. The anteromedial articular facet is ovoidal,
406 having the major axis oblique respect to the sagittal plane. The anteromedial margin is proximally concave
407 and irregular whereas the posterolateral is flattened. The lateral facet is slightly smaller and less inclined with
408 smoother outline. The angle between the two facets is variable between 40° and 45°. The posterolateral
409 articular facet is small and leaf shaped with a very narrow anteroposterior diameter. The posteromedial facet
410 has a subrounded outline and lies attached to the posteromedial margin of the medial primary facet. The
411 proximal portion of the diaphysis is delimited by three crests that follow the main axis of the bone. The
412 posterior surface of the diaphysis is slightly concave to flat in its proximal half, where two faint and shallow
413 longitudinal grooves are present. Toward the distal portion, the shaft flattens and is marked by an ovoidal
414 foramen. The epitrochlear tubercles at the contact between the diaphysis and the distal epiphysis are well
415 developed, more than in the metacarpals; thus, the width at the level of the tubercles is about the same as that
416 between the outer trochlear margins or even larger (e.g., SABAP UMB 20. 1.7328 and SABAP UMB 20.
417 1.7330). The distal epiphysis slightly bends posteriorly. The two trochlear ridges are subparallel relative to
418 the medial and lateral margins of the distal end and converge anteriorly. The lateral and medial trochlear pits
419 are deep and proximally surrounded by radial rugosities.
420
421 4.2. *Comparisons and taxonomic assignment of the Pietrafitta sample*
422 Although the Pietrafitta specimens are characterized by different taphonomic features, on the whole the
423 record is homogeneous, both morphologically and metrically (Figs 2–9; Tables 2–4; Figs S2–S6; Tables S3,
424 S5, S7–S9, S11, S13–S16, S18, S20, S22, S24, S28). The hypothesis that the bovid sample is roughly
425 isochronous is supported by the overall uniformity of the faunal and floral assemblages along the Pietrafitta

426 stratigraphic succession and by the high sedimentation rate estimated for this kind of brown coal deposits
427 (Cameron et al., 1989; Martinetto et al., 2014).

428 The general morphology of the cranial and postcranial remains from Pietrafitta is typical of bovines, and
429 in particular of leptobovines and bison. Most of the systematics of these bovids has been historically based
430 on skulls and metapodials but, as suggested by recent studies (e.g., Sorbelli et al., 2021a), other postcranial
431 bones might provide useful taxonomic information.

432 The Pietrafitta specimens are different from the members of the earliest *Leptobos* species (gr. LSEM) in
433 several cranial features including: shorter braincase (postcornual area), quite reduced intertemporal bridge,
434 shorter and stouter horn-cores, nasal ending at the orbit level, premaxilla not in contact with the nasal, and
435 abundant cement in the upper molars (Figs 6, 7; Table 5). Equally, the larger size and robusticity of all the
436 postcranials clearly separate the Pietrafitta bovid from the LSEM leptobovines (Table 6; Tables S10, S12,
437 S19, S23, S25, S26). At the same time, the increased stoutness and larger limb size of the late representatives
438 of *Leptobos* (gr. LEV) make a comparative distinction from the Pietrafitta bovid more difficult. Indeed, the
439 studied postcranial remains share several morphometric features with this group, and especially with *L.*
440 *vallisarni* from Italy (see section 5.2; Figs 8, 9). In spite of that, taking in consideration the cranium, the
441 differences from *Leptobos* gr. LEV are much more evident. The wider occipital, the anteroposterior
442 compression of the intertemporal bridge, the longer nasals, and the shorter premaxillae clearly differentiate
443 the Pietrafitta bovine from *L. etruscus*. Most interestingly, the double bending of the horn-cores, their wide
444 angle of projection from the frontals, and their short and bulk built are characters that separate the Pietrafitta
445 bovine from both *L. etruscus* and *L. vallisarni*.

446 It is clear that some of the aforementioned features can be interpreted as apomorphies, approaching the
447 Pietrafitta bovine to *Bison* s.l. Nonetheless, the studied sample still retains several features that are generally
448 considered primitive in the evolution of *Bison*, including: small and short horn-cores, weakly tubular orbits,
449 concave frontals, trapezoidal occipital squama, strong indentation of the temporal fossae behind the horn-
450 cores, and relatively short and slender limb bones.

451 On the whole, the Pietrafitta sample shows numerous similarities with the primitive bison forms
452 attributed to the subgenus *Eobison*. In order to identify the samples at species level, within this subgenus, we

provide below detailed comparisons of its most complete and diagnostic elements with several *Leptobos* and *Bison* s.l. species (Figs 6–11; Tables 5, 6).

4.2.1. *Horn-cores*

The best-preserved horn-core (right core of SABAP UMB 19. 2.1179) is plotted in the bivariate diagram that compares the anteroposterior (HAP) and dorsoventral (HDV) diameters of the core bases between various samples of the leptobovine and bisontine groups (Fig. 6a). All early *Bison*, on average, display smaller horns compared to the priscoid group of *B. schoetensacki* and *B. priscus*, with some specimens (e.g., Kalamoto and Dmanisi samples) showing even smaller sizes than *Leptobos*. Most of *Eobison*, *Leptobos* gr. LSEM, and some *B. schoetensacki* specimens are characterized by HAP values considerably higher than HDV ones. These dorsoventrally compressed cores, are clearly different from the more cylindric ones of *Leptobos* gr. LEV and Late Pleistocene-Holocene *Bison*. The Pietrafitta specimen falls within the variability of *Eobison*, in the area occupied by the Salita di Oriolo, Capena, and Dmanisi samples (Fig. 6a). The position of the horn-cores respect to the frontals can give some taxonomic hints (McDonald, 1981). The angle formed by the midline of the core at the base and the sagittal line is wider in *Bison* s.l. and *Leptobos* gr. LSEM than in *Leptobos* gr. LEV (Fig. 6b). In particular, the horns of *B. priscus*, *B. schoetensacki*, and *B. bison* are directed more laterally, forming wide angles, whereas *Leptobos* gr. LSEM, *B. menneri*, and *Eobison* show cores shifted backwards and, in *Leptobos* gr. LEV, even more posteriorly. The two specimens from Pietrafitta exhibit approximated angles of 65° and 70° fitting with the variability of *Bison*, and more specifically of *B.* (*Eobison*).

4.2.2. *Intertemporal bridge and frontals*

The anteroposterior compression of the intertemporal bridge represents an important trend in the evolution of *Leptobos* and *Bison* (Pilgrim, 1947; Masini, 1989, Duvernois, 1990, Cherin et al., 2019). The primitive forms of *Leptobos* are characterized by a well-developed postcornual portion of the neurocranium with a high and narrow intertemporal bridge, posteriorly elongated. Conversely, in later forms (i.e., *Leptobos* gr. LEV), the bridge tends to shorten anteroposteriorly and widen, due to the anterodorsal shifting of the occipital squama and the squeezing outward of the temporal fossae. In *Bison*, the occipital squama is even more advanced and the intertemporal bridge disappears, fusing with the nuchal crest. Following Cherin et al. (2019), in Fig. 7a we show the progressive change in the proportions of the intertemporal bridge from high

and narrow in *Leptobos* to short and wide in *Bison*. This latter condition, in which the bridge is fused with the nuchal crest, is present in the Pietrafitta bovid. Nonetheless, in this form, it is still present a strong indentation of the temporal fossae behind the horn pedicles and, consequently, a constriction of the upper occipital squama; a character which is present in later species of *Leptobos* (i.e., *L. vallisarni*) and in *Eobison* (Flerov, 1972; Toniato et al., 2017; Kostopoulos et al., 2018 among others).

Another evolutionary trend of *Leptobos* and *Bison* is the widening of the frontals and the reduction of their relative length. The biplot in Fig. 7b clearly shows that the earliest representatives of *Leptobos* and *Bison* (gr. LSEM and *Eobison*) have more elongated and narrower frontals compared with their respective descendants (gr. LEV and *B. priscus*). The Pietrafitta specimen SABAP_UMB 19. 2.1178 falls close to the *Eobison* samples from Dmanisi, Capena, and Pirro Nord (Fig. 7b).

4.2.3. *Occipital and basioccipital*

In order to assess the most diagnostic morphometric traits of the occipital and basioccipital in *Leptobos* and *Bison*, a PCA was performed on 41 crania, using six adjusted variables (Fig. 7d; Table S6). According to the results, the first two PCs explain the 79% of the total variance. PC1 (67.9% of variance) is influenced by the distance between the posterior ends of the temporal fossae (IBW positive), by the width of the foramen magnum and of the basioccipital posterior tuberosities (FMW and PPW both negative), and by the shape of the occipital squama (OSHmin negative, MW positive). This component divides the specimens having wide intertemporal bridge and dorsoventrally compressed occipital squama (x positive) from the individuals with narrow intertemporal bridge, high and narrow occipital squama, and wider foramen magnum and basioccipital (x negative). PC2 (11.8% of variance) is dominated by the width of the foramen magnum (FMW negative), the distance between the posterior ends of the temporal fossae (IBW negative), and by the size of the occipital squama and basioccipital tuberosities (MW, OSHmin and PPW positive). Thus, this component helps distinguishing the specimens with more developed occipital squama and basioccipital (y positive) from those with larger foramen magnum and wider intertemporal bridge (y negative). The Pietrafitta specimen SABAP_UMB 19. 2.1179 is found in the top right area, close to the centre of the diagram, fitting with the variability of *Bison* s.l. (Fig. 7d). The bi-condylar width (CW) appears to be the less influencing variable in both PC1 and PC2.

4.2.4. *Teeth*

The comparative study of teeth revealed that the Pietrafitta bovine was characterized by a mixture of plesiomorphic and apomorphic characters and a wide morphological variability. The degree of hypsodonty in bovines tends to increase from the middle Villafranchian on, reaching the highest levels in Late Pleistocene and Holocene forms of *Bison* (Asperen and Kahlke, 2017). The high and columnar teeth of the Pietrafitta bovine are different from those of early *Leptobos*, characterized by more brachydont dentition. On the contrary, the distinction with *Leptobos* gr. LEV is less marked due to their higher hypsodonty (Merla, 1949; Masini 1989; Duvernois, 1990). The amount of cement in the upper molars is another character that may bear diagnostic value, as it is quite scarce or absent in *Leptobos* and more commonly found in *Bison*. All upper teeth from Pietrafitta present abundant cement, especially within the folds of the lingual side. The mesiodistal constriction of the lingual cones of upper molars has been considered as plesiomorphic in *Leptobos* (Cherin et al., 2019). As a matter of fact, this character is recognizable – albeit variably – in all analysed *Leptobos* and some *Eobison* samples (e.g., Pirro, Mygdonia Basin), whereas is less common in more derived species such as *B. schoetensacki* and *B. priscus*. The Pietrafitta sample shows mesiodistal constriction of the lingual cones in all upper teeth, with various degree of development. The presence of a bubaline fold in the upper molars, sometimes considered as a primitive feature (e.g., Cherin et al., 2019), is not a reliable source of taxonomic information, being variably expressed within Bovinae and quite common in *Bison* s.l. (Merla, 1949; McDonald 1981; Asperen and Kahlke, 2017; Sorbelli et al., 2021a). The p4 has been considered one of the most diagnostic anatomical elements of *Eobison*. For instance, a large metaconid with cylindrical shape and lingual projection was considered a distinctive trait in the first description of the *B.* (*E.*) *degiulii* type material by Masini (1989). The latter author, however, suggests that the morphology of the p4 in this species may show a certain variability, confirmed by our personal analysis of the unpublished material from Pirro Nord (IGF collections). The Pietrafitta record shows a wide spectrum of morphologies of the p4 metaconid, from bulky and lingually projected (e.g., SABAP UMB 20. 1.7341) to thin and distally projected (e.g., SABAP UMB 130074), with a prevalence of the former condition (Fig. 4). Raw measurements (Table S4) and $Log_{10}$ ratio plot (Fig. 7c) show that the dimensions of the teeth from Pietrafitta are similar to those from Dmanisi and Capena, with short and relatively wide molars, amongst the largest within the *Eobison* group.

On the whole, the teeth from Pietrafitta are characterized by bison-like morphology, with some noteworthy exceptions. Although over the decades several authors have defined diagnostic characters in the teeth of *Leptobos* and *Bison* (e.g., Masini, 1989; Duvernois 1990; Cherin et al., 2019), we collided with the evidence that dental morphology is highly variable in these taxa. Skinner and Kaisen (1947: 140) exhaustively commented on this issue in their monography on extinct and extant bison "The pronounced similarity in *Bison* teeth has defied the present attempt to establish useful characters that would permit specific or even subgeneric separations based on tooth characters alone. Large population samples suggest tendencies but show no clear-cut differences. Isolated examples of various *Bison* species appear to have tooth characters that would aid in making specific determinations. These characters, however, soon intergrade when a large population sample is examined". Other authors remarked furtherly the wide spectrum of variability in bovines' dental traits when dealing with large samples: "Many students who dealt with very voluminous collections of bovines hold rather sceptical view on the subject, especially concerning isolated teeth" (Sheer, 1997: 114). The Pietrafitta sample reinforces this vision, allowing only trends to be recognized, not defined diagnostic characters. For these reasons, we advocate a cautious approach in using isolated teeth for taxonomic purposed in bovines, especially when small samples are available and/or the putative presence of more than one taxon is inferred.

4.2.5. *Metapodials*

Metapodials (Table 6; Table S26) are the most frequently used postcranial bones in the taxonomy of Bovinae thanks to their abundance in the fossil record and distinct morphology (Schertz, 1936; Sher, 1997; Maniakas and Kostopoulos 2017; Sorbelli et al., 2021a). Recent studies, however, recommend a prudent approach due to the considerable degree of intraspecific variability of these elements, which might be partially caused by ecophenotypic changes (Maniakas and Kostopoulos 2017; Sorbelli et al., 2021a). Comparisons based on Lmax and DEW are widely used to assess the metapodial robusticity, which tends to increase on average from *Leptobos* to *Bison* (Sher, 1997; Kostopoulos et al., 2018; Bukhsianidze, 2020; Sorbelli et al., 2021a). The metacarpal biplot Lmax vs DEW/Lmax% (Fig. 8a) shows the presence of various morphotypes: the left part of the diagram is occupied by the slenderest forms such as *Leptobos* (especially the species of the gr. LSEM); the upper part is occupied by the large-sized and long-legged *B. menneri*; on the right, the more robust species such as *B. schoetensacki* and *B. priscus*, can be found. The Pietrafitta

sample is located in the middle of the diagram, within the variability range of late Villafranchian *Bison*. It is noticeable the partial overlap of the Pietrafitta sample with the most robust specimens of *L. etruscus* and *L.* cf. *vallisarni* from the Valdarno historical collection. Two specimens (SABAP UMB 130038 and SABAP UMB 20. 1.7325) are very short and slender, fitting well with *B.* (*Eobison*) sp. from Venta Micena (Spain), one metacarpal of *B.* (*E.*) *palaeosinensis,* and some of the metacarpals from the Upper Valdarno (Le Ville, La Viesca) referred to *L.* cf. *vallisarni.* Four specimens display larger and stouter built, fitting better with *B.* (*E.*) *degiulii* from the Mygdonia Basin and *B.* (*E.*) *georgicus* from Dmanisi, overlapping with the slenderest specimens of *B. schoetensacki* from various sites of Europe. The two associated metacarpals belonging to the only articulated skeleton from Pietrafitta (SABAP UMB 22. 4.247/7 and SABAP UMB 22. 4.247/8), fall at the left border of the *Eobison* group and overlap with the largest *L. etruscus*. The same plot built for the metatarsals reveals a similar pattern (Fig. 8b). The largest and stoutest sample, on the right, is mainly composed by the priscoid forms (*B. schoetensacki* and *B. priscus*). The upper part is occupied by the tallest specimens (i.e., *B. menneri* and some *B. schoetensacki* individuals), whereas the bottom left is occupied by *Leptobos*, characterized by slenderer and shorter metatarsals. Again, *Eobison* is found in the middle. The Pietrafitta record falls at the left border of the *Eobison* range, partially overlapping with *Leptobos*.

In order to increase taxonomic resolution, we performed a principal component analysis of seven adjusted variables, on both metacarpals and metatarsals (Fig. 9). The two principal components (PC1 and PC2) explain a significant amount of the variance, expressing 80% and 66% of the total variance for metacarpals and metatarsals, respectively. The metacarpal analysis shows that PC1 (71% variance) is negatively influenced by Lmax PET and DET, whereas positively by PEW, DW, and DEW. These results separate the longer and thicker metacarpals (x negative) from the shorter and wider ones (x positive). PC2 (9%) is mainly dominated by Lmax, DW, and DT, for negative values, whereas on the positive axis by PEW, PET, DEW, and DET, so that this axis separates longer metacarpals with larger diaphysis (y negative) from shorter ones with larger epiphyses (y positive). The PCA diagram, although not resolving the overlapping issues between groups, helps us in distinguishing the three major morphotypes without the influence of size effect: the *Leptobos* morphotype with slender diaphysis and deep and narrow epiphyses; the "true bison" morphotype (including *B. schoetensacki*, *B. priscus*, and *B. bonasus*) with robust built and wide diaphysis and epiphyses;

591 the *Eobison* morphotype (including also *B. menneri*) with intermediate features between the two former
592 groups. The Pietrafitta specimens fall within this last group.
593 In the metatarsal analysis (Fig. 9b; Table S27), PC1 (48% variance) is mainly influenced by Lmax for the
594 positive values and by DEW, PEW, DW, DT for the negative ones, thus dividing the long and slender
595 metatarsals (x positive) from the stouter ones with wider shaft and distal end (x negative). PC2 (18%) is
596 determined, positively, by the size of the distal epiphysis (DET and DEW) and the anteroposterior diameter
597 of the proximal end (PET); whereas negatively by the width of the diaphysis (DW), which influences way
598 more than the other variables (PEW, Lmax, and DT). PC2 allows to distinguish the metatarsals with thick
599 ends (y positive) from the ones with wide shafts (y negative). The Pietrafitta specimens, characterized by
600 very thick and wide diaphysis, lie along the negative PC2 axis, occupying an empty space, and partially
601 overlapping the *Eobison* record.
602 Both the PCAs show that the Pietrafitta sample is characterized by metapodials with intermediate
603 proportions between *Leptobos* and *Bison* s.s., fitting with the known *Eobison* variability. It is worth
604 mentioning that some isolated bones from the late Villafranchian of Central Italy referred to *L. etruscus* and
605 *L.* cf. *vallisarni* (Masini, 1989), display proportions similar to some *Eobison* specimens. It has to be
606 considered, in fact, that the first *Bison* and last *Leptobos* likely coexisted in Europe during this period. Thus,
607 it is possible that some of these isolated remains could have been erroneously attributed to *Leptobos* and,
608 instead, pertain to *Bison*.
609 4.2.6. *Radii, astragali, and other postcranials*
610 Among the other postcranial bones, the radii are the most helpful. As already shown by Sorbelli et al.
611 (2021a), their size and built can provide interesting information for taxonomy. The biplot that compares the
612 length and slenderness degree of this bone shows a clear increase in stoutness and size from *Leptobos* to
613 *Bison* (Fig. 8d; Table S12). The Pietrafitta specimens plot in the space occupied by the early *Bison* samples
614 from Pirro Nord, Capena, and the Mygdonia Basin at the upper border of the *Leptobos* cloud. Other
615 postcranials such as calcanei and cubonavicular are not particularly significant due to their considerable
616 dimensional homogeneity between the last *Leptobos* and early *Bison* (Tables S21, S25). Conversely, it is
617 worth noting that the astragali allow a certain separation between "true" *Bison* and *Eobison-Leptobos* based
618 on total length and, secondarily, stoutness (Fig. 8d; Table S23). The low number of complete humeri,

femurs, and tibiae does not allow us to perform dimensional comparisons. In spite of that, the average measurements of these elements in the Pietrafitta sample (and in other roughly coeval samples) are always intermediate between those available for *Leptobos* and *Bison* s.s. (Tables S10, S17, S19).

4.2.7. *Limb proportions and concluding remarks*

Interesting results can also be obtained from the dimensional comparison between different bones. The analysis of the ratio between the metatarsal and metacarpal lengths shows that the latter bone is relatively longer in most primitive forms than in the priscoid group (Fig. 9c). Indeed, in *Leptobos* and most *Eobison*, including the Pietrafitta sample, the metatarsals are less than 15% longer than the metacarpals, whereas in Late Pleistocene *Bison* from Eurasia and North America (including the living species *B. bonasus* and *B. bison*), it is more than 20% longer (Fig. 9c). On the contrary, the ratio between radius and metacarpal lengths shows that the Pietrafitta bovine and other records of *Eobison* share with *Bison* s.s. a relatively elongated radius compared to the metacarpal (Fig. 9c). This analysis reveals that in all late Villafranchian bison the radius length exceeds of more than 30% the metacarpal length, with the exception of the samples from Dmanisi and Venta Micena (Fig. 9c). Interestingly, the earliest members of *Bison* s.s. (i.e., *B. menneri*, *B. schoetensacki*, *B. p. priscus*) differ significantly from their later relatives (i.e., *B. p. mediator*, *B. antiquus*, *B. latifrons*, *B. bison*, *B. bonasus*) in having longer metacarpals compared to both metatarsals and radii.

Considering all the above pieces of evidence, the bovid sample from Pietrafitta can be confidently referred to the subgenus *Eobison*. More specifically, most crania and limb bone morphological and biometric characters are consistent with those described in *B.* (*E.*) *degiulii*, a well-known species from the late Villafranchian of Southern Europe (Italy and Greece) (Fig. 10). Another species with similar morphology is *B.* (*E.*) *georgicus* from Georgia. However, it is represented by a rather scarce sample, which needs to be enriched by new discoveries in order to clarify its taxonomic status (see Discussion).

## 5. Discussion

5.1. Leptobos*: state of the art*

During the twentieth century, several diagnoses of *Leptobos* have been proposed (Pilgrim, 1939; Merla, 1949; Masini, 1989; Duvernois, 1990). Unfortunately, this multiplicity of interpretations has led to a rather vague definition of this genus. Nevertheless, some distinctive characters of *Leptobos* are accepted by the

different authors, including: horn-core bases located not far from the orbits, emerging posterolaterally, slightly to strongly compressed dorsoventrally; horn-cores furrowed in the first half, without evident keel; female hornless; premaxilla in contact with nasal; presence of ethmoidal fenestrae; temporal fossae well developed in the postcornual portion of the cranium; sub-triangular basioccipital; occipital squama from semi-circular to bell-shaped; presence of a more or less developed intertemporal bridge; slender limbs. Below we provide a review of *Leptobos* records in the European Villafranchian.

The first group of species (here called gr. LSEM), generally considered more primitive, includes *L. stenometopon*, *L. elatus*, *L. merlai*, and the poorly-known *L. furtivus*. *Leptobos stenometopon* (Fig. 12b) is a small- to mid-sized species described on the basis of a horned calvarium from the late Pliocene of Dusino (Italy; Rütimeyer, 1867). The taxonomy of this species has been debated over the last decades, being considered either a younger synonym of *L. elatus* (Duvernois and Guérin, 1989; Duvernois, 1990, 1992) or a valid species (Masini, 1989; Geraads, 1992; Rodrigo, 2011; Masini et al., 2013; Cherin et al., 2019). It is also reported - as *L.* cf. *stenometopon* - from the Plio-Pleistocene transition in Montopoli (Italy) and from some sites of uncertain age in the Upper Valdarno (Merla, 1949; Masini, 1989). *Leptobos elatus* is a species described by Depéret (1884) on cranial material from the latest Pliocene of Perrier-Les Étouaires (France). Unfortunately, the type material is no longer available (Viret, 1954; Masini, 1989) and the neo-diagnosis given by Duvernois (1990, 1992) was based only on dental and postcranial remains and on the original descriptions by Depéret (1884). The synonymy between *L. elatus* and *L. stenometopon* proposed by Duvernois and Guérin (1989) and Duvernois (1990) has been questioned by other authors (e.g., Masini et al., 2013; Cherin et al., 2019) due to some flaws in the taxonomic status of *L. elatus* and to significant differences between the material from the type localities of the two species. Other remains attributed to *L. elatus* are from the sites of Rocaneyra (France; dated to the Plio-Pleistocene boundary), Villarroya (Spain; ca. 2.15 Ma), and Tegelen (The Netherlands; ca. 2.0 Ma) (Schreuder, 1946; Viret, 1954; Masini, 1989; Duvernois, 1990; Rodrigo, 2011). *Leptobos merlai* (Fig. 12c) is a mid- to large-sized species from the middle Villafranchian of France (type locality: Saint Vallier) and Italy. First referred to *L. elatus* (Viret 1949) then to *L. stenometopon* (Viret, 1954), De Giuli (1987) recognized diagnostic differences between the remains from Dusino and those from Saint Vallier and erected the species *L. merlai* to accommodate the latter. Later, Duvernois and Guérin (1989) and Duvernois (1990, 1992) similarly to what was done for *L. stenometopon*,

675 proposed *L. merlai* as a subspecies of *L. elatus*. Finally, in their description of the material from Pantalla (ca.
676 2.0 Ma) and other Italian sites, Cherin et al. (2019) supported the validity of *L. merlai* as a distinct species
677 (and questioned the validity of *L. elatus* itself, being based on scanty material). *Leptobos furtivus* is
678 considered the smallest and actually rarest species of this genus in Europe. It was first described by
679 Duvernois and Guérin (1989) on the basis of few teeth, some postcranials, and an isolated horn-core from the
680 middle Villafranchian of Senèze (France), where also the larger *L. etruscus* is recorded. Isolated remains
681 from the late Villafranchian of Italy are also referred to *L. furtivus* (Masini, 1989; Duvernois, 1990). An
682 incomplete cranium and some postcranials from Piana del Cavaliere (Italy) may be attributed to the same or
683 a similar species (*L.* aff. *furtivus* in Masini, 1989; Gentili and Masini, 2005; Fabbi et al., 2021). In spite of
684 the above records, *L. furtivus* remains a little-known species and conclusions on its own validity can only be
685 granted by future discoveries (Cherin et al., 2019).
686 The second group of species (gr. LEV in this manuscript) includes *L. etruscus*, *L. vallisarni*, and the
687 poorly-known *L. bravardi*. *Leptobos etruscus* (Fig. 12e) - erected by Falconer (1868) based on the rich
688 collection from the Upper Valdarno - is the best-known species of the genus, occurring in most Europe
689 during the first stages of late Villafranchian. Fossils of *L. etruscus* have been found in several sites of Spain,
690 France, Italy, Greece, Romania, and possibly the United Kingdom (Merla, 1949; Masini, 1989; Duvernois
691 1990; Kostopoulos, 2006; Garrido, 2008, Breda et al., 2010; Croitor and Popescu 2011; Kostopoulos, 2022
692 and references therein). This species has been considered closely related with *L. vallisarni* based on
693 numerous craniodental similarities (Masini, 1989), to the point that Duvernois (1990) interpreted *L.*
694 *vallisarni* as a junior synonym of *L. etruscus*. *Leptobos vallisarni* (Fig. 12f) - described by Merla (1949)
695 based on a partial cranium from the late Villafranchian of the Upper Valdarno - is characterized by some
696 apomorphic cranial features shared with the earliest bison. Unfortunately, very little is known on the
697 postcranial anatomy of *L. vallisarni* due to absence of sites where associated cranial and postcranial remains
698 were found. Several isolated metapodials from Central Italy were tentatively referred to this species by
699 Masini (1989); however, due to the unclear stratigraphic context (e.g., Upper Valdarno indeterminate
700 localities) and their affinities with the roughly coeval *L. etruscus* and *Eobison* spp., we advocate a prudent
701 approach to their attribution. Two almost complete skulls from the Gonghe Basin (China) were attributed to
702 *L. vallisarni* (Zheng et al., 1985), unfortunately not associated with postcranial bones, again. *Leptobos*

*bravardi* is a mid- to large-sized species described by Duvernois (1990) from Perrier-Les Étouaires, where also *L. elatus* is reported. The same author referred to this species also some of the remains from Villarroya (Spain), where, again, the co-occurrence of *L. elatus* is hypothesized. The validity of *L. bravardi* has been questioned by Rodrigo et al. (2010) and Rodrigo (2011) who attributed the variability recognized in the Spanish and French samples to sexual dimorphism. The fragmented neurocranium of *L. bravardi* from Perrier-Les Étouaires (Duvernois, 1990) was referred to *L. elatus* by Masini (1989).

5.2. Leptobos*: comments on the European taxa*

The crania of LSEM are easily distinguishable from those of LEV and *Bison* s.l. thanks to the peculiar morphology of the cornual and postcornual areas. The double curvature of the horns (anteroposterior and dorsoventral) differentiates these species from *L. etruscus* and *L. vallisarni*. The large size and slenderness of the horns distinguish them from primitive bison, whereas the dorsoventrally compression of the core bases (Fig. 6a) and the strong core curvature distinguish them from *Bison* s.s. The divergence angle between the horn-core axis and the sagittal axis is higher in LSEM than in LEV and fits with the variability of *Bison* s.l. (Fig 6b). The temporal fossae of LSEM are wide and deep, especially in the posterior portion, causing a constriction of the dorsal part in the occipital squama. In addition, the ventral portion of the latter is wider due to massive mastoid processes, resulting in a bell shape of the squama itself (Cherin et al., 2019). These *Leptobos* species, due to the posterior elongation of the temporal fossae, display a distinctly high and narrow intertemporal bridge, which clearly separates the nuchal crest from the frontals. This element, as mentioned above, tends to reduce as a consequence of the progressive shortening of the postcornual portion of the neurocranium in the evolution of *Leptobos* and *Bison*, and disappears in the most derived forms fusing with the nuchal crest (Fig. 7a). LSEM is also distinguished by markedly narrow and elongated frontals (Fig. 7b). Our analyses point out that, on the whole, the cranial morphology of *L. stenometopon*, *L. elatus*, and *L. merlai* is similar to a degree that makes it difficult their distinction at species rank (see PCA in Fig. 7d). The horn-core morphology is very useful also for the taxonomic recognition of LEV. In these species, the horn-core base section is almost perfectly circular (Fig. 6a), and the horn-cores emerge in a more posterior direction than the other bovines considered thus the angle between the middle line of the horn and the sagittal plane is quite reduced (Fig 6b). Moreover, the horn-cores are characterized by simple curvature

731 describing a half-moon shape and lie parallel to the frontal plane, clearly different from both LSEM and
732 *Bison* s.l. In addition, in LEV the intertemporal bridge is much lower and wider than in LSEM; this character
733 is quite evident in *L. vallisarni*, in which the shape of the intertemporal bridge is similar to what is observed
734 in early *Bison* (Fig. 7a). The occipital squama of LEV is semicircular due to the increasing distance between
735 the posterior edges of the temporal fossae and the shortening of the intertemporal bridge. Finally, there is a
736 trend in the widening of the frontals and a general increase of stoutness and size of the cranium from LSEM
737 to LEV as shown by our biometric data and analyses (Fig. 7; Table 5). Other cranial characters (apart from
738 the teeth) are similar between the two *Leptobos* groups (e.g., presence of ethmoidal fenestrae, premaxillae in
739 touch with the nasals, absence of horns in females). The teeth of *Leptobos* are characterized by strong
740 polymorphism, and a relative homogeneity in size (Fig. 7c). Nonetheless, some characters can be useful to
741 discriminate the two groups, provided that sufficiently large samples are available. These characters include
742 the hypsodonty degree, molarization of P4, amount of enamel folds in the central cavities, and cement
743 abundance (see Duvernois, 1990; Cherin et al., 2019).
744 The postcranials of LSEM show small size and overall light built compared with those of LEV and *Bison*
745 s.l. Body mass estimations based on metacarpals give an average value slightly higher than 400 kg for
746 LSEM, that is, the smallest in the studied sample (Fig. 11b). In our analyses, the metapodials and radii are
747 characterized by narrow epiphyses and relatively elongated and slender diaphysis (Figs 8, 9; Table 6; Table
748 S12). Comparing the lengths of different long bones, it emerges that the radius is relatively shorter than the
749 metacarpal, while the latter is relatively longer than the metatarsal (Fig. 9c). The humeri, astragali, and
750 calcanei are among the slenderest of all the studied records (Tables S10, S23, S25). Again, the samples
751 referred to gr. LSEM do not present clear-cut biometric differences in the postcranials, except for the
752 metacarpal sample from Saint Vallier (*L. merlai*), which appears slightly stouter than the others (Fig. 8a).
753 The homogeneity in long bone size and proportions between *L. stenometopon*, *L. elatus*, and *L. merlai* might
754 suggest that they actually represent a single species. From this perspective, the small differences in stoutness
755 between the various records might be correlative with local ecomorphotypes rather than interspecific
756 variation.
757 On the contrary, LEV features larger and stouter bodies compared with early *Leptobos*, and more similar
758 to *Eobison* (Tables S10, S12, S17, S19, S21, S23, S25, S26). The average body mass of LEV is about 500 kg

(Fig. 11b). The radius is characterized by gracile structure and small size (Fig. 8c). The metacarpals are long and slender, but still stouter than those of LSEM (Figs 8a, 9a, 11a). Nonetheless, the low mean value for the length ratio RAD/MC% indicates that the radii are relatively shorter than the forelimb, i.e., the same as in LSEM (Fig. 9c). The low values of the ratio MT/MC% clearly separate *L. etruscus* from *Bison* s.l. (Fig. 9c). The astragali are small compared with those of *Bison* s.l. and overlap in size those of LSEM (Fig. 8d). The lack of postcranial material undoubtedly referrable to *L. vallisarni* makes difficult the comparison between this species and its relatives. In fact, our biometric analyses of metapodials show a significant overlapping of the remains putatively attributed to *L. vallisarni* and those of earliest *Bison*. This issue suggests that isolated bones might have been misinterpreted and their attributions must be taken cautiously (e.g., sample from Le Ville in the Upper Valdarno, which probably belongs to a primitive form of bison).

### 5.3. Eobison *and other "transitional" forms: state of the art*

Several species have been included into *Eobison* since the establishment of this subgenus by Flerov (1979). Unfortunately, over the decades, *Eobison* has become a wastebasket taxon for all bison-like bovid remains found in the Eurasian Villafranchian, hampering its clear definition. The diagnosis provided by Flerov (1979) is rather insufficient, also due to the scarce fossil record available at that time. For this reason, we propose the emended diagnosis in Section 4.

Up to date, the oldest bison fossils belong to *B.* (*E.*) *sivalensis*. This species was erected by Lydekker (1878) on the basis of a partial skull from the Upper Siwaliks (Pakistan); later, Pilgrim (1939) published the diagnosis based on the same cranial material. Since then, few more cranial elements from the Indian Plio-Pleistocene were tentatively attributed to *B. sivalensis*, all chronologically constrained between 3.3 and 2.6 Ma, making thus, this species the first representative of the *Bison* s.l. clade (Khan et al., 2010, 2011). In spite of that, since the holotype skull has apparently been lost (Olsen, 1990) and additional material is too fragmentary for clear attributions, there are no remains that can undoubtfully represent *B.* (*E.*) *sivalensis*. Olsen (1990) and Bukhsianidze (2020) even questioned referral of the type material to the genus *Bison* based on a number of morphological characters.

*Bison* (*E.*) *palaeosinensis* (Fig. 12g) is a small-sized primitive bison occurring in China shortly after *B.* (*E.*) *sivalensis*. The taxonomic status of this species has been debated for a long time. *Bison* (*E.*)

*palaeosinensis* was erected by Teilhard de Chardin and Piveteau (1930) on the basis of three partial skulls - a male (cranium A), a female (cranium B), and a third without sex attribution - and some limb bones from the Nihowan (=Nihewan) Basin. The authors described the characters of this species as "intermediate" between *Leptobos* and *Bison*, sharing more similarities with the latter. Two other incomplete skulls from Yushe and Jinyuan cave in Dalian were referred to this taxon (Teilhard de Chardin and Trassaert, 1938; Jin et al., 2021). Skinner and Kaisen (1947) designated the cranium A as lectotype, evidencing the similarities between cranium B and the holotype of *B.* (*E.*) *sivalensis*, thus not excluding a synonymy between the two species. McDonald (1981) attributed the cranium A to *B. priscus* and the cranium B to *B.* (*E.*) *sivalensis*, hence invalidating the species. Tong et al. (2016) redefined the taxon and described a large number of dentognathic and postcranial remains from the site of Shanshenmiaozui in the Nihowan Basin. These authors also remarked that the cranium B shared some important similarities with *Leptobos*. Up to date, this taxon represents the best-known species of *Eobison* in Asia.

*Bison* (*E.*) *georgicus* (Fig. 12h) is a mid-sized, primitive species, originally defined by Burchak-Abramovich and Vekua (1994) as *Dmanisibos georgicus*, based on material (including a fragmented and reconstructed cranium) from the renowned late Villafranchian site of Dmanisi. Bukhsianidze (2005) revised the material and included it into *Bison* (*Eobison*). The limb bone (in particular metapodials) sample is heterogeneous, showing the presence of two different morphotypes, possibly referrable to another taxon, suggesting that *Eobison* from Dmanisi could have been sympatric with a more primitive bovid, possibly *Leptobos*, as hypothesized in other regions of Eurasia (Tong et al., 2016; Kostopoulos et al., 2018; Sorbelli et al., 2021a).

*Bison* (*E.*) *degiulii* (Fig. 12i, j, k) is, up to date, the best-known species of early *Bison*. It was described informally by Masini (1989) in his PhD dissertation and, later, validated by Masini et al. (2013), based on material from Pirro Nord (latest Villafranchian). The holotype is a partial cranium, associated with several postcranials. An almost complete skeleton from Capena was also referred to this species (Masini, 1989; Masini et al., 2013). Masini (1989) and Sorbelli et al. (2021a) attributed several large bovid remains from Sainzelles (France) to *Eobison* cf. *degiulii*. Kostopoulos et al. (2018) described the rich record from Mygdonia as *B.* (*Bison*) cf. *degiulii*, choosing the open nomenclature due to the lack of clear-cut diagnostic characters in this Greek sample, which seems to display a large number of derived features. The authors,

indeed, stressed that the morphological features of this species can be considered closer to *B.* (*Bison)* than to *B.* (*Eobison*), in agreement with Bukhsianidze (2005), referring this species to the former subgenus. The timespan covered by the aforementioned sites is comprised between 1.7 and 1.2 Ma, thus suggesting that primitive bison, at least in the Mediterranean area, survived until the beginning of the Epivillafranchian and, potentially, co-existed with the larger and more derivate "priscoid" forms of *Bison* s.s., such as *B.* (*B.*) *schoetensacki*, whose first occurrence is at ca. 1.2 Ma (Kostopoulos et al., 2018; Sorbelli et al., 2021a).

*Bison* (*E.*) *tamanensis* was first mentioned, without a diagnosis, by Verestchagin (1959) on scanty cranial material from Tzimbal in the Taman Peninsula (Russia). Later on, the species was validated as member of *Eobison* by Flerov (1979) who gave a diagnosis and designated a lectotype (a partial calvarium). In more recent years, a better-preserved skull was found in Semibalki (Taman Peninsula) and attributed to *B.* cf. *tamanensis* (Baigusheva, 2000). Isolated metapodials and a fragment of horn-core from the three Ukrainian sites of Kairy, Chortkiv, and Cherevychnyy were also referred to this species (David and Svistun, 1981). At present, our knowledge of *B.* (*E.*) *tamanensis* is poor and the taxonomic validity of this species is still discussed (*species inquirenda* in Kostopoulos et al., 2018).

The species *Eobison suchovi* was erected by Alekseeva (1967) based on a single horn-core and few postcranial bones from Dolinskoye (Ukraine). Due to the quite scanty record, the taxonomic validity of this species has been questioned and it has been often synonymized with *B. tamanensis* (Flerov, 1975; Gromov and Baranova, 1981; Croitor, 2016).

*Adjiderebos cantabilis* (Fig. 12d) was described by Dubrovo and Burchak-Abramovich (1986) on the basis of a nearly complete skull from the middle-late Villafranchian of Kushkuna (Azerbaijan; Bukhsianidze and Koiava, 2018; Krijgsman et al., 2019). Bukhsianidze (2005) suggested that this species might belong to an early form of *Eobison*. No postcranials are known to date. From older layers of the same locality, scanty remains of another bovid were described by Burchak-Abramovich et al. (1980) and referred to *Protobison kushkunensis*. This latter taxon, dated to the late early Villafranchian, could be the first "bisontine" form outside Asia (Bukhsianidze and Koiava, 2018). This type material of this species although poorly preserved, share some plesiomorphic characters with LSEM (Bukhsianidze, 2005).

*Probison dehmi* is a small bovid from the Tatrots of the Upper Siwaliks (Pakistan) described by Shani and Khan (1968). The holotype is a badly preserved partial cranium with one horn-core, showing common traits with the Asian *Leptobos falconeri* and *B.* (*E.*) *sivalensis* (Shani and Khan, 1968; Kahn et al., 2010).

Over the decades, several other samples of bison-like bovids were described from late Villafranchian sites of Europe and referred to as "early *Bison*" or "*Eobison*", but without a specific attribution. The largest of these samples is from Venta Micena. This site, dated between 1.6 and 1.5 Ma (Palmqvist et al., 2022), yielded a large number of bovid taxa (Moyà Solà, 1987). This last author recognized, in the larger-sized form, some bison-like characters and attributed the remains to *Bison* sp. Later on, the study of a partial juvenile calvarium confirmed that a relatively small and primitive bison was present in Venta Micena during the late Villafranchian (Martinez-Navarro et al., 2011). The postcranial bones from the site are slightly stouter compared with those of *Leptobos* but shorter and more gracile than those of *Bison* s.s., resembling those of *Eobison* although characterized by relatively smaller size (Masini, 1989; Sorbelli et al., 2021a).

A well-preserved neurocranium with both horn-cores from Salita di Oriolo (Italy) was referred to *Bison* (*Eobison*) sp. by Toniato et al. (2017) due to primitive characters in the occipital and temporal. To *Bison* (*Eobison*) sp. were attributed other scanty records from the Italian peninsula, including an isolated horn-core from Mugello and few postcranial bones from Cava Redicicoli (Italy) (Masini, 1989; Caloi and Palombo, 1995). Bonnoure and Dimitrijevic (2006) referred to an undefined primitive bison several fragmentary remains from the lower layers of Trlica cave (Montenegro). A skull fragment from the Early Pleistocene of Maar du Riege (France) may belong to the same group (Ambert et al., 1996). Finally, from the late Villafranchian site of Taurida cave (Crimea, Ukraine), the putative co-occurrence of *Leptobos* and *Eobison* is reported (Loopatin et al., 2019), but no further information of the fossils is available. Due to the scarcity of data, the last three records are not further discussed and were not included in our comparisons.

### 5.4. Eobison *and other "transitional" forms: comments*

#### 5.4.1. *Dmanisi*

The Dmanisi bovid has been considered the first bison reaching Europe in the first part of the late Villafranchian. The few remains attributed to *B.* (*E.*) *georgicus* include a neurocranium and some postcranials, although more elements are pending to be published (Bukhsianidze, 2020). The neurocranium

(MG D354) is broken at the level of the orbits, posteriorly to the nasals. The occipital and basioccipital regions are well preserved on the whole. The right horn-core and the base of the left are present, although the reconstruction of their original orientation is not trustworthy (Bukhsianidze, pers. comm.). In agreement with Bukhsianidze (2005), the neurocranium from Dmanisi shows many features supporting its attribution to *Eobison*, including: trapezoidal occipital squama, high temporal fossae strongly indenting within the postcornual area, weakly tubular orbits, arched nuchal crest in dorsal view, long pedicles and posterolaterally directed horns (angle of 55° with the sagittal axis). Our biometric comparisons of cranial districts reveal that the Dmanisi bovid is well-fitting with the variability of *Bison* s.l., and in particular with the most primitive forms (Figs 7, 8). The postcranial elements evidence a certain heterogeneity, which might suggest the presence of two different taxa in Dmanisi (Kostopoulos et al., 2018; Sorbelli et al., 2021a), as advocated in Taurida cave (Lopatin et al., 2019) and Tsiotra Vryssi (Kostopoulos et al., 2018). The three most complete metacarpals from Dmanisi have been re-measured and the analyses show that two of them (MG D2812 and MG D3426) have proportions compatible with *Eobison* and one (MG D2288) features slenderer proportions, fitting with the variability of the largest *Leptobos* (Fig. 8a). The two complete radii from Dmanisi (MG D2165 and MG D2962) have short and stout appearance, recalling robust forms of *Eobison* and differing from the smaller radii of *Leptobos* spp. and Venta Micena *Bison* (Fig. 8c). In our opinion, at least the two stouter metacarpals and the radii can be confidently referred to *Eobison* and not to *Leptobos*. The same goes for the cranium MG D354, which shows *Eobison* features. The more pronounced concavity of the forehead and the stronger constriction of the upper occipital squama, are traits that distinguish the Dmanisi specimen from the younger remains of *B.* (*E.*) *degiulii* from Pirro Nord and Kalamoto (Figs 6, 7, 11; Table 5). However, as far as our current knowledge is concerned, it is not possible to attest if these differences can be due by inter- on intraspecific variability (e.g., sexual dimorphism, which we know to play an important role in determining the cranial morphology in bison). Pending new discoveries, we consider *B.* (*E.*) *georgicus* as a distinct taxon. Although we cannot exclude the presence of both *Leptobos* and *Eobison* in Dmanisi, new fossils and more evidence are needed to attest the coexistence of these two genera in the Georgian site. It is worth remembering that, in Southern Europe, in the interval corresponding to the age of the Dmanisi assemblage (ca. 1.8 Ma; early late Villafranchian), *Leptobos* was the only bovine present. It will be replaced by *Eobison* only after ca. 1.6 Ma (latest Villafranchian).

897 5.4.2. *Venta Micena*

898 The postcranials Venta Micena represents one of the richest records of late Villafranchian *Bison*. Our
899 analyses of metapodials show that this bovine was relatively small and had quite short metacarpals (few
900 specimens exceed 230 mm in length) and elongated metatarsals (most of the specimens exceed 260 mm in
901 length), which is a common feature of *Bison* species (Fig. 8a). The robusticity biplots and PCAs show that
902 the metapodial record from Venta Micena falls within the variability of *Eobison*, mostly in the area occupied
903 by the smallest and slenderest specimens. As stated by other authors (Moyà-Solà, 1987; Palmqvist et al.,
904 2022), the wide biometric variability of the sample is the result of marked sexual dimorphism (Sorbelli et al.,
905 2021a). The overall small size of the specimens from Venta Micena (estimated average body mass of 440 kg;
906 Fig. 11b) might be related to the fact that most fossils are part of a biogenic concentration interpreted as a
907 *Pachycrocuta brevirostris* den (Arribas and Palmqvist, 1998; Palmqvist et al., 2022). It has been
908 hypothesized that this fossil assemblage is strongly biased in favour of females and young individuals,
909 characterized by small sizes and, thus, more commonly hunted by predators like hyaenas (Arribas and
910 Palmqvist, 1998). On the other hand, the three complete radii from the site display an oddly primitive
911 proportions with reduced lengths (Figs 8c, 9c); indeed, the value for RAD/MC% is similar to those found in
912 *Leptobos*. Nonetheless, the lack of an abundant sample of complete radii might affect these results, as does
913 the aforementioned sex ratio bias in metacarpals. The juvenile cranium of *Bison* sp. MAEGR VM 8000
914 described by Martinez-Navarro et al. (2011) is strongly damaged and quite uninformative. Even so, the
915 estimated diameters of the horn-core bases are within the variability of *Eobison* (Fig. 6a). Its reduced size is
916 most probably due to the early ontogenetic stage. Waiting for a comprehensive reappraisal of the Venta
917 Micena sample, we agree with previous scholars in referring it to the subgenus *Eobison* without further
918 conclusions on its specific attribution. The possible co-occurrence between *Leptobos* and *Bison* in Venta
919 Micena (Sorbelli et al., 2021a) might be suggested by the presence of two metacarpals and one metatarsal
920 with a slightly elongated morphology, fitting with the variability of gr. LEV. However, in both biplots and
921 PCAs, the larger *Leptobos* and *Eobison* are similar each other, making it difficult to differentiate them in the
922 overlapping areas (Figs 8a-b, 9a-b).

923 5.4.3. *Pirro Nord and Mygdonia Basin*

924 The vertebrate assemblage from the karstic site of Pirro Nord is dated, on a biochronological basis, to
925 1.6–1.3 Ma, although some authors lean towards the upper part of this interval (ca. 1.4–1.3 Ma; Arzarello et
926 al., 2015 and references within). The holotype of *B.* (*E.*) *degiulii* (IGPB s.n., temporarily hosted in DST), a
927 partial cranium of an elder individual, is broken just anteriorly to the orbits. Only horn-core pedicles are
928 partially preserved. It clearly shows bison-like features such as enlarged occipital, laterally placed horn-
929 cores, and protruding orbits. In the first descriptions by De Giuli et al. (1986) and Masini (1989), the authors
930 emphasized the primitive aspect of the cranium, fitting with the original definition of *Eobison* by Flerov
931 (1979). On the contrary, Bukhsianidze (2005) and Kostopoulos et al. (2018) suggested that the Pirro Nord
932 bovine already shows a derived morphology, referrable to "true" *Bison*. In fact, the deep and narrow
933 temporal fossae and doomed frontals are apomorphic character observed in the Pirro Nord cranium.
934 Nonetheless, the section of the horn-core base and shape of the occipital squama, the size of the teeth, and
935 the proportions of the limb bones are still primitive (Figs 10, 12; Table 5). The intertemporal bridge biplot
936 (Fig. 7a) shows that the Pirro Nord specimen exhibits a marked dorsal constriction of the occipital squama,
937 resembling the *Eobison* remains from Dmanisi and Pietrafitta and *L. vallisarni* from the Upper Valdarno.
938 The biplots on frontal and horn-core dimensions highlight the same similarities (Figs 7, 8). Teeth from Pirro
939 Nord are characterized by quite small size (Fig. 7c). Their morphology is variable, as already mentioned by
940 Masini (1989). The Pirro Nord bovine displays, on average, more robust metacarpals than the slightly older
941 primitive bison from the Iberian and Italian Peninsulas (Figs 8a, 11a). The metatarsals, on the contrary, are
942 less stout and fit better with the smaller specimens of *Eobison* (Fig. 8b). These discrepancies in metapodial
943 proportions, however, might be caused by the strong sexual dimorphism of these bovids, thus to a possible
944 sex bias in the Pirro Nord record. The length ratio between metatarsal and metacarpal points out that the
945 former is less than 15% longer than the latter, fitting with the variability of *Eobison* and some *Bison* s.s.
946 species (Fig. 9c). Taking in consideration that the younger age estimations for the Pirro Nord assemblage are
947 around 1.3 Ma, it is possible that this record represents one of the last and most derived forms of *Eobison*,
948 roughly coeval with the stout *B.* (*E.*) cf. *degiulii* from Apollonia. The latter locality lies in the Mygdonia
949 Basin as well as the sites of Tsiotra Vryssi, Krimni, and Kalamoto-2, with an overall age spanning from 1.78
950 to 1.2 Ma (Kostopoulos et al., 2018; Konidaris et al., 2021). Among the most interesting remains of *B.* (*E.*)
951 cf. *degiulii* from this area, a fragmentary cranium and several complete limb bones including metapodials

and radii stand out. The cranium (NHCK KLT-638; Fig. 10f) from Kalamoto-2, lacks the horn-cores and most of the splanchnocranium, being broken at the level of the P3. Most of its features, including the morphology of the orbits, occipital, and frontals, are similar to those of the holotype of *B.* (*E.*) *degiulii* from Pirro Nord (Kostopoulos et al., 2018). The horn-core bases from Mygdonia sites are among the smallest and dorsoventrally compressed among those examined, fitting with other *Eobison* samples and with *B. menneri* (Fig. 6a). The intertemporal bridge is not preserved; however, the occipital squama shows a constriction in its upper section due to the posterior elongation of the temporal fossae, as in all *Eobison*. The robusticity biplot performed on the metapodials shows that, compared with the other records of *Eobison*, the Mygdonia sample (especially the Apollonia specimens), is characterized by marked stoutness, which causes a partial overlap with the records of *B. schoetensacki* (Fig. 8a). In spite of that, PCAs confirm that the Mygdonia bovine clearly falls within the variability of early bison (Fig. 9a). In the metrical analysis, the four complete radii from Apollonia fall at the upper limit of the *Eobison* range, reinforcing the idea that this record can be referred to a short-legged, but still relatively slender form of *Biso*n, different from the larger and stouter *B. schoetensacki* and *B. priscus* from the Epivillafranchian onwards. This is also supported by length rations between metacarpals, metatarsals, and radii (Fig. 9c; Table 6; Table S12, S26).

In sum, the records of *B.* (*E.*) *degiulii* from Pirro Nord and the Mygdonia Basin clearly represent a derived stage of this group, marked by a greater expression of bisontine characters and larger body size (i.e., estimated body mass of ca. 600 kg, on average; Fig. 11b). In particular, the metacarpals from Apollonia (ca. 1.2 Ma) are the most robust among all primitive bison, setting a turning point, at the late Villafranchian-Epivillafranchian transition, towards increased forelimb stoutness. This might be related to an aridification of the habitat, already inferred for the locality (Maniakas and Kostopoulos, 2017; Kostopoulos et al., 2018). Based on our review, we agree with Bukhsianidze (2005) and Kostopoulos et al. (2018) that *B.* (*E.*) *degiulii* is not completely fitting with the original diagnosis of *Eobison* by Flerov (1979). However, we have provided compelling evidence that this species is markedly different from *Bison* s.s. and conforms to our emended diagnosis of the subgenus.

5.4.4. *Capena, Salita di Oriolo, and other Italian sites*

The bovid skeleton (MUST (ex MPUR) s.n.) recovered from Capena (late Early Pleistocene) in 1970, has been recently restored allowing its study in this paper (Fig. 10b1-3). Masini (1989), in his preliminary

980 description of the material, recognized clear bisontine features and attributes this specimen to the newly
981 erected species *B.* (*E.*) *degiulii* due to some primitive traits of the appendicular skeleton. The skeleton is
982 almost complete and in good state of preservation, although the skull is severely cracked and deformed. In
983 spite of that, the horn-cores are almost intact; they are large-sized and emerge laterally, dorsoventrally
984 flattened at the base, and with single curvature (directed downward at the base then upward at the tips). The
985 biplot in Fig. 6a shows that this specimen has the most compressed and large horns in the *Eobison* group
986 (although dorsoventral compression might be slightly exaggerated by taphonomic deformation). The
987 postcornual portion is shortened and the occipital region is wide and flattened (Fig. 10b2). The left
988 premaxilla is partially intact, and its posterior margin does not reach the nasal; the latter has a bifid anterior
989 edge (Fig. 10b1). The rest of the cranium is severely damaged thus providing poor information. Teeth do not
990 differ significantly from those of other bovines. The bubaline fold is present in all upper molars, which
991 present faint constriction of the lingual lobes. The cement is abundant, especially on the labial side,
992 concentrated in the recess between the protocone and metacone. The entostyle of the upper molars has a
993 relatively simple outline. The p4 is characterized by a large and cylindrical metaconid. In the $Log_{10}$ diagrams,
994 dental dimensions follow the general trend of *Eobison*. Based on the size of the appendicular skeleton, the
995 Capena bovine stands out for being particularly large (estimated body mass of about 600 kg; Fig. 11b). The
996 metapodials and radii are among the stoutest and largest in *Eobison*, always placed in the upper range of
997 variability of this group in both biplots and PCAs, very close to *Bison* s.s. (Figs 8, 9). Moreover, the
998 metatarsal and radius are elongated with respect to the metacarpal, recalling the typical condition of more
999 derived species of *Bison*. Consequently, the size and proportions of this skeleton may lead to the question of
1000 whether it belongs to a relatively large and derived species *Eobison*, such as the specimens from Pirro Nord
1001 and Apollonia, or a to small-sized form of true *Bison* (e.g., female of *B. schoetensacki*). The lack of any other
1002 fossil from Capena does not help dispel this doubt. Even if we are more inclined to agree with Masini (1989)
1003 and Masini et al. (2013) in referring this specimen to *B.* (*E.*) *degiulii*, here we prefer cautiously to use the
1004 open nomenclature *B.* (*E.*) cf. *degiulii*.
1005 The calvarium of *Eobison* (MCSNF s.n.) from the "Sabbie Gialle" formation of Salita di Oriolo (Fig.
1006 10c), dated to the late Early Pleistocene (Toniato et al., 2017), was found associated with a fragment of
1007 mandible, some upper teeth, and a cervical vertebra. The fossil is strongly weathered but not fractured or

deformed except for the left jugular process and some portions of the occipital which are missing (Fig. 10c1-4). The dorsal edge of the right orbit is still preserved as well as the basioccipital region. The horn-cores are virtually intact. The occipital is characterized by a large but narrow squama with a marked bell-shape. The intertemporal bridge is wide and dorsoventrally compressed. The frontals are wide and slightly inflated between the horn-core bases; as a result, the forehead is concave except for a small crest running along the interfrontal suture. The orbits are weakly tubular. The pedicles are relatively long. The horn-cores are massive and relatively short, without an evident keel; they emerge in posterolateral direction (ca. 72° with the sagittal axis; Fig. 6b), bend laterally after the first third, and point posteriorly toward the tips; in posterior view posterior, they are directed downward and then curve markedly upward. The horn-core base is wide, with strong dorsoventral compression (Fig. 6a). The teeth are heavily worn, ma. This, affected also their morphology, making their description difficult (e.g., the metaconid, entoconid, and entostylid of p4 are fused). However, it is possible to recognize constricted lingual lobes in the upper molars and a bubaline fold in the P4. To sum up, the general morphology of the material from Salita di Oriolo is primitive (see, in particular, the strong constriction of the upper occipital squama, the high intertemporal fossae, the concave frontals, and the overall small size). Similarities with *B.* (*E.*) *degiulii*, *B.* (*E.*) *palaeosinensis*, and *B.* (*E.*) *georgicus*, especially in the occipital region, are striking (Figs 10, 12; Table 5). In our PCA of neurocranial variables, the Salita di Oriolo specimen falls within the range of variation of *Bison* s.l. (Fig. 7d), but it stands out as one of the smallest known crania of *Eobison* (Fig. 10). Based on this evidence, we support the attribution of the Salita di Oriolo sample to a primitive form of *Bison*, with strong affinities with *B.* (*E.*) *degiulii*. The age of the fossils is debated (Toniato et al., 2017). Considering the similarities between the bovine material and *B.* (*E.*) *degiulii*, we tend to consider the "Sabbie Gialle" formation of late Villafranchian age, that is, slightly older than previously estimated (ca. 1.0 Ma; Toniato et al., 2017).

An isolated right horn-core (MGCB s.n.) from Mugello, although damaged and badly restored, appears to preserve its original morphology. It is relatively short and has a wide base. In dorsal view, it slightly curves posteriorly, then anteriorly, then again posteriorly, toward the tip. In anterior view, it bends downward and then markedly upward. The base is dorsoventrally compressed. Furrows are mainly concentrated on the posteroventral portion. The shape and size (Fig. 6a) are well fitting with the variability of primitive bison, as already suggested by Masini (1989). For these reasons, we confirm referral of this specimen to *B.* (*Eobison*)

1036 sp. This specimen might be the same coming from the lignite mine of Lumena (Mugello) and referred to
1037 *Leptobos* sp. by Merla (1949).
1038 From Cava Redicicoli, dated around 0.8 Ma, the co-occurrence of the large *B. schoetensacki* and the
1039 smaller *B.* (*Eobison*) cf. *degiulii* is reported, due to the presence of few metapodials of different sizes (Caloi
1040 and Palombo, 1995; Masini et al., 2013). The two complete metacarpals, however, show a feeble discrepancy
1041 in size and proportions that might be explainable by sexual dimorphism. In the PCA (Fig. 8a), they fall
1042 within the variability of larger *Eobison* and smaller *B. schoetensacki*. Even if the Cava Redicicoli sample is
1043 surely referrable to *Bison* s.l., and most probably to a single species, further studies are needed to assess their
1044 specific taxonomy.
1045 Several metapodials from the Upper Valdarno area were ascribed to *Leptobos* cf. *vallisarni* and *L.* cf.
1046 *etruscus* by Masini (1989) due to their large size and relatively stout appearance. Our comprehensive
1047 comparative analysis reveals that some of these fossils might be attributed to *Eobison*. Of the four
1048 metacarpals from Le Ville previously referred to L. cf. *vallisarni*, two (IGF 3279, IGF 2374) show different
1049 preservation and are characterized by shorter diaphysis and stouter structure, fitting better with the variability
1050 shown by the *Eobison* group. The same goes for the metacarpal IGF VA661 from La Viesca (Figs 8a, 9a).
1051 For these three specimens we propose a new identification under *B.* (*Eobison*) sp.
1052 5.4.5. *Eastern Europe and Asia*
1053 The (lost) holotype of *B.* (*E.*) *sivalensis* is a partial skull missing of the horn-cores and part of the
1054 splanchnocranium. In our revision of the species original definition, we found an incongruence in the horn-
1055 core description by Lydekker (1878). The author states: "The horn-cores are compressed antero-posteriorly;
1056 their anterior surface is flat from above downwards and concave from within outwards; their posterior
1057 surface is convex in both directions" (Lydekker, 1878: 23). However, in the drawing of the specimen
1058 (Lydekker, 1878: pl. XV) the figured section of the horn is clearly dorsoventrally compressed and, in the
1059 measurement given by the same author (Lydekker, 1878: 125–138), the anteroposterior diameter is 3.4
1060 inches (=86.4 mm) whereas the transverse (dorsoventral?) diameter is 2.6 inches (=66 mm), suggesting,
1061 again, a dorsoventral compression of the horn-core. This issue led to a series of misleading conceptions of
1062 this species. For example, Khan et al. (2010) attributed to *B.* (*E.*) cf. *sivalensis* two complete horn-cores from
1063 late Pliocene deposits of the Tatrot formation, distinguishing from *L. etruscus* for their anteroposterior

compression, absence of torsion, and shorter length. Taking in consideration that the latter two characters are not diagnostic in differencing this sample from *L. etruscus* (the length of the horn-cores actually fit with the variability of *L. etruscus*, which in addition, shows only a feeble torsion), and, if it is true that the holotype of *B.* (*E.*) *sivalensis* had dorsoventrally compressed horn-core bases, then these horn-cores from the Tatrot more resemble the sub-cylindrical sections typical of *L. etruscus* and *Bison* s.s. (Fig. 6a). Based on literature data and available figures, the shape of the occipital area of *B.* (*E.*) *sivalensis*, with its markedly indenting temporal fossae, recalls the typical condition of primitive bison. Olsen (1990) and Bukhsianidze (2020), following the idea of Lydekker (1878), suggested that this species could belong to a different *Bison* subgenus and attributed it to cf. *Poephagus*, in light of similarities with the wild yak. Although we agree that several aspects (e.g., morphology, chronological and geographical ranges) may lead to the same conclusion, the lack of available material does not allow us to infer further on the taxonomy of this form.

*Bison* (*E.*) *palaeosinensis* is considered one of the most primitive forms of bison, unfortunately suffering from a confused taxonomic definition, only partially solved by the emended diagnosis recently given by Tong et al. (2016). One of the main concerns lies in the differences between the two most complete syntypic specimens, cranium A and cranium B, originally attributed to a male and female, respectively (Teilhard de Chardin and Piveteau, 1930). We were not able to study directly the type material, but the measurements and figures available in the literature, clearly show that cranium B is actually different from cranium A, somewhat resembling *L. vallisarni* in various traits of the horn-cores and occipital. However, we still know too little about the intraspecific variability of primitive bison to rule out that the differences between the two crania may actually be due to sexual dimorphism (Tong et al., 2016). The idea by McDonald (1981) that cranium A belongs to a small form of *B. priscus* is debatable due to the clearly primitive features of the occipital squama and temporal fossae, as well as its age. Some similarities especially in the shape and orientation of the horn-cores, can be observed between cranium B and the holotype *B.* (*E.*) *sivalensis* figured by Lydekker (1878). However, the unavailability of the type material of the latter species imposes caution in taxonomic conclusions. Biometric comparisons support affinities of both cranium A and cranium B with other records of *Eobison* (Table 5). The same goes for cranial morphology, which shows an array of primitive characters including flattened to concave frontals marked by a sagittal crest along the suture, long pedicles, short postcornual section, high temporal fossae. Moreover, cranium A shares with *L. vallisarni* and

*Eobison* the intertemporal bridge proportions (Fig. 7a), again disproving its possible inclusion in *B. priscus*. The postcranials referred to *B.* (*E.*) *palaeosinensis* are characterized by a relatively slender built and small size, fitting with the largest *Leptobos* specimens and most *Eobison* (Figs 6, 7; Table 6; Tables S12, S19, S23, S25, S26).

The holotype of *B.* (*E.*) *tamanensis* is a portion of left horn-core still attached to fragments of occipital, temporal, and frontal bones (ZIN RAS 26010). Although the postorbital constriction is visible, it seems to be less developed than in most primitive forms of *Bison*. The temporal fossa is slightly indenting the occipital area, ending not far from the horn-core base, which has a relatively short pedicle. The horn-core is dorsoventrally flattened and has a faint keel on the posterior side. As shown in the biplot in Fig. 6a, the specimen is quite large compared to other records of *Eobison*, falling not far from the area occupied by *B. schoetensacki* from Süssenborn and Mauer. David and Svistun (1981) assigned to this species three isolated metacarpals from different Ukrainian localities (Cherevichny, Chertkov, and Kairy) but, as already suggested by Sher (1997), there is strong heterogeneity in the sample and their attribution to *B.* (*E.*) *tamanensis* is mainly based on the pre-Tiraspolian age of the deposits in which they were found. Croitor (2010) referred the metacarpals from Kairy and Chertkov to *B.* cf. *menneri* and the one from Cherevichny to *Eobison* sp. The robusticity biplot (Fig. 8a) shows that the Chertkov specimen is, in fact, similar to the largest *B. menneri* individuals, whereas the Kairy one fits better with the variability of *B. schoetensacki*, and the slenderest specimen from Cherevichny falls in the overlapping range between *Eobison* and *B. menneri*. Therefore, as for the first two specimens, we agree with the identification by Croitor (2010), while we prefer to attribute the metacarpal from Kairy to *B.* cf. *schoetensacki* due to its robustness. The poor preservation of the holotype of *B.* (*E.*) *tamanensis* prevents to define clear-cut diagnostic characters for this species which, however, seems to be overall similar to *B. schoetensacki*. The presence of a more complete cranium from Semibalki attributed to *B.* (*E.*) cf. *tamanensis* (Baigusheva et al., 2000) could help in assessing the validity of this taxon. Kostopoulos et al. (2018) noticed some similarities between the cranium from Semibalki and that of *B. schoetensacki* suggesting, again, a possible synonymy between the two species. If confirmed, this may reinforce the idea that large and stout priscoid *Bison* had already arrived at the gates of Europe at the end of the Villafranchian and reached the Mediterranean area during the Epivillafranchian (e.g., Le Vallonnet and Vallparadís Section; Sorbelli et al., 2021a).

*Bison* (*E.*) *suchovi* is the less known species of *Eobison*. The holotype, described by Alekseeva (1967), is a distal fragment of juvenile female horn-core from Dolinskoye (GIN RAS 391-2) characterized by stout built and subtriangular section with flattened base. This scanty material does not allow to assess the validity of this species. Croitor (2010) suggested that the alleged differences between this horn-core and the holotype of *B.* (*E.*) *tamanensis* are due to sexual dimorphism, hence considering *B.* (*E.*) *suchovi* as a junior synonym of *B.* (*E.*) *tamanensis*. Sher (1997) stated that the metapodials from Dolinskoye are similar to those from Süssenborn, Mauer, and Mosbach, which, at least for the first two localities, belong to *B. schoetensacki* (Sorbelli et al., 2021a). Based on these pieces of evidence, *B.* (*E.*) *suchovi* is an invalid species in our opinion.

The almost complete cranium of *Adjiderebos cantabilis* (PIN 3723-1) from Kushkuna is one of the best preserved and yet under-considered specimens of Villafranchian large bovid in Eurasia. The cranium misses a portion of the occipital area and fragments of the splanchnocranium, but is in a very good state of preservation on the whole. The first descriptions of this outstanding fossil were given by Dubrovo and Burchak-Abramovich (1983, 1986), who erected this new genus of bovine evidencing its similarities with *Bison* and *Leptobos*. In fact, this cranium shows several features shared with these two genera, but also some autapomorphies including: zygomatic arc elevated over the mandibular articulation and unciform rims at the external borders of the occipital condyles (Dubrovo and Burchak-Abramovich 1986; Bukhsianidze, 2005). Both these characters, however, can be found in other genera of bovines. The zygomatic elevation at the mandibular articulation is clearly visible in some specimens of *Leptobos*, *Bos*, and *Bison* s.l. (e.g., the female *L. etruscus* NHMB VA605 from the Upper Valdarno and the holotype of *B.* (*E.*) *degiulii*) and the hooked process of the occipital condyles is well known in *Bison* s.s. (McDonald, 1981: 187, pl. 26). Our morphometric analyses show that the horn-core bases share the same proportions with the smallest *Eobison* specimens whereas the postcornual constriction is quite developed with a marked posterior indentation of the temporal fossae, which resembles the condition found in the most primitive *Leptobos* forms (Fig. 7a). In addition, the frontals are extremely narrow (Fig. 7b). The well-developed intertemporal bridge, the premaxilla in contact with the nasal, and the presence of ethmoidal fenestrae are all leptobovine features. On the other side, the nasals ending posteriorly to the anterior border of the orbits and the wide angle of horn-core insertion are bisontine features. On the whole, the characters that would distinguish *Adjiderebos* from

*Leptobos* and *Eobison* seem to be not diagnostic, thus, most probably, this species actually belongs to one of these two genera. A direct revision of the Kushkuna material, paired with a phylogenetic study of these clades, are requested in order to clarify the taxonomic position of this extremely interesting "transitional" form between *Leptobos* and *Eobison*.

The holotype of *Probison dehmi* is a fragmented cranium from the Tatrots stage of the Upper Siwaliks (DGPU B/7), dated to the late Pliocene (Shani and Khan, 1968). The cranium is severely damaged and badly restored. Nevertheless, it shows interesting characters in common with gr. LSEM including: long frontals, shallow and high temporal fossae, strong constriction of the upper occipital squama, developed mastoid processes, premaxilla in contact with nasal, presence of ethmoidal vacuity. Shani and Khan (1968) stated that the only complete horn-core is anteroposteriorly compressed; in fact, observing the holotype pictures, it is clear that the horn-core is markedly compressed in dorsoventral direction. It shows a peculiar orientation, bending downward and forward. According to Bukhsianidze (2005), it is most probable that the horn-core was mounted on reverse (the base is completely hidden by plaster). This hypothesis is supported by the fact that the well-marked ribs and furrows visible on the convex surface of the horn-core, are normally present on the ventral side and not on the dorsal. If the horn-core was actually mounted incorrectly, it would originally emerge posterolaterally, then bend upward and forward with a strong posterior twist as in gr. LSEM lineage. A revision and new restoration of the material is required to assess the validity of this taxon or the possible incorporation of *P. dehmi* into *Leptobos*.

### 5.5. *Comments on the evolutive trends in limb proportions and body mass*

Several studies on the morpho-functional adaptations of bovid limb bones in response to climate/environmental changes over the Pleistocene, have been published in the last decades (Scott, 1985; Plummer and Bishop, 1994; Klein et al., 2013; Scott and Barr, 2014; Maniakas and Kostopoulos, 2018; Etienne et al., 2021; among others). The comprehensive study by Scott (1979) on the proportions of bovid limbs showed that long-legged small-sized taxa typical of open habitats rely on their cursorial skills to outrun the predators, whereas in other taxa, passive defence strategies based on large body size and/or gregarious behaviour are preferred. Consequently, small-sized cursorial forms underwent to an elongation of the distal limb elements, while similar evolutionary changes are not expected in large bovids living in the same open

environments (Scott, 1979, 1985). On the contrary, in these forms, it is observed a marked increase in limbs width against length, most probably as an allometric response to heavier bodies (Biewener, 2005; Etienne et al., 2020). This is indirectly confirmed by regression equations for body mass prediction that, if performed on the length of distal bones, overestimate the mass of small bovids of open/arid habitats (i.e., Antilopini, Alcelaphini) and largely underestimate the mass of larger bovines, whereas the epiphysis measurements give much more reliable estimations (Scott, 1983). In addition, it has been proved that bovids exceeding 300 kg in body mass are characterized by an allometric pattern of the anterior zygopodium (Scott, 1985; Etienne et al., 2020), in the fact that this section underwent to a stronger increase of size and robusticity, compared to the other forelimb sections, as a response to heavier mass and subsequent change in posture. In their analysis of several samples of *Bison* from the Pleistocene of Europe, Sorbelli et al. (2021a) suggested that the robusticity of metacarpals in bison is inversely related to the amount of tree cover in the environment.

The present study, including data from numerous species of *Leptobos* and *Bison* covering a wide chronological range, supports the above observations and gives further hints on the morphological response of these bovines to environmental changes over the last 2 Ma in Western Palearctic. *Leptobos* (especially LSEM) is considered as typical of relatively closed environments (Rook and Martinez-Navarro, 2010). In fact, it is inferred that one of the main causes of the extinction of these forms was the progressive contraction of wooded areas started at the end of the Pliocene and specially during the late Villafranchian (Head and Gibbard, 2005, 2015; Maslin and Brierley, 2015). *Bison*, due to its capability to adapt to a wider spectrum of environments, occupied the new available niches, in particular after the onset of new asymmetric glacial/interglacial cycles and the increase of seasonality during the EMPT (Maslin and Brierley, 2015). Our results show a clear trend towards an increased robusticity of metapodials from the Pliocene onwards (Fig. 11a). The violin boxplot of body mass estimations (Fig. 11b) highlights a constant increase of average weight starting from the late Pliocene and reaching a peak during the late Middle Pleistocene, before recording an opposite trend in the Late Pleistocene and Holocene (see also Maniakas & Kostopoulos 2017). Similarly, the biplot of radius robusticity (Fig. 8d) and the RAD/MC% histogram (Fig. 9c) show that *Leptobos* and *Bison* underwent to a clear increase in size and stoutness of the anterior zygopodium correlated with larger body masses (Fig. 11b).

1203 It is even possible to observe the same parallel trends within *Leptobos* and *Bison* at smaller scale. In
1204 *Leptobos*, there is a transition from the slender and short metapodials of LSEM to the stouter and longer ones
1205 of LEV, paired with an increase of radius size, body mass, and hypsodonty, following the first contraction of
1206 forested environments at the middle-late Villafranchian transition (Rook and Martinez-Navarro, 2010;
1207 Madurell-Malapeira et al., 2014). In *Bison*, due to their long history, wide geographic distribution, and
1208 abundant fossil record, the situation is much more complex. The primitive *Eobison*, roughly coeval to the last
1209 *Leptobos*, features increased body mass and robusticity, characterized by larger and heavier heads and limbs,
1210 although not yet displaying the massive appearance of later forms. Their limb structure shows a wide
1211 spectrum of variability (e.g., slender morphology from Pietrafitta, stouter from Apollonia), which could
1212 reflect either separate taxa or ecophenotypic variations. It is clear, however, that close to the beginning of the
1213 Epivillafranchian, their size and stoutness started to increase, especially in the most arid environments such
1214 as those of Pirro Nord and Apollonia. An even wider variability is present in *Bison* s.s. due to the extremely
1215 widespread geographic distribution of these derived forms. It is true indeed, that if both *Leptobos* and
1216 *Eobison* are mainly (if not exclusively) found between the 45th and 35th parallels, later forms of *Bison* (i.e.,
1217 priscoid group) populated all the Palearctic, from Siberia to the Mediterranean area (Fig. 1a) (Kahlke, 1999).
1218 This wide distribution led to the evolution of several morphotypes adapted to the dominant habitats and
1219 climatic conditions, in a timespan that covers more than 1 Ma. The very slender *B. menneri* and the stouter *B.*
1220 *schoetensacki* were the most common forms in Europe during the Early-Middle Pleistocene boundary (Sala,
1221 1986; Moullé, 1992; Brugal, 1995; Sher, 1997; Sorbelli et al., 2021a). Although characterized by large size
1222 and priscoid characters, they still featured slender built compared with the extremely stout *B. priscus*. As
1223 already pointed out by Sher (1997) and Sorbelli et al. (2021a), the common misconception that *B.*
1224 *schoetensacki* was a small-sized forest-adapted form, is disproved by the records from Le Vallonnet and
1225 Vallparadís Section, which prove that these animals were adapted to a wider spectrum of habitats and very
1226 large body mass, even reaching 1,000 kg (Fig. 11b). The first occurrence of *B. priscus* is still debated.
1227 Between 0.9 and 0.5 Ma, bison with priscoid morphologies started to appear in fossil records such as those
1228 from the Kuznetsk Basin, Tiraspol, and Mosbach, which are, however, still pending a clear taxonomic status
1229 (Freudenberg; 1914; Sher, 1997; Foronova, 2001; Sorbelli et al., 2021a). In the late Middle Pleistocene, giant
1230 and massive forms such as *B. p. gigas* and *B. p. priscus* from Riverenert, Châtillon-Saint-Jean, Romain-La-

Roche, and Taubach, are recorded (body mass reaching 1,600 kg; Fig. 11b) (Mourer-Chauvire, 1972; Flerov, 1977a, 1977b; Vercoutère and Guerin, 2010). Some of these animals, however, were still characterized by relatively elongated metacarpals (Fig. 11a). From the Late Pleistocene on, the body mass and metapodial length of *B. priscus* (often referred to the subspecies *B. p. mediator*; Kahlke, 1999) started to decrease. In agreement with the aforementioned model by Sorbelli et al. (2021a), the slenderer forms of *Bison* s.s. (e.g., the long-legged *B. menneri* from Untermassfeld or the samples of *B. schoetensacki* from Le Vallonnet and Mauer) are found in more humid, heterogeneous habitats (i.e., mosaic of forested and open patches), while the samples of *B. schoetensacki* from more arid sites such as Süssenborn, Durfort, and Vallparadís Section exhibit stouter proportions (Fig. 11a). Similarly, the tallest and slenderest specimens of *B. priscus* are those from Taubach, a site characterized by a fully developed interglacial conditions with warm and forested environment (Kahlke, 1977), whereas the stouter members of this species inhabited open, steppe/prairie-like habitats during the last glacial both in Eurasia and North America (Fig. 11a). The common misconception that the smallest and stoutest forms of *B. priscus* living during MIS 3 and MIS 2 (*B. p. mediator* sensu Flerov, 1979) were typical of forested areas, was already questioned with reason by Sala (1986), Guérin and Valli (2000), and Castaños (2012). These authors emphasized how *B. p. mediator* is always associated with horses and reindeer (e.g., in Kiputz IX), suggesting that the typical habitat of this subspecies was the cold steppe of the last glaciation tundra. Our robusticity analysis confirms this idea, evidencing that *B. p. mediator* was well adapted to open environments thanks to its robust and stout limbs (Fig. 11a). This correlation is maintained also in Pleistocene *Eobison* from the Mediterranean area and in Holocene species. *Bison* (*E.*) *degiulii* from Pietrafitta lived in the surroundings of a humid and wooded habitat (see Section 2) and featured slender metapodials (slightly stouter than those of *L. etruscus*); conversely, members of the same species from Pirro Nord and Apollonia, adapted to drier or rocky environments, bear more robust limbs, similar to those shown by the stouter *B. schoetensacki* (Maniakas and Kostopoulos, 2017; Blain et al., 2019). The extant subspecies *B. bison bison* populates the open grasslands of North America and is characterized by the shortest metacarpals among living bison, whereas the taller and slenderer woodland bison *B. bison athabascae* and European wisent *B. bonasus* prefer sub-hygric and mixed habitats (McDonald, 1982; Stephenson et al., 2001).

These multiple pieces of evidence are furtherly supported by the dietary habits inferred for extinct and extant taxa by Asperen and Kahlke (2017). Based on tooth wear analysis, these authors showed that the extremely tall *Bison* from Taubach and Untermassfeld, as well as *B. b. athabascae* are better defined as browser-mixed feeders, whereas the stouter *Bison* from Süssenborn and extant *B. bonasus* feature more grazer signatures. The North American plain bison *B. b. bison*, namely a species with extremely short metacarpals, shows typical dental wear features of an open habitat grazer.

It has been already remarked by several scholars that the mean size of *Bison*, except for few exceptions, decreased after the last interglacial in the Holarctic region (Vasiliev, 2008; Saarinen et al., 2016; Maniakas and Kostopoulos, 2017). Our body mass estimations computed on a large sample of *Leptobos* and *Bison* confirm this statement, showing a clear trend toward gigantism from *Leptobos* to *Eobison* and to *Bison* s.s. and an opposite trend from the Late Pleistocene on (Fig. 11b). In particular, during the latest Middle Pleistocene (e.g., MIS 6–MIS 5e), the largest forms are recorded (e.g., samples from Châtillon-Saint-Jean, Romain-La-Roche, and Taubach). The main driving factors of increasing body size throughout the Early-Middle Pleistocene, are still matter of debate. Maniakas and Kostopoulos (2017) observed that bison specimens from Joint Mitnor Cave mammal assemblage were significantly smaller than the roughly isochronous ones from Taubach (ca. 0.12 Ma). This apparently contrasts with the Bergmann's rule, which expects a positive correlation between body size and latitude. Meiri et al. (2007) pointed out that in taxa with wide geographical ranges (such as *Bison*), body size can be influenced by a complex array of factors, including not only ecogeographical rules but also - often predominantly - food availability and interspecific competition. During the MIS 5e interglacial, the presence of numerous geothermal springs at Taubach would have favoured the development of a humid dense forest with a large amount of food (Asperen and Kahlke, 2017), while the paleoenvironmental conditions of the British islands would have been harsher. Therefore, the Taubach bison may have reached gigantic size thanks to extremely favourable trophic conditions, while the Joint Mitnor Cave bison may have kept smaller dimensions due to the combination of severe environmental context and geographic isolation. A recent study on *B. priscus* inhabiting the Yukon territory in the last 0.05 Ma demonstrated that they experienced body mass increase and population growth during warmer periods and opposite trends in harsher phases (Abigail et al., 2021). In their comprehensive analysis of *Bison* s.s. records from the Middle-Late Pleistocene of Germany and UK, Saarinen et al. (2016) showed

that populations living in open arid landscapes had smaller body size than those living in wooded humid landscapes. The same pattern was found in other large herbivores such as caballine horses, in which body mass increased in relatively closed, highly productive environments as a result of the combined effect of resource availability, habitat partitioning, inter- and intraspecific competition, and herd density (Asperen et al., 2010; Saarinen et al., 2021).

Our study provides further evidence to support the above inferences. The progressive harshening of climate during the Last Glacial Maximum did not allow the development of very large body size in *Bison*, which in most Late Pleistocene sites (e.g., Roter Berg, Habarra, Gral), are characterized by mean body mass lower than 1,000 kg, in contrast with the considerably heavier weights reached during MIS 5e and previous interglacial stages (e.g., Romain-La-Roche, Taubach) (Fig. 11b). Going further back in time, the Pietrafitta sample fits perfectly into this model. The primitive bison from this locality was characterized by relatively slender limbs but large body on the whole (i.e., slightly heavier than 600 kg; Fig. 11b). Slender limbs and large body size can be related with a warm climate environment rich in forested patches, as suggested by palaeobotanical and paleoherpetological evidence (Martinetto et al., 2014; Sorbelli et al., 2021b). The excellent ecological suitability would have allowed the Pietrafitta bison to develop larger dimensions than, for example, the almost contemporary Venta Micena bison, which lived in a more arid environment and with greater competition in the herbivore guild.

## 6. Conclusions

Pietrafitta (ca. 1.5 Ma) is one of the key sites of the European late late Villafranchian thanks to the extremely rich paleozoological and paleobotanical evidence (Martinetto et al., 2014; Sorbelli et al., 2021b). The abundant large-sized bovid record from Pietrafitta, which was preliminarily believed to represent an advanced form of *Leptobos* (Masini, 1989; Gentili and Masini, 2005), is here referred to *B.* (*E.*) *degiulii* based on a combination of characters found in several skeletal districts (e.g., cranium and metapodials). *Bison* (*E.*) *degiulii* represents one of the earliest representatives of its genus that appeared in Western Palearctic.

The study of the Pietrafitta material triggered the reappraisal of all available records of Villafranchian *Leptobos* and *Bison*, with a focus on the subgenus *Eobison*. Our revision of the taxonomy and variability of this group of early bison has resulted in the emended diagnosis provided in this paper, which has served as a

basis for the summary of comparative characters in Table 7. As far as the available data are concerned, we think that among all the species of *Eobison* described so far, only three can be considered valid, namely *B.* (*E.*) *palaeosinensis*, *B.* (*E.*) *georgicus*, and *B.* (*E.*) *degiulii*. Among these, the best-known species - also thanks to the very rich sample from Pietrafitta - is *B.* (*E.*) *degiulii*, which occurred in Mediterranean Europe during the latest Villafranchian. Additional fossils would be desirable to enrich our knowledge of *B.* (*E.*) *palaeosinensis* and *B.* (*E.*) *georgicus* which, thanks to their older age and geographical distribution, could clarify further aspects on the evolutionary transition between *Leptobos* and *Bison*.

In agreement with previous works, our study also confirms the validity of limb bone dimensions and proportions as (1) reliable taxonomic tools, (2) proxies for the estimation of body mass, and (3) predictors of paleoenvironmental preferences in bovines. Thanks to these data, we suggest that European *Leptobos* and *Bison* responded to the progressive Pleistocene climatic deterioration through changes in limb proportions and average body mass. In particular, the contraction of forested habitats and the spread of open environments under colder and more arid climate, led to an increase in metapodial stoutness and in body size, and to higher hypsodonty associated with grazing-based diet. This trend can be along the transition from *Leptobos* to *Bison*, but also on a smaller scale, within the two groups.

Despite the average tendency to increase in size, a more detailed analysis of the *Bison* s.l. record in the interval 1.8–0.01 Ma (Fig. 11) shows that there have been fluctuations. In our opinion, it is probable that these may be attributable to punctual habitat changes and/or shifts between glacial and interglacial stages, but often the paleoenvironmental data and dating available for the various paleontological sites do not have sufficient resolution to verify this hypothesis. It should not be forgotten that these phenomena of variation in body size and proportions were determined by a complex combination of factors, including ecogeographical patterns (e.g., Cope-Depéret and Bergmann's rules), resource availability, intraspecific competition, and predatory pressure.

**Acknowledgments**

This work is funded by the Agencia Estatal de Investigación European Regional Development Fund of the European Union (CGL2016-76431-P and CGL2017-82654-P, AEI/FEDER-UE) and the Generalitat de Catalunya (CERCA Programme). LS is supported by the FI AGAUR fellowship (ref. 2020 FI_B1 00131)

funded by the Secretaria d'Universitats i Recerca de la Generalitat de Catalunya and the European Social Fund. The present manuscript has been prepared during a Visiting Professor fellowship at the Earth Sciences Department of the University of Florence awarded to JM-M in May–June 2021. The present manuscript is part of the PhD thesis of LS within the Geology PhD program of the Universitat Autonoma de Barcelona. We would like to thank Paola Romi (Soprintendenza Archeologia Belle Arti e Paesaggio dell'Umbria) for the possibility to study the Pietrafitta bovid collection at the MPLB and for her kindness and availability; Elisabetta Cioppi and Luca Bellucci for the possibility to study the Valdarno bovid collections at the IGF; Lorenzo Rook for the possibility to study the Pirro Nord bovid collection at the DST; Maia Bukshianidze for having sent to us the 3D model and pictures of *B.* (*E.*) *georgicus* holotype and for precious information about the Dmanisi bovid; Marco Sami for having sent to us measurements and pictures of the Salita di Oriolo bovid; Michela Contessi for having sent to us pictures of the Mugello bovid; Roman Croitor for having sent to us measurements of some East European *B.* (*B.*) *priscus*; Omar Cirilli for the help in the bibliographic and data collection at the DST; Dawid Adam Iurino for the useful discussions about the methodological approach; Grant Zazula and Elizabeth Hall for having sent to us some comparative *B.* (*B.*) *bison* pictures; and Elpiniki Maria Parparousi, for the digital data elaboration.

## References

Agadzhanyan, A.K., Vislobokova, I.A., Shunkov, M.V. and Ulyanov, V.A., 2017. Pleistocene mammal fauna of the Trlica locality, Montenegro. Fossil Imprint, 73(1–2), 93–114.

Alekseeva, L.I., 1967. To the history of subfamily Bovinae during the Pleistocene in the European USSR. In: Paleontologiya, geologiya i poleznye iskopaemye Moldavii Vyp. 2. Shtiintsa, Kishinev, pp. 123–127 (in Russian).

Ambrosetti, P., Cattuto, C. and Gregori, L., 1989. Geomorfologia e neotettonica nel bacino di Tavernelle/Pietrafitta (Umbria). Il Quaternario, 2, 57–64.

Ambrosetti, P., Argenti, P., Basilici, G., Gentili, S. and Ikome, F.E., 1992. The pleistocenic fossil vertebrata of the Pietrafitta basin (Umbria, Italy): preliminary taphonomic analyses. In Taphonomy: processes and products. European Paleontological Association Workshop, Strasbourg (pp. 20-21).

1369 Ambrosetti, P., Basilici, G., Capasso Barbato, L., Carboni, M.G., Di Stefano, G., Esu, D., Gliozzi, E.,
1370 Petronio, C., Sardella, R. and Squazzini, E., 1995. Il Pleistocene inferiore nel ramo Sud-Occidentale
1371 del Bacino Tiberino (Umbria): aspetti litostratigrafici e biostratigrafici. Il Quaternario, 8(1), 19–36.
1372 Arribas, A. and Palmqvist, P., 1998. Taphonomy and palaeoecology of an assemblage of large mammals:
1373 hyaenid activity in the lower Pleistocene site at Venta Micena (Orce, Guadix-Baza Basin, Granada,
1374 Spain). Geobios, 31, 3–47.
1375 Arzarello, M., Peretto, C. and Moncel, M.H., 2015. The Pirro Nord site (Apricena, Fg, Southern Italy) in the
1376 context of the first European peopling: Convergences and divergences. Quat. Int., 389, 255–263.
1377 Asperen E.N. van, 2010. Ecomorphological adaptations to climate and substrate in late Middle Pleistocene
1378 caballoid horses. Palaeogeogr. Palaeoclimatol. Palaeoecol. 297: 584–596.
1379 Asperen van, E.N., Kahlke, R.D., 2017. Dietary traits of the late early Pleistocene *Bison menneri* (Bovidae,
1380 Mammalia) from its type site Untermassfeld (Central Germany) and the problem of Pleistocene
1381 'wood bison'. Quat. Sci. Rev. 177, 299–313.
1382 Baigusheva, V.S., 2000. New data on Tasmanian faunal assemblage from the excavation site near Semibalki
1383 village (Azov Area). Historical-Archaeological in Azov and Lower Don in 1998, 16, 27–57.
1384 Biewener, A.A., 2005. Biomechanical consequences of scaling. J. Exp. Biol., 208(9), 1665–1676.
1385 Blain, H.A., Fagoaga, A., Ruiz-Sánchez, F.J., Bisbal-Chinesta, J.F. and Delfino, M., 2019. Latest
1386 Villafranchian climate and landscape reconstructions at Pirro Nord (southern Italy). Geology, 47(9),
1387 829–832.
1388 Breda, M., Collinge, S.E., Parfitt, S.A., Lister, A.M., 2010. Metric analysis of ungulate mammals in the early
1389 Middle Pleistocene of Britain, in relation to taxonomy and biostratigraphy: I: Rhinocerotidae and
1390 Bovidae. Quat. Int. 228, 136–156.
1391 Brugal, J.-P., 1995. Le bison (Bovidae, Artiodactyla) du Pléistocène moyen ancien de Durfort (Gard,
1392 France). Bull. Mus. Natl. Hist. Nat. 16C 2–4, 349–381.
1393 Bukhsianidze, M., 2005. The fossil Bovidae of Dmanisi. Ph.D. Dissertation, Università degli Studi di
1394 Ferrara.

1395 Bukhsianidze, M. and Koiava, K., 2018. Synopsis of the terrestrial vertebrate faunas from the Middle Kura
1396 Basin (Eastern Georgia and Western Azerbaijan, South Caucasus). Acta Palaeontol. Pol. 63(3), 441–
1397 461.
1398 Bukhsianidze, M., 2020. New Results on Bovids from the Early Pleistocene site of Untermassfeld. In:
1399 Kahlke, R.D. (Ed.), Das Pleistozänvon Untermaßfeld bei Meiningen (Thüringen). Teil 4. Habelt-
1400 Verlag, Bonn, pp. 1169–1195.
1401 Burchak-Abramovich, N.I., Gadzhiev, D.D., Vekua, A.K., 1980. Concerning ancestral form of bisons from
1402 the Akchagyl of Southern Caucasus. Bull. Georgian Natl. Acad. Sci. 97(2), 48–488 (in Russian).
1403 Burchak-Abramovich, N.I., Gadzhiev, D.V., Vekua, A.K., 1994. On a new Pleistocene Bovine from Eastern
1404 Georgia. Teriologii Paleoteriologija, 253–261 (in Russian).
1405 Caloi, L. and Palombo, M.R., 1995. The early Galerian fauna of Redicicoli. XIV INQUA Congress, Berlin.
1406 Cameron, C.C., Esterle, J.S. and Palmer, C.A., 1989. The geology, botany and chemistry of selected peat-
1407 forming environments from temperate and tropical latitudes. Int. J. Coal. Geol. 12(1–4), 105–156.
1408 Castaños, J., Castaños, P., Murelaga, X. and Alonso-Olazabal, A., 2012. Kiputz IX: un conjunto singular de
1409 bisonte estepario (*Bison priscus* Bojanus, 1827) del Pleistoceno Superior de la Península Ibérica.
1410 Ameghiniana, 49(2), 247–261.
1411 Castelló, J. 2016. Bovids of the World: Antelopes, Gazelles, Cattle, Goats, Sheep, and Relatives. Princeton:
1412 Princeton University Press, 664 p.
1413 Cherin, M., Bizzarri, R., Buratti, N., Caponi, T., Grossi, F., Kotsakis, T., Pandolfi, L., Pazzaglia, F., Barchi,
1414 M.R., 2012. Multidisciplinary study of a new Quaternary mammal-bearing site from Ellera di
1415 Corciano (central Umbria, Italy): preliminary data. Rend. Onl. Soc. Geol. Ital., 21, 1075–1077.
1416 Cherin, M., D'Allestro, V., Masini, F., 2019. New bovid remains from the Early Pleistocene of Umbria
1417 (Italy) and a reappraisal of *Leptobos merlai*. J. Mamm. Evol. 26, 201–224.
1418 Cignoni, P., Callieri, M., Corsini, M., Dellepiane, M., Ganovelli, F. and Ranzuglia, G., 2008. Meshlab: an
1419 open-source mesh processing tool. In Eurographics Italian chapter conference, 2008, pp. 129-136.
1420 Clark, P.U., Archer, D., Pollard, D., Blum, J.D., Rial, J.A., Brovkin, V., Mix, A.C., Pisias, N.G., Roy, M.,
1421 2006. The middle Pleistocene transition: characteristics, mechanisms, and implications for long-term
1422 changes in atmospheric $pCO_2$. Quat. Sci. Rev. 25, 3150–3184.

1423 Coltorti, M., Feraud, G., Marzoli, A., Peretto, C., Ton-That, T., Voinchet, P., Bahain, J.J., Minelli, A.,
1424 Hohenstein, U.T., 2005. New 40Ar/39Ar, stratigraphic and palaeoclimatic data on the Isernia la
1425 Pineta Lower Palaeolithic site, Molise, Italy. Quat. Int. 131, 11–22.
1426 Conti, M.A. and Esu, D., 1981. Considerazioni sul significato paleoclimatico e geodinamico di una serie
1427 lacustre pleistocenica inferiore presso Tavernelle (Perugia, Umbria). Geogr. Fis. Din. Quat., 4, 3–10.
1428 Conti, M.A. and Girotti, O., 1977. Il Villafranchiano nel "Lago Tiberino", ramo sud-occidentale: schema
1429 stratigrafico e tettonico. Geol. Romana, 16, 67–80.
1430 Croitor, R., 2010. Critical remarks on genus *Bison* (Bovidae, Mammalia) from Pleistocene of Moldova.
1431 Revista Archeologica 5, 172–188. (in Russian)
1432 Croitor R., 2016. Genus *Bison* (Bovidae, Mammalia) in Early Pleistocene of Moldova. In: E. Coropceanu
1433 (Ed.), Materialele Conferinţei ştiinţifi ce naţionale cu participare internaţională "Mediul și dezvoltare
1434 durabilă", Ediţia a III-a, Chișinău, pp. 14–20.
1435 Croitor, R. and Popescu, A., 2011. Large-sized ruminants from the Early Pleistocene of Leu (Oltenia,
1436 Romania) with remarks on biogeographical aspects of the" *Pachycrocuta* event". Neues Jahrb. fur
1437 Geol. Palaontol. - Abh., 261(3), 353–371.
1438 David, A.I. and Svistun, V.I., 1981. Bison remains from Upper Pliocene and Lower Pleistocene deposits of
1439 Moldova and South Ukraine.In: Biostratigraphy of Anthropogene and Neogene of South-West of
1440 USSR. Shtiintsa; Kishinev pp. 3–15 (in Russian).
1441 De Giuli, C., 1987. Late Villafranchian faunas in Italy: The Selvella Local Fauna in southern Chiana Valley -
1442 Umbria. Palaeontogr. Ital. 74, 11–50.
1443 De Giuli, C., Masini, F. and Torre, D., 1987. The latest villafranchian faunas in Italy: the Pirro Nord fauna
1444 (Apricena, Gargano). Palaeontogr. Ital. 74, 51–62.
1445 Depéret, C., 1884. Nouvelles études sur les ruminants pliocenes et quaternaires d'Auvergne. Bull. Soc. Geol.
1446 Fr. 22, 247–284
1447 Dong, W., 2008. Nouveau matériel de *Leptobos* (*Smertiobos*) *crassus* (Artiodctyla, Mammalia) du
1448 Pléistocène inférieur à Renzidong (Chine de l'Est). Geobios 41: 355–364.
1449 Dubrovo, I.A., and Burchak-Abramovich, N.I., 1983: A New Pliocene Bovid Genus, *Adjiderebos* gen. nov.,
1450 from Transcaucasia. Dokl. Akad. Nauk SSSR, 276(3), 717–720.

1451 Dubrovo, I.A. and Burchak-Abramovich, N.I., 1986. New data on the evolution of Bovine of the tribe
1452 Bovini. Quartärpaläontologie, 6,13–21.
1453 Duvernois, M.P., 1990. Les *Leptobos* (Mammalia, Artiodactyla) du Villafranchien d'Europe Occidentale.
1454 Doc. lab. géol. Fac. sci. Lyon 113, 1–213.
1455 Duvernois, M.P., 1992. Mise au point sur le genre *Leptobos* (Mammalia, Artiodactyla, Bovidae);
1456 implications biostratigraphiques et phylogénétiques. Geobios 25, 155–166.
1457 Duvernois, M.P., Guérin, C., 1989. Les Bovidae (Mammalia, Artiodactyla) du Villafranchien Supérieur
1458 d'Europe Occidentale. Geobios 22: 339–379.
1459 Etienne, C., Filippo, A., Cornette, R. and Houssaye, A., 2021. Effect of mass and habitat on the shape of
1460 limb long bones: A morpho- functional investigation on Bovidae (Mammalia: Cetartiodactyla). J.
1461 Anat. 238(4), 886–904.
1462 Fabbi S., Romano M., Strani F., Sardella R., Bellucci L. (2021) The Pleistocene vertebrate fauna of the
1463 Oricola-Carsoli intermontane Basin (Latium-Abruzzi, Italy): state of the art and historical review.
1464 Boll. Soc. Pal. Ital. 60: 255–268.
1465 Falconer, H., 1868. Paleontological memoirs and notes, vol. II, I. R. J. Murchison (Ed.), London, 590 p.
1466 Flerov, C.C., 1972. The Most Ancient Bisons and the History of Genus *Bison*. In: Teriologiya, vol 1. Nauka,
1467 Novosibirsk, pp. 81–86 (in Russian).
1468 Flerow, K.K., 1975. Die Bison-reste aus den travertinen von Weimar-ehringsdorf. Abh. Zentr. Geol. Inst. 23,
1469 171–199.
1470 Flerov, K.K., 1977a. Gigantic Bisons of Asia. J. Palaeontol. Soc. India. 20, 77–80.
1471 Flerov, K.K., 1977b. Die fossilen Bisonreste von Taubach und ihre Stellung in der Entwicklungsgeschichte
1472 der Gattung Bison in Europa, In: Kahlke, R.-D. (Ed.), DasPleistozan von Untermaßfeld bei
1473 Meiningen (Thuringen), Teil 1. Quartarpalaontologie 2, pp. 179–208.
1474 Flerov, K.K., 1979. Morphology, systematic, evolution, ecology. In: Sokolov, E.V. (Ed.), European Bison.
1475 Nauka, Moscow, pp. 9–127 (in Russian).
1476 Foronova, I.V., 2001. Quaternary Mammals of the South-East of Western Siberia (Kuznetsk Basin).
1477 Phylogeny, Biostratigraphy, and Paleoecology. A.V. Kanygin (Ed.), Publishing house of SB RAS.
1478 Branch "GEO", 234 p. (in Russian).

1479 Freudenberg, W., 1914. Die saugetiere des alteren Quartas von Mitteleuropa. Geol. Paleont, Abh, 12,
1480 pp.455–670.
1481 Garrido, G., 2008. Primera cita de *Leptobos etruscus* (Falconer, 1868) (Bovidae, Artiodactyla, Mammalia)
1482 en la Península Ibérica (Fonelas P-1, Cuenca de Guadix, Granada). Cuadernos del Museo Geominero
1483 10: 489–516.
1484 Gentili, S., Abbazzi, L., Masini, F., Ambrosetti, P., Argenti, P. and Torre, D. 1996. Voles from the Early
1485 Pleistocene of Pietrafitta (central Italy, Perugia). Acta Zool. Cracov., 3: 185–199.
1486 Gentili, S., Barili, A., Ambrosetti, P., 2000. Un museo per i fossili di Pietrafitta. Nuova Museologia, 2, 16–
1487 17.
1488 Gentili, S., Masini F., 2005. An outline of Italian *Leptobos* and a first sight on *Leptobos* aff. *vallisarni* from
1489 Pietrafitta (early pleistocene, Perugia) Quaternarie Hors Series, 2, 81–89.
1490 Gliozzi, E., Abbazzi, L., Argenti, P., Azzaroli, A., Caloi, L., Barbato, L.C., Di Stefano, G., Esu, D.,
1491 Ficcarelli, G., Girotti, O., Kotsakis, T., 1997. Biochronology of selected mammals, molluscs and
1492 ostracods from the Middle Pliocene to the Late Pleistocene in Italy. The state of the art. Riv. Ital.
1493 Paleontol. Stratigr, 103, 369–388.
1494 Geraads, D., 1992. Phylogenic analysis of the tribe Bovini (Mammalia: Artiodactyla). Zoological Journal of
1495 the Linnean Society 104, 193–207.
1496 Gromov, I.M., Baranova, G.I. (Eds.), 1981. Catalogue of Mammals of the USSR (Pliocene-Recent). Nauka,
1497 Leningrad, 456 p. (in Russian).
1498 Groves, C. and Grubb, P., 2011. Ungulate Taxonomy. The John Hopkins University Press, Baltimore, 309 p.
1499 Guérin, C., 1982. Première biozonation du Pléistocène européen, principal résultat biostratigraphique de
1500 l'étude des Rhinocerotidae (Mammalia, Perissodactyla) du Miocène terminal au Pléistocène
1501 supérieur d'Europe occidentale. Geobios, 15(4), pp.593–598.
1502 Guérin, C. and Valli, A.M., 2000. Le gisement pléistocène supérieur de la grotte de Jaurens à Nespouls,
1503 Corrèze, France: les Bovidae (Mammalia, Artiodactyla). Publications du musée des Confluences,
1504 1(1), 7–39.
1505 Hammer, Ø., Harper, D.A., Ryan, P.D., 2001. PAST: Paleontological statistics software package for
1506 education and data analysis. Paleontol. Electron. 4, 1–9.

1507 Hassanin, A., 2014. Systematic and Evolution of Bovini, in Melletti, M. and Burton, J. (eds), Ecology,
1508 Evolution and Behavior of Wild Cattle: Implications for Conservation. Cambridge University Press,
1509 Cambridge: 7-20.
1510 Head, M.J., Gibbard, P.L., 2005. Early-Middle Pleistocene transitions: an overview and recommendation for
1511 the defining boundary. Geol. Soc. London Special Publications 247, 1–18.
1512 Head, M.J. and Gibbard, P.L., 2015. Early–Middle Pleistocene transitions: linking terrestrial and marine
1513 realms. Quat. Int. 389, 7–46.
1514 Jin, C., Wang, Y., Liu, J., Ge, J., Zhao, B., Liu, J., Zhang, H., Shao, Q., Gao, C., Zhao, K. and Sun, B., 2021.
1515 Late Cenozoic mammalian faunal evolution at the Jinyuan Cave site of Luotuo Hill, Dalian,
1516 Northeast China. Quat. Int. 577,.15–28.
1517 Jungers, W.L., Falsetti, A.B., Wall, C.E., 1995. Shape, relative size, and size-adjustments in morphometrics.
1518 Am. J. Phys. Anthropol. 38, 137–161.
1519 Kahlke, H.-D. (Ed.), 1977. Das Pleistozän von Taubach bei Weimar. Quartärpaläontologie, vol. 2, 1–509 p.
1520 Kahlke, R.D., 1999. The History of the Origin, Evolution and Dispersal of the Late Pleistocene *Mammuthus-*
1521 *Coelodonta* Faunal Complex in Eurasia (large mammals). Fenske Companies, Rapid City (1999),
1522 218 p.
1523 Kelly, A., K., Miller, Joshua, H., DeSantis, L., Wooller, M., Zazula, G., 2021. Niche Stability Through
1524 Environmental Change: A Late Pleistocene Chronology of Bison Priscus Paleoecology from Yukon
1525 Territory, Canada. SVP 2021 Annual Meeting. 2021 Program and Abstract Book, pp. 157.
1526 Khan, M.A., Kostopoulos, D.S., Akhtar, D.S., Nazir, M., 2010. Bison remains from the upper Siwaliks of
1527 Pakistan. N. Jahrb. Geol. Palaontol. Abh. 258, 121–128.
1528 Khan, M.A., Nasim, S., Ikram, T., Ghafoor, A. and Akhtar, M., 2011. Dental remains of early bison from the
1529 Tatrot formation of the upper Siwaliks, Pakistan. J Anim Plant Sci, 21(4), 862–867.
1530 Klein, R.G., Franciscus, R.G., Steele, T.E., 2010. Morphometric identification of bovid metapodials to genus
1531 and implications for taxon-free habitat reconstruction. J. Archaeol. Sci. 37, 389–401.
1532 Konidaris, G.E., Kostopoulos, D.S., Maron, M., Schaller, M., Ehlers, T.A., Aidona, E., Marini, M.,
1533 Tourloukis, V., Muttoni, G., Koufos, G.D. and Harvati, K., 2021. Dating of the Lower Pleistocene

1534 vertebrate site of Tsiotra Vryssi (Mygdonia Basin, Greece): Biochronology, magnetostratigraphy,
1535 and cosmogenic radionuclides. Quat., 4(1), 1.
1536 Kostopoulos, D.S., Maniakas, I., Tsoukala, E., 2018. Early bison remains from Mygdonia Basin (Northern
1537 Greece). Geodiversitas 40, 283–319.
1538 Kottek, M., Grieser, J., Beck, C., Rudolf, B., Rubel, F., 2006. World map of the Köppen-Geiger climate
1539 classification updated. Meteorol. Z., 15, 259–263.
1540 Krijgsman, W., Tesakov, A., Yanina, T., Lazarev, S., Danukalova, G., Van Baak, C.G., Agustí, J., Alçiçek,
1541 M.C., Aliyeva, E., Bista, D. and Bruch, A., 2019. Quaternary time scales for the Pontocaspian
1542 domain: Interbasinal connectivity and faunal evolution. Earth-Sci. Rev. 188, 1–40.
1543 Lydekker, R., 1878. Crania of ruminants from the Indian Tertiaires. Pal. Indica 10 (1), 88–171.
1544 Lopatin, A.V., Vislobokova, I.A., Lavrov, A.V., Startsev, D.B., Gimranov, D.O., Zelenkov, N.V.,
1545 Maschenko, E.N., Sotnikova, M.V., Tarasenko, K.K. and Titov, V.V., 2019. The Taurida Cave, a
1546 new locality of Early Pleistocene vertebrates in Crimea. Dokl. Biol. Sci. 485(1), 40–43.
1547 Lona, F. and Bertoldi, R. 1972. La storia del Plio-Pleistoceno Italiano in alcune sequenze vegetation-ali
1548 lacustri e marine. Atti Accad. Naz. Lincei Cl. Sci. Fis. Mat. Natur. Memorie Serie 8 (11), 1–47.
1549 Madurell-Malapeira, J., Ros-Montoya, S., Espigares, M.P., Alba, D.M., Aurell-Garrido, J., 2014.
1550 Villafranchian large mammals from the Iberian Peninsula: paleobiogeography, paleoecology and
1551 dispersal events. J. Iber. Geol. 40, 167–178.
1552 Maniakas, I., Kostopoulos, D.S., 2017. Morphometric-palaeoecological discrimination between *Bison*
1553 populations of the western Palaearctic. Geobios 50, 155–171.
1554 Martinetto, E., Bertini, A., Basilici, G., Baldanza, A., Bizzarri, R., Cherin, M., Gentili, S., Pontini, M.R.,
1555 2014. The plant record of the Dunarobba and Pietrafitta sites in the Plio-Pleistocene
1556 palaeoenvironmental context of Central Italy. Alp. Mediterr. Quat. 27, 29–72.
1557 Martinetto, E., Momohara, A., Bizzarri, R., Baldanza, A., Delfino, M., Esu, D., Sardella, R., 2017. Late
1558 persistence and deterministic extinction of "humid thermophilous plant taxa of East Asian affinity"
1559 (HUTEA) in southern Europe. Palaeogeogr. Palaeoclimatol. Palaeoecol., 467, 211–231.
1560 Martínez-Navarro, B., Pérez-Claros, J.A., Palombo, M.R., Rook, L., Palmqvist, P., 2007. The Olduvai
1561 buffalo *Pelorovis* and the origin of *Bos*. Quat. Res. 68, 220–226.

1562 Martínez-Navarro, B., Ros-Montoya, S., Espigares, M.P., Palmqvist, P., 2011. Presence of the Asian origin
1563 Bovini, *Hemibos* sp. aff. *Hemibos gracilis* and *Bison* sp., at the early Pleistocene site of Venta
1564 Micena (Orce, Spain). Quat. Int. 243, 54–60.
1565 Masini, F., 1989. I bovini villafranchiani dell'Italia. Ph.D. Dissertation, Università di Modena-Bologna-
1566 Firenze-Roma.
1567 Masini, F., Palombo, M.R., Rozzi, R., 2013. A reappraisal of the Early to Middle Pleistocene Italian
1568 Bovidae. Quat. Int. 288, 45–62.
1569 Maslin, M.A. and Brierley, C.M., 2015. The role of orbital forcing in the Early Middle Pleistocene
1570 Transition. Quat. Int. 389, 47–55.
1571 McDonald, J. N., 1981. North American Bison: their Classification and Evolution. University of California
1572 Press, Berkeley, 316 p.
1573 Mead, J.I., Jin, C., Wei, G., Sun, C., Wang, Y., Swift, S.L. and Zheng, L., 2014. New data on *Leptobos*
1574 *crassus* (Artiodactyla, Bovidae) from Renzidong Cave, Early Pleistocene (Nihewanian) of Anhui,
1575 China, and an overview of the genus. Quat. Int. 354, 139–146.
1576 Meiri, S., Yom- Tov, Y. and Geffen, E., 2007. What determines conformity to Bergmann's rule?. Glob. Ecol.
1577 Biogeogr., 16(6), 788–794.
1578 Merla, G., 1949. I *Leptobos* Rütim. italiani. Palaeontogr. Ital. 46, 41–155.
1579 Moullé, P. É., 1992. Les grands mammifères du Pléistocène inférieur de la grotte du Vallonnet (Roquebrune-
1580 Cap-Martin, Alpes-Maritimes). Étude paléontologique des Carnivores, Équidés, Suidés et Bovidés.
1581 Ph.D. Dissertation, Muséum national d'Histoire naturelle, Paris.
1582 Mourer-Chauviré, C., 1972. Etude de nouveaux restes de vertébrés provenant de la carrière Fournier à
1583 Châtillon-Saint-Jean. III. Artiodactyles, chevaux, oiseaux. Quaternaire 9, 271–305.
1584 Moyà-Solà, S., 1987. Los bóvidos (Artiodactyla, Mammalia) del yacimiento del Pleistoceno inferior de
1585 Venta Micena (Orce, Granada, Espana). Paleontol. Evol. Mem. Esp. 1, 181–236.
1586 Olsen, S.J., 1990. Fossil ancestry of the yak, its cultural significance and domestication in Tibet. Proc. Acad.
1587 Nat. Sci. Philadelphia, pp.73–100.
1588 Palmqvist, P., Espigares, M.P., Pérez-Claros, J.A., Figueirido, B., Guerra-Merchán, A., Ros-Montoya, S.,
1589 Rodríguez-Gómez, G., García-Aguilar, J.M., Granados, A. and Martínez-Navarro, B., 2022. Déjà vu:

1590 a reappraisal of the taphonomy of quarry VM4 of the Early Pleistocene site of Venta Micena (Baza
1591 Basin, SE Spain). Sci. Rep. 12(1), 1–16.
1592 Pazzaglia, F., Barchi, M.R., Buratti, N., Cherin, M., Pandolfi, L. and Ricci, M., 2013. Pleistocene calcareous
1593 tufa from the Ellera basin (Umbria, central Italy) as a key for an integrated paleoenvironmental and
1594 tectonic reconstruction. Quatern. Int., 292, 59–70.
1595 Pilgrim, G.E., 1937. Siwalik antelopes and oxen in the American Museum of Natural History. Bull. Am.
1596 Mus. Nat. Hist. 72, 7.
1597 Pilgrim, G.E., 1939. The fossil Bovidae of India. Mem. Geol. Surv. India, Pal. Indica, n.s. 26 (1), 356 p.
1598 Plummer, T.W., Bishop, L.C., 1994. Hominid paleoecology at Olduvai Gorge, Tanzania as indicated by
1599 antelope remains. J. Hum. Evol. 27, 47–75.
1600 Rodrigo, M.A., 2011. Los Bóvidos Villafranquienses de La Puebla de Valverde y Villarroya: sistemática,
1601 filogenia y paleobiología. Ph.D. Dissertation, Universidad de Zaragoza.
1602 Rook, L. and Martínez-Navarro, B., 2010. Villafranchian: the long story of a Plio-Pleistocene European large
1603 mammal biochronologic unit. Quat. Int. 219(1–2), 134–144.
1604 Rütimeyer, L., 1867. Versuch einer natürlichen Geschichte des Rindes. Neuen Denkschr. Algem. Schweiz.
1605 Ges. Naturwiss. II (Vol. 22).
1606 Saarinen, J., Eronen, J., Fortelius, M., Seppä, H. and Lister, A.M., 2016. Patterns of diet and body mass of
1607 large ungulates from the Pleistocene of Western Europe, and their relation to vegetation. Palaeontol.
1608 Electron. 19(3), 1–58.
1609 Saarinen, J., Cirilli, O., Strani, F., Meshida, K. and Bernor, R.L., 2021. Testing Equid Body Mass Estimate
1610 Equations on Modern Zebras—With Implications to Understanding the Relationship of Body Size,
1611 Diet, and Habitats of Equus in the Pleistocene of Europe. Front. Ecol. Evol. 9, 90.
1612 Sala, B., 1986. *Bison schoetensacki* Freud. from Isernia la Pineta (early Mid-Pleistocene – Italy) and revision
1613 of the European species of bison. Palaeontogr. ital. 74, 113–170.
1614 Schertz, E., 1936. Zur Unterscheidung von *Bison priscus* Boj. und *Bos primigenius* Boj. an Metapodien und
1615 Astragalus, nebst Bemerkungen über einige diluviale Fundstellen. Seckenbergiana 18, 37–71.
1616 Schreuder, A., 1946. The Tegelen fauna, with a description of new remains of its rare components (*Leptobos*,
1617 *Archidiskodon meridionalis*, *Macaca*, *Sus strozzii*). Arch. Neerl. Zool., 7(1), 153–204.

1618 Scott, K.M., 1979. Adaptation and allometry in bovid postcranial proportions. Ph.D. Dissertation. Yale
1619 University, New Haven.
1620 Scott, K.M., 1983. Prediction of body weight of fossil Artiodactyla. Zool. J. Linn. Soc. 77(3), 199–215.
1621 Scott, K.M., 1985. Allometric trends and locomotor adaptations in the Bovidae. Bull. Am. Mus. Nat. Hist.
1622 197, 197–288.
1623 Scott, R.S., Barr, W.A., 2014. Ecomorphology and phylogenetic risk: implications for habitat reconstruction
1624 using fossil bovids. J. Hum. Evol. 73, 47–57.
1625 Shani, M. R. and Khan, E., 1968. *Probison dehmi* n. g. n. sp., a recent find of the Upper Siwalik bovid. Mitt.
1626 Bayer. Staatssamml. Paläontol. Hist. Geol. 8, 247–251.
1627 Sher, A.V., 1997. An Early Quaternary *Bison* population from Untermaßfeld: *Bison menneri* sp. nov. In:
1628 Kahlke, R.D. (Ed.), Das Pleistozänvon Untermaßfeld bei Meiningen (Thüringen). Teil 2. Habelt-
1629 Verlag, Bonn, pp. 101–180.
1630 Simpson, G.G., 1941. Large Pleistocene felines of North America. Am. Mus. Novit. 1136, 1–27.
1631 Skinner, M.R., Kaisen, O.C., 1946. The fossil *Bison* of Alaska and preliminary revision of the genus. Bull.
1632 Am. Mus. Nat. Hist. 89, 123–256.
1633 Sorbelli, L., Alba, D.M., Cherin, M., Moullé, P.É., Brugal, J.P. and Madurell-Malapeira, J., 2021a. A review
1634 on *Bison schoetensacki* and its closest relatives through the early-Middle Pleistocene transition:
1635 Insights from the Vallparadís Section (NE Iberian Peninsula) and other European localities. Quat.
1636 Sci. Rev. 261, 106933.
1637 Sorbelli, L., Villa A., Gentili S., Cherin M., Carnevale, G., Tschopp E., and Delfino, M., 2021b. The Early
1638 Pleistocene ectothermic vertebrates of Pietrafitta (Italy) and the last Western European occurrence of
1639 *Latonia* Meyer, 1843. C. R. Palevol. 20(26), 555–583.
1640 Soubrier, J., Gower, G., Chen, K., Richards, S.M., Llamas, B., Mitchell, K.J., Ho, S.Y., Kosintsev, P., Lee,
1641 M.S., Baryshnikov, G., Bollongino, R., 2016. Early cave art and ancient DNA record the origin of
1642 European bison. Nat. Commun. 7, 13158.
1643 Stephenson, R.O., 2001. Wood bison in late Holocene Alaska and adjacent Canada: paleontological,
1644 archaeological and historical records. In: SC Gerlach and MS Murray (Eds), Wildlife and People in

Northern North America. Essays in Honor of R. Dale Guthrie. British Archaeological Reports, International Series, pp. 944.

Teilhard de Chardin, P., Piveteau, J., 1930. Les mammifères fossiles de Nihowan (Chine). Ann. Paleontol. 19, 1–134.

Teilhard de Chardin, P. and Trassaert, M., 1938. Caviconia of South-Eastern Shansi. Pal. Sin. New Ser. C, 6, 1–106.

Tong, H.W., Chen, X., Zhang, B., 2016. New fossils of *Bison palaeosinensis* (Artiodactyla, Mammalia) from the steppe mammoth site of early Pleistocene in Nihewan Basin, China. Quat. Int. 445, 450–468.

Toniato, G., Marabini, S., Sala, B. and Vai, G.B., 2017. Revised bison skull from the Salita di Oriolo quarry near Faenza, "sabbie gialle", Pleistocene, Northern Apennines. Alp. Mediterr. Quat. 30(1), 11–23.

Torre, D., Ficcarelli, G., Masini, F., Rook, L. and Sala, B., 1992. Mammal dispersal events in the early Pleistocene of Western Europe. Cour. Forsch. Inst. Senckenberg, 153, 51–58.

Vasiliev, S.K., 2008. Late Pleistocene bison (*Bison p. priscus* Bojanus, 1827) from the southeastern part of western Siberia. Archaeol. Ethnol. Anthropol. Eurasia 34, 34–56.

Vercoutère, C. and Guérin, C., 2010. les Bovidae (Mammalia, Artiodactyla) du Pléistocène moyen final de l'Aven de Romain-La-Roche (Doubs, france). Rev. de Paleobiologie 9, 655–696.

Verestchagin, N.K., 1959. The Mammals of the Caucasus. A History of the Fauna. Academia Nauk, Leningrad (translated from Russian; Israel Program for Scientific Translations, Jerusalem 1967).

Viret, J., 1949. La vie dans la moyenne vallée du Rhône au début des temps quaternaires (Essai d'écologie de la faune des mammifères fossiles de Saint-Vallier). Bull. Mens. Soc. Linn. Lyon 18, 20–24

Viret, J., 1954. Le loess à banc durcis de Saint-Vallier (Drôme) et sa faune de mammifères villafranchiens. Avec une analyse granulométrique. Nouv. Arch. Mus. Hist. Nat. Lyon 4, 1–200.

Zheng, S.H., Wu, W.Y., Li, Y., Wang, G.D., 1985. Late Cenozoic mammalian faunas of Guide and Gonghe Basins, Qinghai Province. Vert. PalAs. 23, 89–134 (in Chinese).

Zucchetta, G., Gentili, S. and Pavia, M., 2003.: A new early Pleistocene bird association from Pietrafitta (Perugia, Central Italy). Riv. Ital. Paleontol. S., 109, 527–538.

**Figures Captions**

**Fig. 1** a, Major Eurasian sites with the occurrence of primitive *Bison*: 1, Venta Micena (Spain); 2, Sainzelles (France); 3, Maar du Riege (France); 4, Salita di Oriolo (Italy); 5, Central Italy (Upper Valdarno, Pietrafitta, Capena); 6, Pirro Nord (Italy); 7, Trlica (Montenegro); 8, Mygdonia Basin (Greece); 9, Taurida Cave (Ukraine); 10, Dmanisi (Georgia); 11, Kushkuna (Azerbaijan); 12, Upper Siwaliks (Pakistan); 13, North-West China (Bajjazui, Huiduipo, Zhangjiapo, Yangguo, Genjiagou, Gonghe); 14, South Shanxi area (Yushe, Linyi, Pinglu, Mianchi; China); 15, Nihewan Basin area (Jiajiashan, Chifeng, Xiashagou, Shanshenmiaozui, Cenjiawan; China). Shaded blue area: putative geographic distribution of *B. priscus* during the Pleistocene (taken from Kahlke, 1999). b, Time scale showing the chronological/biochronological distribution of the studied taxa in Europe and the most important Plio-Pleistocene sites of Europe and Western Asia mentioned in the text. Abbreviations: Ma, mega annum; GC, geochronology; ELMA, European Land Mammal Age; C, glacial/interglacial cyclicity; MS, magnetostratigraphy.

**Fig. 2** Cranial remains of *Bison* (*Eobison*) *degiulii* from Pietrafitta. a, Cranium SABAP UMB 19. 2.1178 in dorsal view; b Cranium SABAP UMB 19. 2.1179 in posterior (b1) and ventral (b2) views; c, Atlas SABAP UMB 21. 4.1314 in anterior (c1), posterior (c2), dorsal (c3), and ventral (c4) views; d, Occipital and basioccipital fragments SABAP UMB 21. 4.1177 in posterior (d1) and ventral (d2) views; e, Occipital and basioccipital fragments SABAP UMB 19. 2.1179 in posterior (e1) and ventral (e2) views. Scale bar: 100 mm.

**Fig. 3** Cranial remains of *Bison* (*Eobison*) *degiulii* from Pietrafitta. a, Basioccipital SABAP UMB 20. 1.6802/4 in ventral (a1) and lateral (a2) views; b, Basioccipital SABAP UMB 20. 1.6803/2 in ventral (b1) and lateral (b2) views; c, Horn-core tip SABAP UMB 21. 4.1323; d, Left horn-core SABAP UMB 19. 2.1179/1 in posterior (d1), dorsal (d2), and ventral (d3) views; e, Left horn-core SABAP UMB 21. 4.1179 in posteroventral view; f, Nasal fragments SABAP UMB 20. 1.6802/3 in dorsal view; g, Right horn-core SABAP UMB 19. 2.1179/2 in anterior view; h, Right premaxilla SABAP_UMB 20.1.6802/2 in lateral view; i, Left horn-core SABAP UMB 20. 1.6803/1 in posterior view; j, Left horn-core SABAP UMB 20. 1.6802/5 in anterior view; k, Right (?) horn-core tip SABAP_UMB 20.1.7345 in posterior (k1) and dorsal (k2) views. Scale bar: 50 mm.

**Fig. 4** Dentognathic remains of *Bison* (*Eobison*) *degiulii* from Pietrafitta. a, Right M3 SABAP UMB 20. 1.7346/1 in occlusal (a1), labial (a2), and lingual (a3) views; b, Right M3 SABAP UMB 20. 1.6804/2 in occlusal view; c, Right M2 SABAP UMB 20. 1.7348 in occlusal (c1) and labial (c2) views; d, Right M2 SABAP UMB 21. 4.1325 in occlusal view; e, Left M1 SABAP UMB 20. 1.6804/5 in occlusal (e1) and lingual (e2) views; f, Right M1 SABAP UMB 20. 1.7350 in occlusal view; g, Right P4 SABAP UMB 21 .4.1230 in occlusal (g1) and labial (g2) views; h, Right P4 SABAP UMB 20. 1.6804/7 in occlusal view; i, Left P3 SABAP UMB 20. 1.6802/14 in occlusal (i1) and labial (i2) views; j, Left P2 SABAP UMB 20. 1.7361 in occlusal (j1) and labial (j2) views; k, Right m3 SABAP UMB 20. 1.1227 in occlusal (k1), labial (k2), and lingual (k3) views; l, Left m2 SABAP UMB 20. 1.7365 in occlusal (l1) and labial (l2) views; m, Left m1 SABAP UMB 20. 1.1228 in occlusal (m1) and labial (m2) views; n, Right hemimandible with p4-m1 SABAP UMB 21. 4.1235 in occlusal (n1) and lingual (n2) views; o, Right hemimandible with p2-p4 SABAP UMB 21. 4.1236 in labial (o1) and occlusal (o2) views; p, Fragment of right mandibular ramus SABAP UMB 21. 4.1298 in lateral view; q, Right hemimandible with p2-m3 SABAP UMB 130074 in occlusal (q1) and lingual (q2) views; r, Right hemimandible with p2-m3 SABAP UMB 20. 1.7341 in occlusal (r1) and labial (r2) views; s, Left hemimandible with p2-m3 SABAP UMB 20. 1.7342 in occlusal (s1) and labial (s2) views. Scale bars: 30 mm (top) and 50 mm (bottom).

**Fig. 5** Metapodials of *Bison* (*Eobison*) *degiulii* from Pietrafitta. a, Left metacarpal SABAP UMB 20. 1.7325 in anterior (a1) and proximal (a2) views; b, Right metacarpal SABAP UMB 130038 in anterior (b1) and proximal (b2) views; c, Right metacarpal SABAP UMB 22. 4.247/8 in anterior (c1) and proximal (c2) views; d, Left metacarpal SABAP UMB 20. 1.7324 in anterior (d1) and proximal (d2) views; e, Right metatarsal SABAP UMB 20. 1.7330 in anterior (e1) and proximal (e2) views; f, Right metatarsal SABAP UMB 20. 1.7331 in anterior (f1) and proximal (f2) views; g, Left metatarsal in anterior (g1) and proximal (g2) views; h, Right metatarsal SABAP_UMB 20.1.7332 in anterior (h1) and proximal (h2) views. Scale bars: 50 mm.

**Fig. 6** Horn-core morphology in several species of *Leptobos* and *Bison* s.l. a, Biplot of the horn-core section at the base. Measurement abbreviations are explained in Table S2 and shown in Fig. S1. Measurements are in mm. b, Diagram of the angle between the sagittal axis of the cranium and the horn-core midline.

**Fig. 7** Biometric comparisons of cranial and dental variables in several species of *Leptobos* and *Bison* s.l. a, Biplot of the intertemporal bridge shape. b, Biplot of the frontal shape. Measurement abbreviations are

explained in Table S2 and shown in Fig. S1. Measurements are in mm. c, $Log_{10}$ ratio of upper molars and third lower molar; d, Principal component analysis of six selected variables of the occipital and basioccipital areas.

**Fig. 8** Bivariate plots of postcranial stoutness in several species of *Leptobos* and *Bison* s.l. a, Metacarpals; b, Metatarsals; c, Radii; d, Astragali. Measurement abbreviations are explained in Table S2 and shown in Fig. S1. Measurements of Lmax are in mm.

**Fig. 9** Comparisons of limb bone dimensions and proportions in several species of *Leptobos* and *Bison* s.l. a–b, Bivariate plots of the first two principal component (PC) scores resulting from PCA of metacarpals (a) and metatarsals (b), based on seven selected variables presented in Table 1; c, Histogram representing the ratio between the lengths of metacarpal (MC), radius (RAD), and metatarsal (MT).

**Fig. 10** Morphological comparison between *Bison* (*Eobison*) specimens from the Mediterranean area, studied in this work. a, *B.* (*E.*) *degiulii* from Pietrafitta, SABAP UMB 19. 2.1178 in dorsal view; b, *B.* (*E.*) *degiulii* from Pietrafitta, SABAP UMB 21. 4.1177 in posterior view; *B.* (*E.*) *degiulii* from Pietrafitta, SABAP UMB 19. 2.1179 in posterior (c1) and ventral (c2) views; d, *B.* (*E.*) cf. *degiulii* from Capena, MUST (ex MPUR) s.n., in dorsal (d1), posterior (d2), and ventral (d3) views; e, *B.* (*E.*) cf. *degiulii* from Salita di Oriolo, MCSNF s.n., in dorsal (e1), posterior (e2), right lateral (e3), and ventral (e4) views; f, *B.* (*E.*) *degiulii* holotype from Pirro Nord, IGPB s.n.., in dorsal (f1), posterior (f2), right lateral (f3), and ventral (f4) views; g, *B.* (*E.*) *degiulii* from Kalamoto-2, NHCK KLT-638, in dorsal (g1), posterior (g2), left lateral (g3), and ventral (g4) views; f, *B.* (*Eobison*) sp. from Mugello, MGCB s.n., in anterior (h1) and dorsal (h2) views. Scale bar: 100 mm.

**Fig. 11** Evolutionary trends in *Leptobos* and *Bison* over the last 3 Ma. a, Stoutness violinplot of metacarpals; b, Body mass estimation violinplot. The numbers at the base of the plots indicate the number of specimens for each sample. At the bottom, the age of the samples is shown on a chronological and paleoclimatological diagram of LR04 Benthic Stack (from Lisiecki and Raymo, 2005); each paleontological locality is associated with the predominant paleoenvironment in Western Palearctic in the considered time span. European Land Mammal Ages are indicated at the bottom. Abbreviations: Ta, Taubach; CSJ, Chatillon St. Jean; RLR, Romain-la-Roche; JMCMA, Joint Mitnor Cave Mammal Assemblage sites; Ha, Habarra; Gr, Gral; CF, Cava Filo; Si, Sirejol; RB, Roter Berg.

**Fig. 12** Comparisons of Bovinae considered in this review. a, Life reconstructions of *Leptobos* and *Bison* species from the late Pliocene (left) to Late Pleistocene (right). From left to right: *Leptobos* gr. LSEM, *Leptobos* gr. LEV, *Bison* (*Eobison*) *degiulii*., *Bison* (*Poephagus*) *menneri*, *Bison* (*Bison*) *schoetensacki*, *Bison* (*Bison*) *priscus*. b–o, Morphological comparison between craniums of several species of Bovinae mentioned in this work: b, *L. stenometopon* from Dusino in dorsal (b1) and posterior (b2) views; c, *L. merlai* from St. Vallier in dorsal (c1) and posterior (c2) views; d, *A. cantabilis* from Kushkuna in dorsal (d1) and posterior (d2) views; e, *L. etruscus* from Upper Valdarno in dorsal (e1) and posterior (e2) views; f, *L. vallisarni* Le Fratte (Upper Valdarno) in dorsal (f1) and posterior (f2) views; g, *B.* (*E.*) *palaeosinensis* from Nihowan in dorsal (g1) and posterior (g2) views; h, *B.* (*E.*) *georgicus* from Dmanisi in dorsal (h1) and posterior (h2) views; i, *B.* (*E.*) *degiulii* from Pietrafitta in dorsal view; j, *B.* (*E.*) *degiulii* from Pirro Nord in dorsal (j1) and posterior (j2) views; k, *B.* (*E.*) *degiulii* from Kalamoto-2 in dorsal (k1) and posterior (k2) views; l, *B.* (*P.*) *menneri* from Untermassfeld in dorsal (l1) and posterior (l2) views; m, *B.* (*B.*) *schoetensacki* from Mauer in dorsal (m1) and posterior (m2) views; n, *B.* (*B.*) *priscus* from Po River in dorsal (n1) and posterior (n2) views; o, *B.* (*B.*) *bonasus* from Białowieża in dorsal (o1) and posterior (o2) views. Specimens not in scale. Artworks by LS.

Figure 1


1
2
3
4
5
6
7
8
9
10
11
12
13
14
15
60°N
45°N
30°N
a

b

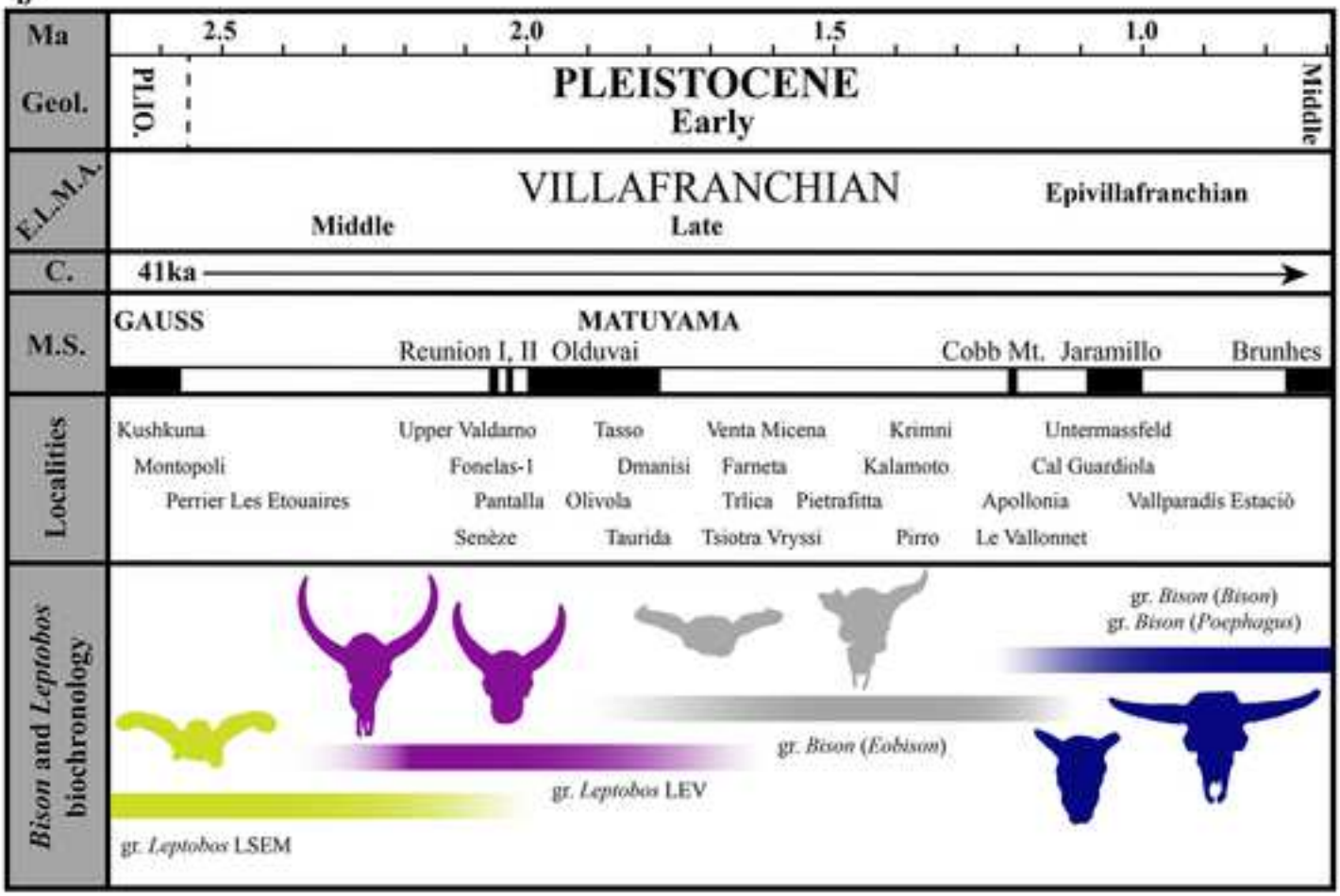
Ma
2.5
2.0
1.5
1.0
Geol.
PLIO.
PLEISTOCENE
Early
Middle
E.L.M.A.
VILLAFRANCHIAN
Middle
Late
Epivillafranchian
C.
41ka
M.S.
GAUSS
MATUYAMA
Reunion I, II
Olduvai
Cobb Mt.
Jaramillo
Brunhes
Localities
Kushkuna
Montopoli
Perrier Les Etouaires
Upper Valdarno
Fonelas-1
Pantalla
Senèze
Tasso
Dmanisi
Olivola
Taurida
Venta Micena
Farneta
Trlica
Tsiotra Vryssi
Krimni
Kalamoto
Pietrafitta
Pirro
Untermassfeld
Cal Guardiola
Apollonia
Le Vallonnet
Vallparadis Estaciò
Bison and Leptobos biochronology
gr. Bison (Bison)
gr. Bison (Poephagus)
gr. Bison (Eobison)
gr. Leptobos LEV
gr. Leptobos LSEM

Figure 2

Figure 4


a1
a2
c1
e2
e1
g1
h
i1
j1
g2
i2
j2
a3
b
d
f
e2
o1
o2
k1
l1
m1
n1
n2
k2
k3
l2
m2
q1
p
q2
r1
r2
s2
s1

Figure 3

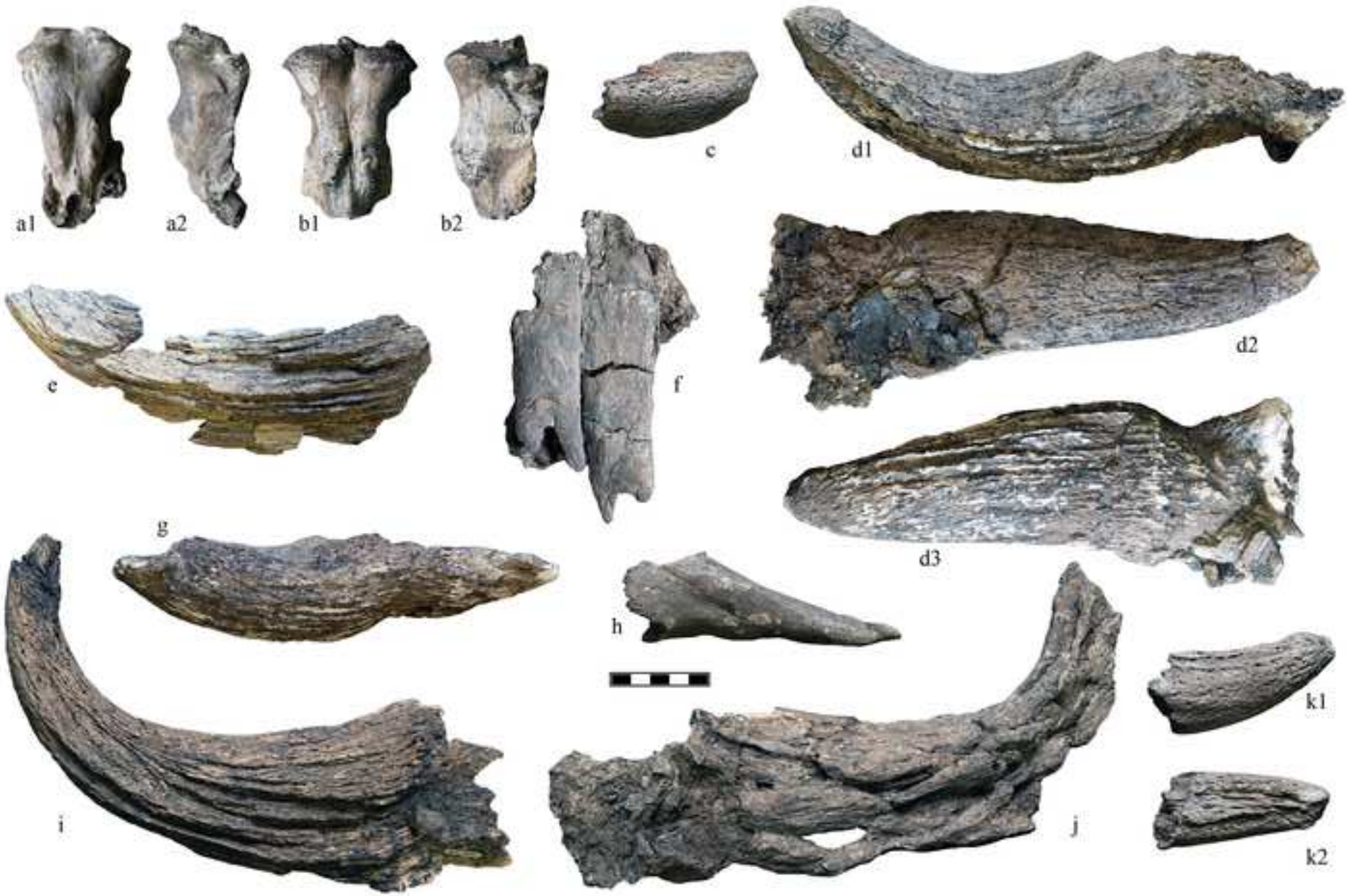

Figure 5

Figure 6

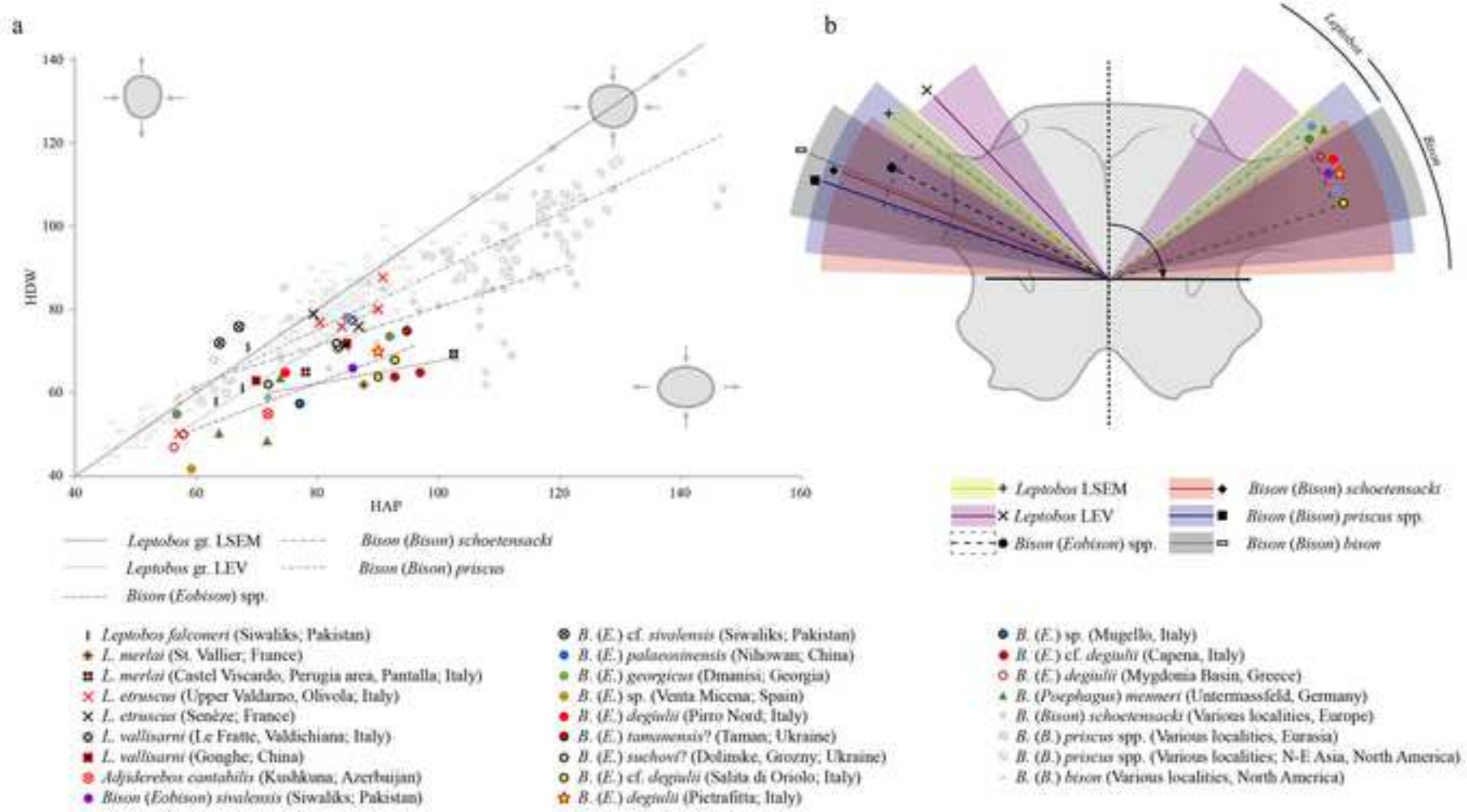
a
b
HDW
HAP
Leptobos
Bison
Leptobos gr. LSEM
Leptobos gr. LEV
Bison (Eobison) spp.
Bison (Bison) schoetensacki
Bison (Bison) priscus
Leptobos falconeri (Siwaliks; Pakistan)
L. merlai (St. Vallier; France)
L. merlai (Castel Viscardo, Perugia area, Pantalla; Italy)
L. etruscus (Upper Valdarno, Olivola; Italy)
L. etruscus (Senèze; France)
L. vallisarni (Le Fratte, Valdichiana; Italy)
L. vallisarni (Gonghe; China)
Adjidaumo cantabilis (Kushkuna; Azerbaijan)
Bison (Eobison) sivalensis (Siwaliks; Pakistan)
B. (E.) cf. sivalensis (Siwaliks; Pakistan)
B. (E.) palaeosinensis (Nihowan; China)
B. (E.) georgicus (Dmanisi; Georgia)
B. (E.) sp. (Venta Micena; Spain)
B. (E.) degiulii (Pirro Nord; Italy)
B. (E.) tamanensis? (Taman; Ukraine)
B. (E.) suchovi? (Dolinske, Grozny; Ukraine)
B. (E.) cf. degiulii (Salita di Oriolo; Italy)
B. (E.) degiulii (Pietrafitta; Italy)
B. (E.) sp. (Mugello, Italy)
B. (E.) cf. degiulii (Capena, Italy)
B. (E.) degiulii (Mygdonia Basin, Greece)
B. (Poephagus) menneri (Untermassfeld, Germany)
B. (Bison) schoetensacki (Various localities, Europe)
B. (B.) priscus spp. (Various localities, Eurasia)
B. (B.) priscus spp. (Various localities; N-E Asia, North America)
B. (B.) bison (Various localities, North America)

Figure 7

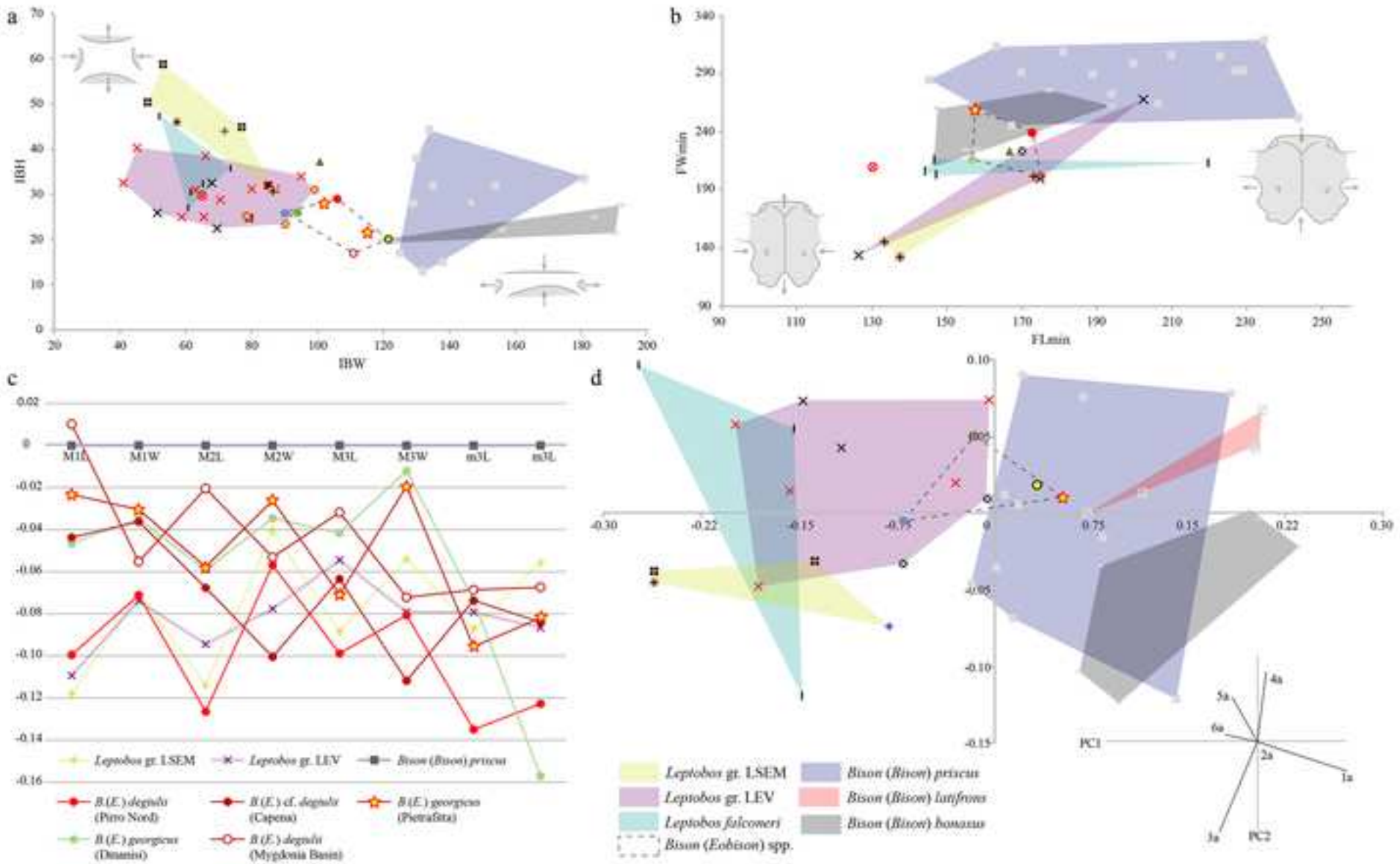


- *Leptobos falconeri* (Siwaliks; Pakistan)
- *L. merlai* (St. Vallier; France)
- *L. merlai* (Castel Viscardo, Perugia area, Pantalla; Italy)
- *L. etruscus* (Upper Valdarno, Olivola; Italy)
- *L. etruscus* (Senèze; France)
- *L. vallisarni* (Le Fratte, Valdichiana; Italy)
- *L. vallisarni* (Gonghe; China)
- *Adjiderebos cantabilis* (Kushkuna; Azerbaijan)
- *Bison* (*Eobison*) *palaeosinensis* (Nihowan; China)
- *B.* (*E.*) *georgicus* (Dmanisi; Georgia)
- *B.* (*E.*) *degiulii* (Pitro Nord; Italy)
- *B.* (*E.*) cf. *degiulii* (Salita di Oriolo; Italy)
- *B.* (*E.*) *degiulii* (Pietrafitta; Italy)
- *B.* (*E.*) cf. *degiulii* (Capena, Italy)
- *B.* (*E.*) *degiulii* (Mygdonia Basin, Greece)
- *B.* (*Poephagus*) *menneri* (Untermassfeld, Germany)
- *B.* (*Bison*) *schoetensacki* (Various localities, Europe)
- *B.* (*B.*) *priscus* spp. (Various localities, Eurasia)
- *B.* (*B.*) *priscus* spp. (Various localities; N-E Asia, North America)
- *B.* (*B.*) *latifrons* (Various localities, North America)
- *B.* (*B.*) *bison* (Various localities, North America)
- *B.* (*B.*) *bonasus* (Bialowieża, Polonia)

Figure 8

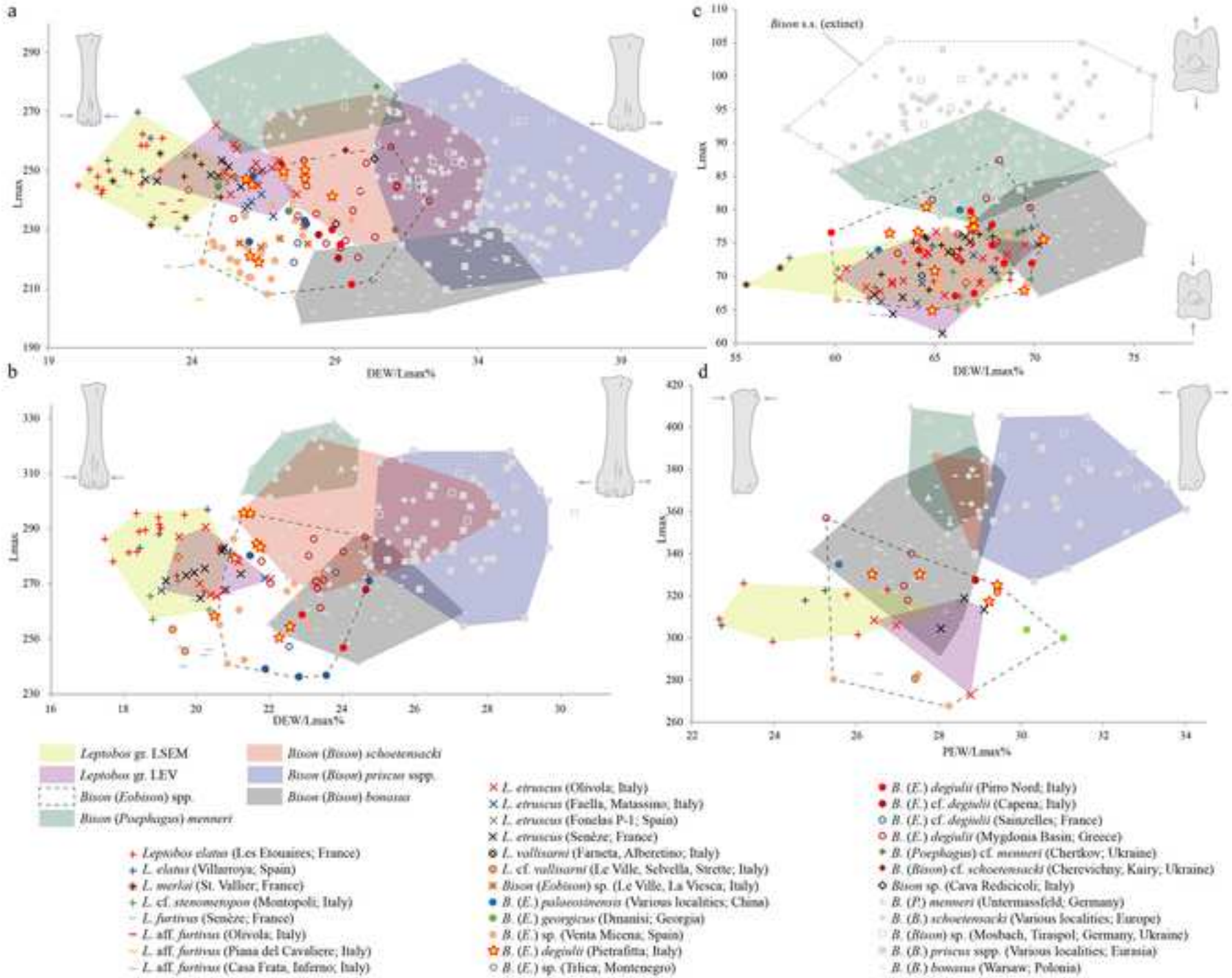
a
b
c
d
Lmax
DEW/Lmax%
PEW/Lmax%
Bison s.s. (extinct)
Leptobos gr. LSEM
Leptobos gr. LEV
Bison (Eobison) spp.
Bison (Poephagus) mennerti
Bison (Bison) schoetensacki
Bison (Bison) priscus ssgp.
Bison (Bison) bonasus
+ Leptobos elatus (Les Etouaires; France)
+ L. elatus (Villarroya; Spain)
+ L. merlai (St. Vallier; France)
+ L. cf. stenomenyxon (Montopoli; Italy)
– L. fortivus (Senèze; France)
– L. aff. fortivus (Olivola; Italy)
– L. aff. fortivus (Piana del Cavaliere; Italy)
– L. aff. fortivus (Casa Frata, Inferno; Italy)
× L. etruscus (Olivola; Italy)
× L. etruscus (Faella, Matassino; Italy)
× L. etruscus (Fonelas P-1; Spain)
× L. etruscus (Senèze; France)
L. vallisarni (Farneta, Alberetino; Italy)
L. cf. vallisarni (Le Ville, Selvella, Strette; Italy)
Bison (Eobison) sp. (Le Ville, La Viesca; Italy)
B. (E.) palaeosinensis (Various localities; China)
B. (E.) georgicus (Dmanisi; Georgia)
B. (E.) sp. (Venta Micena; Spain)
B. (E.) degiulii (Pietrafitta; Italy)
B. (E.) sp. (Tilica, Montenegro)
B. (E.) degiulii (Pirro Nord; Italy)
B. (E.) cf. degiulii (Capena; Italy)
B. (E.) cf. degiulii (Saintzelles; France)
B. (E.) degiulii (Mygdonia Basin; Greece)
B. (Poephagus) cf. mennerti (Chertkov; Ukraine)
B. (Bison) cf. schoetensacki (Cherevichny; Kairy, Ukraine)
Bison sp. (Cava Redicicoli; Italy)
B. (P.) mennerti (Untermassfeld; Germany)
B. (B.) schoetensacki (Various localities; Europe)
B. (Bison) sp. (Mosbach, Tiraspol; Germany, Ukraine)
B. (B.) priscus ssgp. (Various localities; Eurasia)
B. (B.) bonasus (Warsaw; Polonia)

Figure 9

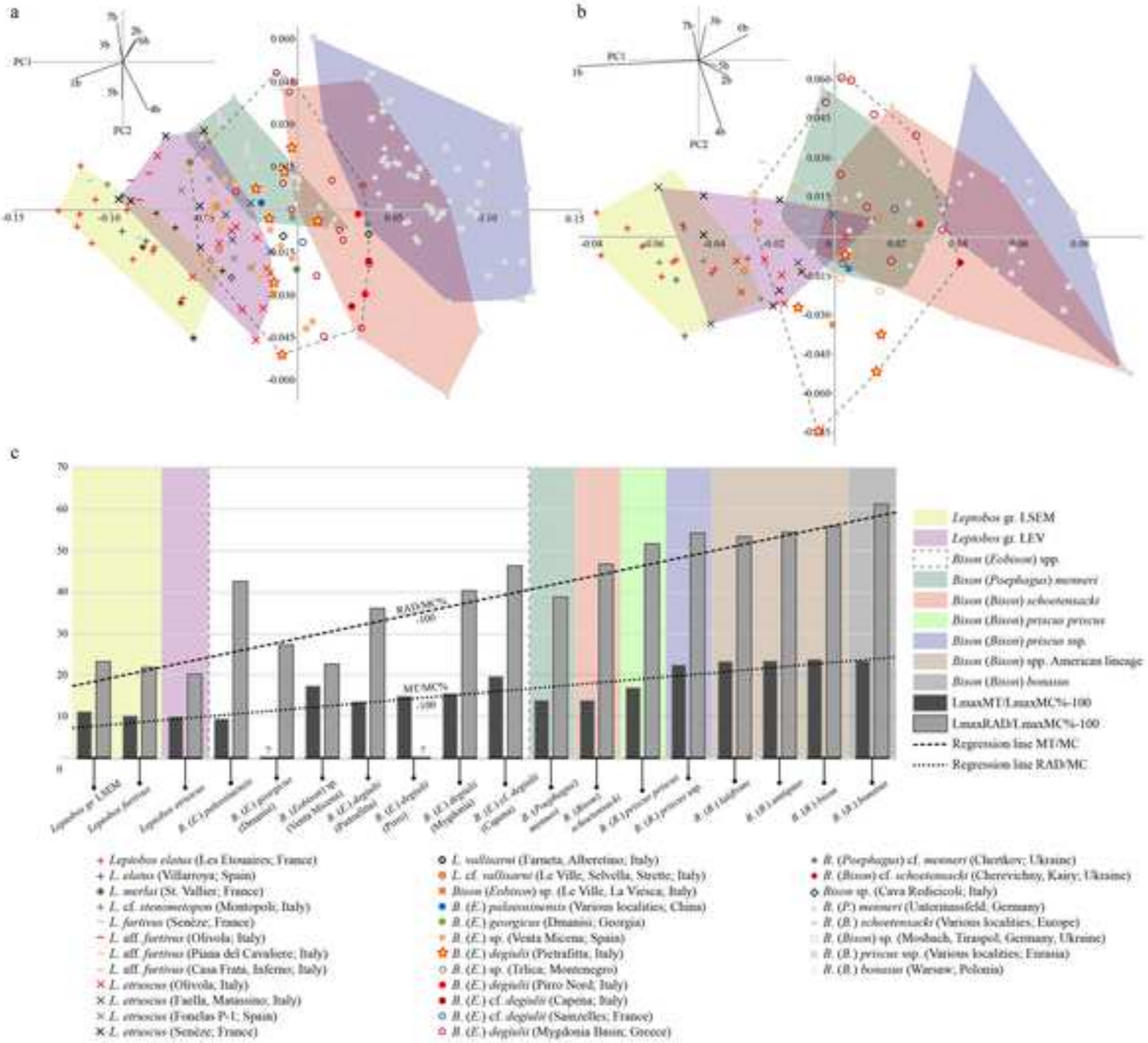
a
b
c
PC1
PC2
RAD/MC%
-100
MT/MC%
-100
Lmax MT/Lmax MC%-100
Lmax RAD/Lmax MC%-100
Regression line MT/MC
Regression line RAD/MC
Lepidobos gr. LSEM
Lepidobos gr. LEV
Bison (Eobison) spp.
Bison (Poephagus) menneri
Bison (Bison) schoetensacki
Bison (Bison) priscus priscus
Bison (Bison) priscus ssp.
Bison (Bison) spp. American lineage
Bison (Bison) bonasus
L. elatus (Les Etouaires; France)
L. elatus (Villarroya; Spain)
L. meridionalis (St. Vallier; France)
L. cf. stenometopon (Montopoli; Italy)
L. fortivus (Senèze; France)
L. aff. fortivus (Olivola; Italy)
L. aff. fortivus (Piana del Cavaliere; Italy)
L. aff. fortivus (Casa Frati, Inferno; Italy)
L. etruscus (Olivola; Italy)
L. etruscus (Faella, Matassino; Italy)
L. etruscus (Fontalas P-1; Spain)
L. etruscus (Senèze; France)
L. vallisarni (Tarneta, Alberetino; Italy)
L. cf. vallisarni (Le Ville, Selvella, Stretto; Italy)
Bison (Eobison) sp. (Le Ville, La Vecica; Italy)
B. (E.) palaeosinensis (Various localities; China)
B. (E.) georgicus (Dmanisi; Georgia)
B. (E.) sp. (Venta Micena; Spain)
B. (E.) degiulii (Pietrafitta; Italy)
B. (E.) sp. (Trlica; Montenegro)
B. (E.) degiulii (Pirro Nord; Italy)
B. (E.) cf. degiulii (Capena; Italy)
B. (E.) cf. degiulii (Saint-Prest; France)
B. (E.) degiulii (Mygdonia Basin; Greece)
B. (Poephagus) cf. menneri (Chertkov; Ukraine)
B. (Bison) cf. schoetensacki (Cherevichny, Kairy; Ukraine)
Bison sp. (Cava Rodicicoli; Italy)
B. (P.) menneri (Untermassfeld, Germany)
B. (B.) schoetensacki (Various localities; Europe)
B. (Bison) sp. (Mosbach, Tiraspol, Germany, Ukraine)
B. (B.) priscus ssp. (Various localities; Eurasia)
B. (B.) bonasus (Warsaw; Polonia)

Figure 10

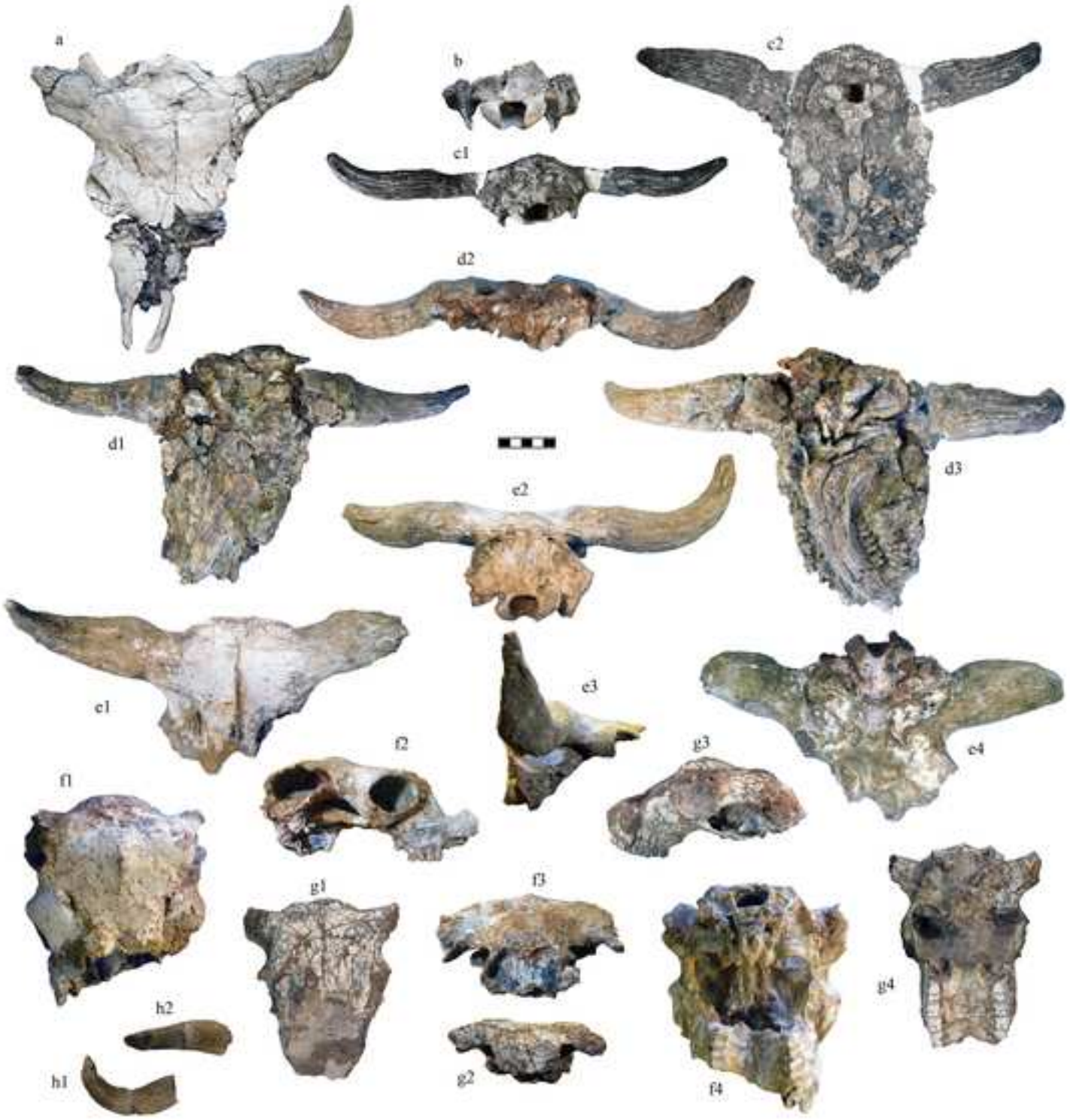

Figure 11

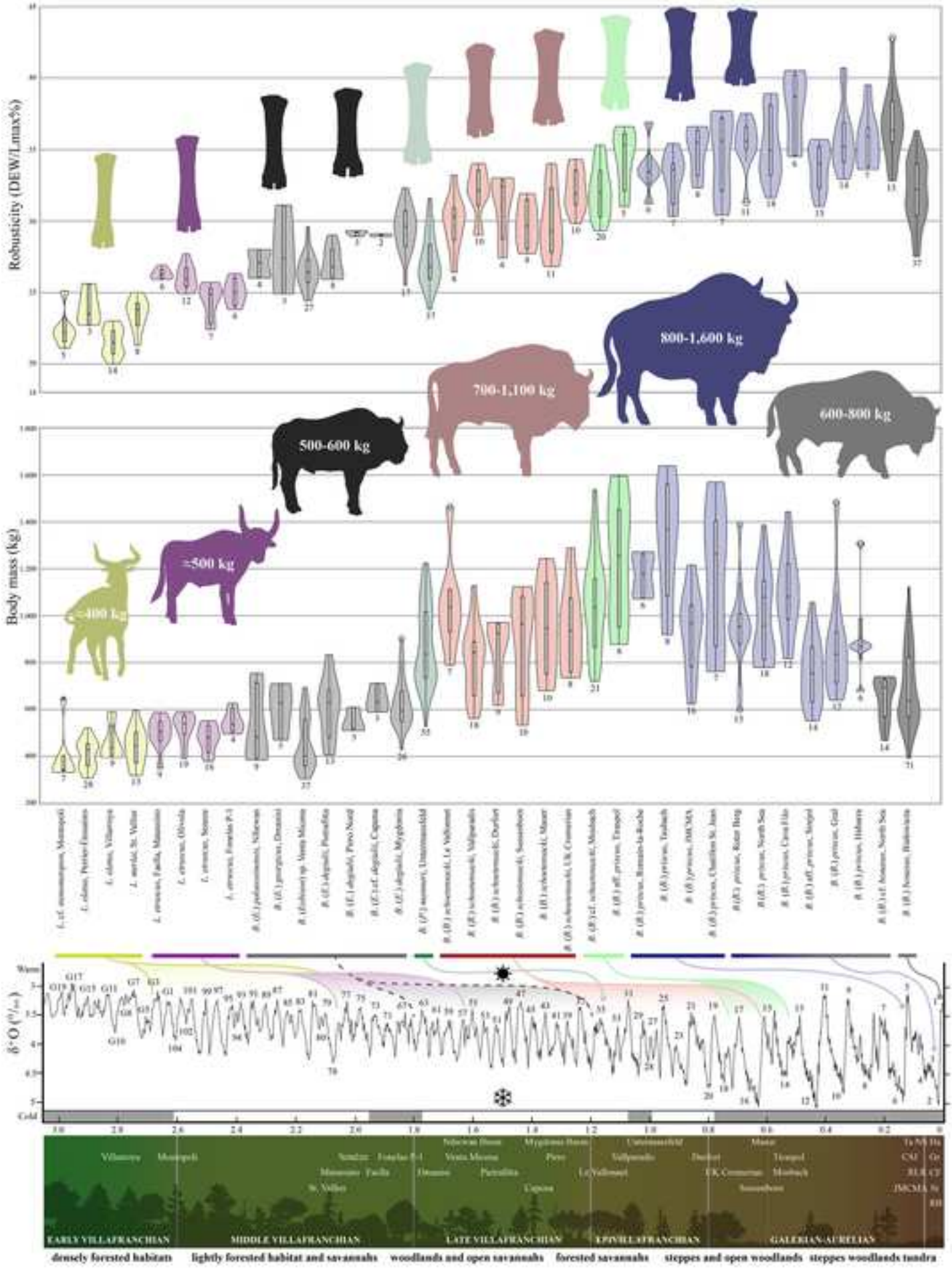
Robusticity (DEW/Lmax%)
Body mass (kg)
≈400 kg
≈500 kg
500-600 kg
700-1,100 kg
800-1,600 kg
600-800 kg
δ18O (‰)
Warm
Cold
EARLY VILLAFRANCHIAN
MIDDLE VILLAFRANCHIAN
LATE VILLAFRANCHIAN
EPIVILLAFRANCHIAN
GALERIAN-AURELIAN
densely forested habitats
lightly forested habitat and savannahs
woodlands and open savannahs
forested savannahs
steppes and open woodlands
steppes woodlands tundra

Figure 12

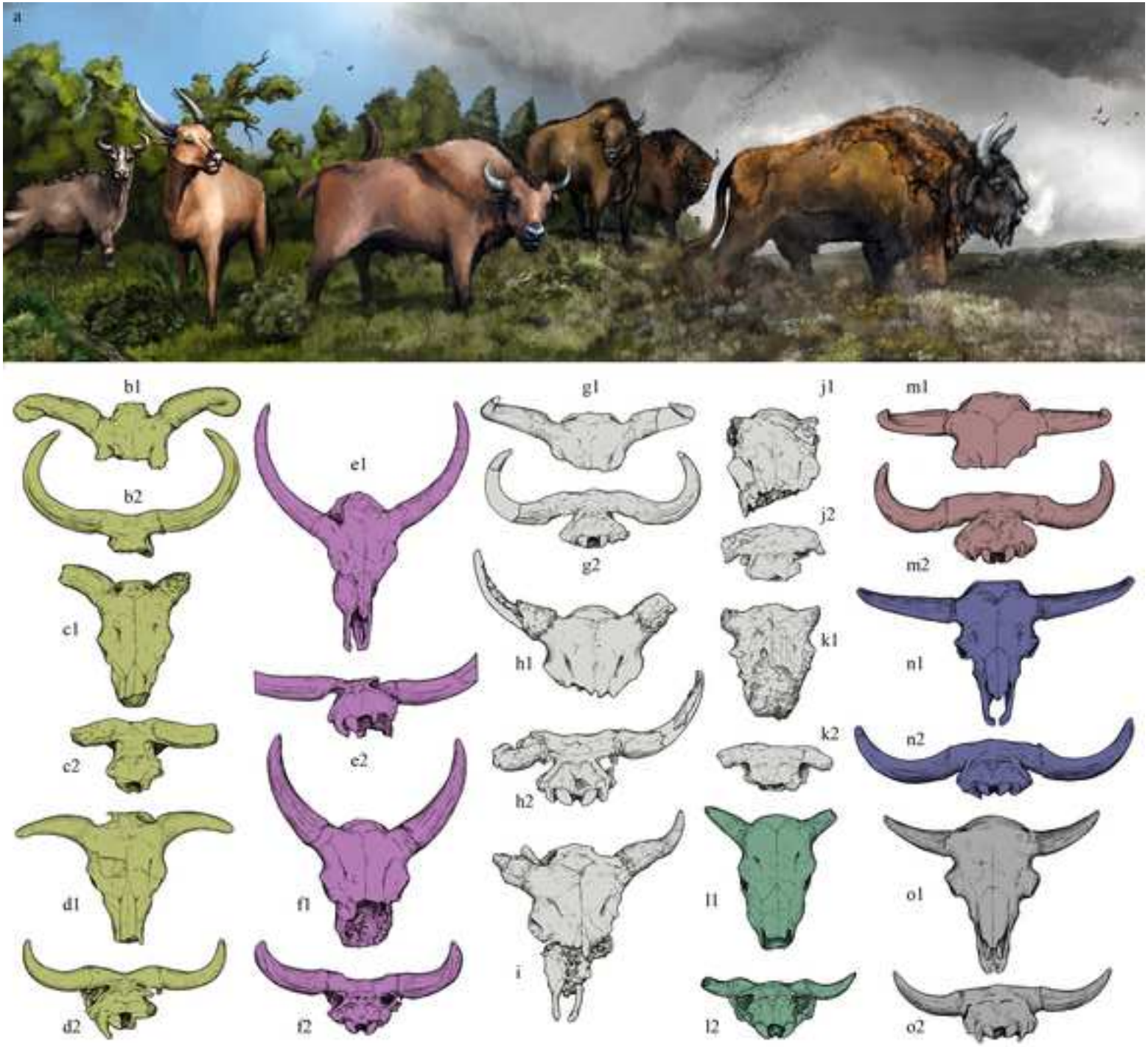
a
b1
b2
c1
c2
d1
d2
e1
e2
f1
f2
g1
g2
h1
h2
i
j1
j2
k1
k2
l1
l2
m1
m2
n1
n2
o1
o2

**Table 1.** Shape variables used for the principal component analysis. Abbreviations: ms, Mosimann shape variable; GM, Geometric Mean. Abbreviations of measurements as in Fig. S1 and Table S2.

| Selected Mosimann shape variables for cranium | Fig. 7 | Selected Mosimann shape variables for metapodials | Fig. 9 |
|---|---|---|---|
| msIBW = Log (IBW/ GM) | 1a | msLmax = Log (Lmax/GM) | 1b |
| msCW = Log (CW/ GM) | 2a | msPEW = Log (PEW/GM) | 2b |
| msFMW = Log (FMW/ GM) | 3a | msPET = Log (PET/GM) | 3b |
| msMW = Log (MW/ GM) | 4a | msDW = Log (DW/GM) | 4b |
| msOSHmax = Log (OSHmax/ GM) | 5a | msDT = Log (DT/GM) | 5b |
| msPPW = Log (PPW/ GM) | 6a | msDEW = Log (DEW/GM) | 6b |
| | | msDETm = Log (DETm/GM) | 7b |

**Table 2**. Measurements (mm) of the crania of *Bison* (*Eobison*) *degiulii* from Pietrafitta. Estimated measurements are in italics. Abbreviations as in Fig. S1 and Table S2.

| **Measurements** | SABAP UMB 19. 2.1178 | SABAP UMB 19. 2.1179 | SABAP UMB 20. 1.6803 | SABAP UMB 20. 1.6802 | SABAP UMB 21. 4.1177 |
|---|---|---|---|---|---|
| **HS°** | 65.0 | *75* | - | - | - |
| **IBW** | *102.0* | *115.0* | - | - | - |
| **IBH** | *28.0* | *22.0* | - | - | - |
| **CW** | - | 116.0 | - | - | 101.0 |
| **FMH** | - | 36.0 | - | - | 35.0 |
| **FMW** | - | 34.0 | - | - | 39.9 |
| **MW** | - | 202.0 | - | - | 217.4 |
| **OSHmin** | - | *90.0* | - | - | - |
| **OSHmax** | - | *130.0* | - | - | - |
| **PW** | *146.0* | - | - | - | - |
| **BAW** | *90.0* | - | - | - | - |
| **HLmax** | - | - | *340.0* | *310.0* | - |
| **HAP** | - | *90.0* | - | - | - |
| **HDV** | - | *70.0* | 77.0 | - | - |
| **HLmin** | *206.0* | *226.0* | *223.0* | *215.0* | - |
| **HBWmax** | *326.0* | 335.0 | - | - | - |
| **HBWmin** | *250.0* | *270.0* | - | - | - |
| **FFW** | *144.0* | - | - | - | - |
| **HOD** | *77.0* | - | - | - | - |
| **FWmin** | *259.0* | - | - | - | - |
| **FFLmin** | *231.0* | - | - | - | - |
| **FLmax** | *157.0* | - | - | - | - |
| **FLmin** | *157.0* | - | - | - | - |
| **PPW** | *58*.0 | 67.0 | 69.0 | 59.0 | 66.0 |
| **APW** | *33*.0 | 33.0 | 38.0 | 34.0 | 36.0 |

Table 3

**Table 3**. Measurements (mm) of the metacarpals of *Bison* (*Eobison*) *degiulii* from Pietrafitta. Estimated measurements are in italics. Abbreviations as in Fig. S1 and Table S2.

| ID Specimen | Side | Lmax | Lf | PEW | PET | DW | DT | DDW | DEW | DETm | DETl | PFWm | PFWl | ABETm | ABETl | AETm | AETl |
|---|---|---|---|---|---|---|---|---|---|---|---|---|---|---|---|---|---|
| SABAP UMB 20. 1.7324 | L | 249.6 | 239.1 | 74.2 | 51.1 | 42.5 | 31.6 | 67.2 | 68.0 | 39.4 | 38.8 | 43.1 | 29.3 | 30.8 | 28.0 | 37.3 | 36.8 |
| SABAP UMB 20. 1.7325 | L | 220.8 | 211.6 | 59.7 | *40.8* | 36.7 | 24.9 | 58.2 | 57.5 | 33.3 | 32.9 | 35.1 | 21.9 | 26.6 | 23.4 | 31.0 | 31.0 |
| SABAP UMB 22. 4.247/7 | L | *245.0* | - | 66.4 | *45.4* | 42.5 | 30.0 | 61.8 | 64.0 | 35.7 | 35.7 | - | - | 27.6 | 26.1 | 33.8 | 33.1 |
| SABAP UMB 20. 1.7329/1 | R | *250.2* | - | - | - | *50.0* | - | *70.0* | *69.0* | *38.0* | - | - | - | *30.8* | *28.5* | *35.9* | *36.5* |
| SABAP UMB 22. 4.247/8 | R | 249.0 | 240.4 | 66.4 | 42.8 | 44.9 | 31.0 | 60.1 | 64.0 | 35.7 | 37.5 | 37.8 | 26.3 | - | - | - | - |
| SABAP UMB 20. 1.7326 | R | 247.3 | 238.0 | *73.1* | 43.5 | *44.6* | *30.5* | 66.7 | 69.2 | 39.2 | 38.6 | 37.0 | 33.0 | 28.6 | 27.3 | 36.5 | 35.6 |
| SABAP UMB 130038 | R | 218.9 |  | 60.2 | 38.9 | 37.0 | 26.0 | 57.8 | 57.7 | 33.5 | 33.3 | 34.7 | 24.9 | 25.8 | 24.8 | 31.0 | 30.8 |
| IGF 1011 | R | 241.0 | 230.0 | 69.9 | 44.4 | 40.5 | 30.5 | 65.2 | 69.8 | 39.5 | 39.4 | 39.5 | 28.6 | 31.6 | 31.1 | 37.9 | 37.3 |

Table 4

**Table 4**. Measurements (mm) of the metatarsals of *Bison* (*Eobison*) *degiulii* from Pietrafitta. Estimated measurements are in italics. Abbreviations as in Fig. S1 and Table S2.

| ID Specimen | Side | Lmax | Lf | PEW | PET | DW | DT | DDW | DEW | DETm | DETl | PFOm | PFOl | ABETm | ABETl | AETm | AETl |
|---|---|---|---|---|---|---|---|---|---|---|---|---|---|---|---|---|---|
| SABAP UMB 20. 1.7330 | R | 258.2 | 248.2 | 47.8 | 48.2 | 34.8 | 33.3 | 54.2 | 52.9 | 33.8 | 33.0 | 33.9 | 31.8 | 24.9 | 24.1 | 29.8 | 31.2 |
| SABAP UMB 20. 1.7331 | R | 284.3 | 270.5 | 58.8 | 55.0 | 36.9 | 36.0 | 63.0 | 61.5 | 37.6 | 35.0 | 36.6 | 34.0 | 28.5 | 23.0 | 33.5 | 33.3 |
| SABAP UMB 20. 1.7332 | R | 295.3 | 283.9 | 64.5 | 56.8 | 42.8 | 36.9 | - | 63.3 | 38.5 | 36.9 | 40.1 | - | 28.4 | 27.1 | 33.3 | 34.7 |
| SABAP UMB 20. 1.7333 | L | 254.3 | - | - | - | 37.0 | - | 56.8 | 57.4 | 33.5 | 35.0 | 43.7 | - | 25.1 | 26.7 | 32.7 | 30.6 |
| SABAP UMB 20. 1.7335 | R | 288.0 | - | - | - | - | - | - | - | 40.0 | 37.6 | - | - | 28.7 | 28 | 36.2 | 36.4 |
| SABAP UMB 20. 1.7336 | R | 296.0 | - | - | - | - | - | 62.3 | 63.0 | 38.5 | 37.4 | 41.4 | 37.6 | 29.2 | 26.7 | 33.9 | 35.6 |
| SABAP UMB 20. 1.7338 | R | - | - | - | - | - | - | 63.3 | 65.6 | 41.2 | 40.0 | - | - | 30.6 | 29.3 | 36.1 | 37.9 |
| SABAP UMB 20. 1.7328 | R | 250.3 | - | 53.2 |  | 34.5 | 35.7 | 57.1 | 55.7 | 34.3 | 33.8 | - | - | 26.1 | 25.9 | 30.8 | 31.7 |
| SABAP UMB 20. 1.7327 | R | - | - | - | - | - | - | 66.0 | 71.3 | 39.1 | 39.0 | - | - | 31.5 | 28.5 | 36.8 | 37.9 |
| SABAP UMB 130037 | L | 283.0 | - | 58.2 | 35.9 | 36.6 | 36.5 | 62.2 | 61.5 | 38.7 | 36.6 | 40.0 | 35.9 | 29.4 | 25.7 | 32.7 | 34.5 |
| SABAP UMB 22. 4.247/15 | R | 278.9 | - | 59.5 | 54.8 | 38.2 | 40.6 | 59.7 | 58.7 | 35.5 | 35.1 | 39.5 | 39.8 | 26.3 | 25.4 | 31.6 | 33.9 |

Table 5

**Table 5**. Comparative cranial measurements (mm) of selected *Leptobos* and *Bison* s.l. samples. Abbreviations of taxa: LF, *Leptobos falconeri*; LSEM, *Leptobos* gr. *stenometopon-elatus-merlai*; LE, *Leptobos etruscus*; LV, *Leptobos vallisarni*; AC, *Adjiderebos cantabilis*; EP, *Bison* (*Eobison*) *palaeosinensis*; EGDm, *Bison* (*Eobison*) *georgicus* from Dmanisi; EDPf, *Bison* (*Eobison*) *degiulii* from Pietrafitta; EDPr, *Bison* (*Eobison*) *degiulii* from Pirro Nord; EDKm, *Bison* (*Eobison*) *degiulii* from Kalamoto; EcfDSO, *Bison* (*Eobison*) cf. *degiulii* from Salita di Oriolo; BM, *Bison* (*Poephagus*) *menneri*; BS, *Bison* (*Bison*) *schoetensacki*; BP, *Bison* (*Bison*) *priscus* sspp. Estimated measurements are in italics. Abbreviations of measurements as in Fig. S1 and Table S2. Data taken from: [a]Masini (1989); [b]Dubrovo and Burchak-Abramovich (1986); [c]Teilhard de Chardin Piveteau (1930); [d]Bukshianidze (2005); [e]this work; [f]Kostopoulos et al. (2018); [g]Bukshianidze (2020); [h]Sala (1986); [i]Anfossi et al., 1999; [j]Prat et al. (2003); [k]Vercoutère and Guerin (2010); [l]Castaños et al. (2012).

| Meas. | Stat. | LSEM [a] | LE [a] | LV [a] | AC [b] | EP [a, c] | EGDm [d, e] | EDPf [e] | EDPr [a, e] | EDKm [f] | EcfDSO [e] | BM [g] | BS [e, h] | BP [e, h, i, j, k, l] |
|---|---|---|---|---|---|---|---|---|---|---|---|---|---|---|
| **IBW** | **Mean (N)** | 61.5 (5) | 66.2 (13) | 86.36 (5) | 65.0 (1) | 92.0 (2) | 94.0 (1) | 108.5 (2) | 106.0 (1) | 111.0 (1) | 122.0 (1) | 100.8 (1) | 146.0 (1) | 172.7 (25) |
| | **Min-Max** | 48.4-77.0 | 41.0-95.0 | 78.5-99.0 | - | 90.0-94.0 | - | 102.0-115.0 | - | - | - | - | - | 125-230 |
| **IBH** | **Mean (N)** | 48.8 (5) | 30.6 (13) | 27.32 (5) | *30* (1) | 25.8 (1) | 26.0 (1) | 25.0 (2) | 29.0 (1) | 17.0 (1) | *20.0* (1) | 37.0 (1) | 28.0 (1) | 60.3 (16) |
| | **Min-Max** | 44.0-59.0 | 22.5-40.0 | 23.4-32 | - | - | - | 22-28 | - | - | - | | - | 13-147 |
| **CW** | **Mean (N)** | 92,4 (3) | 89.5 (11) | 93.75 (4) | 106 (1) | 100.3 (2) | 99.8 (1) | 108.4 (2) | - | - | *118.0* (1) | 110.2 (1) | 136.7 (11) | 135.3 (39) |
| | **Min-Max** | 84.5-103.0 | 56.5-101 | 88.3-97 | - | 100-100.5 | - | 101.3-115.5 | - | - | - | - | 129.0-145.0 | 107.5-156.0 |
| **FMH** | **Mean (N)** | 35.5 (4) | 35.8 (10) | 36.6 (3) | - | 42.5 (1) | 30.0 (1) | 35.5 (2) | - | - | 46.0 (1) | - | 40.3 (11) | 44.0 (37) |
| | **Min-Max** | 30.3-41.4 | 32.0-41.0 | 31.9-40.0 | - | - | - | 35.0-36.0 | - | - | - | - | 30.0-52.0 | 33.6-53.0 |
| **FMW** | **Mean (N)** | 42.9 (4) | 36.4 (10) | 38.2 (3) | - | 42.8 (1) | 33.0 (1) | 36.95 (2) | - | - | 43 (1) | 40.7 (1) | 44 (11) | 41.9 (37) |
| | **Min-Max** | 37.5-46.7 | 28.9-39.4 | 35.1-42.1 | - | - | - | 34.0-39.9 | - | - | - | - | 36.0-52.0 | 19.6-59.0 |
| **MW** | **Mean (N)** | 162.7 (4) | 193.5 (8) | 177.96 (5) | 220.0 (1) | 217.0 (2) | 200.0 (1) | 209.7 (2) | 204 (1) | 165 (1) | 246 (1) | - | 269.1 (7) | 274.4 (35) |
| | **Min-Max** | 131.9-200.0 | 155.3-220 | 145-200.8 | - | 210.0-224.0 | - | 202-217.4 | | | | - | 208-322 | 218-350 |
| **OSHmin** | **Mean (N)** | 101.9 (4) | 90.9 (12) | 92.1 (2) | - | 94.8 (1) | 100.0 (1) | 90.0 (1) | 90.7 (1) | | *120.0 (1)* | 97.4 (1) | 104 (8) | 122.8 (30) |
| | **Min-Max** | 96.8-106.8 | 75.4-103.0 | 91.2-93.0 | - | - | - | - | - | - | - | - | 72.0-130.0 | 93.0-151.0 |
| **OSHmax** | **Mean (N)** | 134.5 (4) | 128 (8) | 108.5 (4) | 102.0 (1) | 131.5 (2) | 134.0 (1) | 130.0 (1) | - | - | 143.0 (1) | 131.7 (1) | 136.0 (8) | 160.9 (31) |
| | **Min-Max** | 125.8-141.0 | 115.6-141.0 | 85.0-130.5 | - | 129.0-134.0 | - | - | - | - | - | - | 120-164 | 132.6-188.0 |
| **PW** | **Mean (N)** | 125.3 (5) | 144.4 (11) | 155.5 (2) | - | 208.0 (1) | 143.0 (1) | 146.0 (1) | 177.0 (1) | | 205.0 (1) | - | 233.0 (1) | 239.4 (16) |
| | **Min-Max** | 94.0-161.0 | 85.5-220.0 | 151.0-160.0 | - | - | - | - | - | - | - | - | - | 205.0-259.0 |
| **BAW** | **Mean (N)** | 86.5 (5) | 87.1 (10) | 70.375 (4) | - | 55.3 (2) | 63.0 (1) | 90.0 (1) | - | 48.0 (1) | - | 47.6 (1) | 74.0 (1) | 98.6 (17) |
| | **Min-Max** | 80.0-99.0 | 61.0-101.6 | 53.0-78.0 | - | 50.0-60.5 | - | - | - | - | - | - | - | 69.0-149.0 |
| **HLmax** | **Mean (N)** | 435.0 (1) | 490.0 (3) | 322.0 (3) | 280.0 (1) | 450.0 (1) | 344.0 (1) | 325.0 (2) | 435.0 (1) | - | - | - | 344.7 (9) | 440.6 (9) |
| | **Min-Max** | | 440.0-540 | 270.0-360.0 | - | - | - | 310.0-340.0 | - | - | - | - | 310.0-420.0 | 285.0-570.0 |
| **HAP** | **Mean (N)** | 79.3 (3) | 82.2 (4) | 80.3 (3) | 65.0 (1) | 85 (1) | 92.1 (1) | 90 (1) | 75 (1) | 58 (1) | 106 (1) | 67.8 (1) | 105.1 (8) | 110.2 (10) |
| | **Min-Max** | 72.0-87.8 | 79.5-84.5 | 70-86 | - | - | - | - | - | - | - | - | 91.0-116.0 | 74.5-140.0 |

| | | | | | | | | | | | | | | |
|---|---|---|---|---|---|---|---|---|---|---|---|---|---|---|
| **HDV** | **Mean (N)** | 62.0 (3) | 75.9 (4) | 70.8 (3) | 85.0 (1) | 78.2 (1) | 73.6 (1) | 73.5 (2) | 60.0 (1) | 50.0 (1) | 80.0 (1) | 49.4 (1) | 75.1 (8) | 108.2 (10) |
| | **Min-Max** | 59.0-65.0 | 71.5-79.0 | 63.0-77.5 | - | - | - | 70.0-77.0 | - | - | - | - | 58-87 | 77.5-136.5 |
| **HLmin** | **Mean (N)** | 245.0 (1) | 374.3 (3) | 275.5 (3) | 173.0 (1) | 210 (2) | 245 (1) | 217.5 (4) | - | - | - | 159.9 (1) | 276 (10) | 395.1 (8) |
| | **Min-Max** | | 343.0-400.0 | 250.0-296.5 | - | 200.0-220.0 | | 206.0-226.0 | - | - | - | - | 235.0-325.0 | 255.0-505.0 |
| **HBWmax** | **Mean (N)** | 238.5 (2) | 306.3 (3) | 303.3 (1) | - | 317.0 (1) | 294.3 (1) | 330.5 (2) | 245.0 (1) | - | - | - | 314.1 (10) | - |
| | **Min-Max** | 232.0-245.0 | 283.0-320.0 | - | - | - | - | 326.0-335.0 | - | - | - | - | 280.0-350.0 | - |
| **HBWmin** | **Mean (N)** | 135.5 (2) | 268 (3) | 202 (1) | - | 247.5 (2) | 195 (1) | 260 (2) | 153 (1) | - | 310 (1) | - | - | 314.4 (6) |
| | **Min-Max** | 118.0-153.0 | 224.0-350.0 | - | - | 220.0-275.0 | - | 250.0-270.0 | - | - | - | - | - | 236.5-390 |
| **FFW** | **Mean (N)** | 102.4 (6) | 105.7 (8) | 126.9 (3) | - | 152 (2) | 127.4 (1) | 144 (1) | 134.3 (1) | 122.0 (1) | 132.0 (1) | 142.1 (1) | - | 195.8 (15) |
| | **Min-Max** | 84.0-123.0 | 77-159 | 107.6-144 | | 143.0-161.0 | - | - | - | - | - | - | - | 180.5-217.0 |
| **HOD** | **Mean (N)** | 93.8 (2) | 102.8 (2) | 92.0 (1) | 75.0 (1) | - | 72.0 (1) | 77.0 (1) | 65.0 (1) | 60.0 (1) | 90.0 (1) | - | - | 97.1 (18) |
| | **Min-Max** | 85.0-102.5 | 95.0-110.5 | - | - | - | - | - | - | - | - | - | - | 73.0-111.0 |
| **FWmin** | **Mean (N)** | 159.2 (5) | 205.3 (7) | 249.5 (3) | 210.0 (1) | 237.0 (1) | 241.8 (1) | 259.0 (1) | 239.5 (1) | 202.0 (1) | 244.0 (1) | 223.5 (1) | 290.9 (11) | 296.6 (37) |
| | **Min-Max** | 132.0-201.0 | 133.7-267.4 | 223.4-280.0 | - | - | - | - | - | - | - | - | 255.0-335.0 | 232.0-344.0 |
| **FFLmin** | **Mean (N)** | 134.3 (3) | 150.2 (8) | 166.0 (1) | - | 150.0 (1) | 154.5 (1) | 231.0 (1) | 182.9 (1) | 175.0 (1) | - | - | - | 208.4 (15) |
| | **Min-Max** | 105.0-153.0 | 132.1-174.4 | - | - | - | - | - | - | - | - | - | - | 167.0-249.0 |
| **FLmax** | **Mean (N)** | 234.1 (2) | 226.2 (3) | - | - | - | 223.0 (1) | 157.0 (1) | 230.0 (1) | - | 225.0 (1) | 214.4 (1) | - | 274.6 (16) |
| | **Min-Max** | 231.2-237.0 | 196-282 | - | - | - | - | - | - | - | - | - | - | 233.0-303.0 |
| **FLmin** | **Mean (N)** | 148.0 (3) | 160.9 (4) | 157.7 (3) | 130.0 (1) | - | 147.5 (1) | 157.0 (1) | 194.0 (1) | 175.0 (1) | 159.0 (1) | 166.8 (1) | | 196.0 (12) |
| | **Min-Max** | 133.0-173.5 | 126.4-202 | 150-170 | - | - | - | - | - | - | - | - | - | 145.4-244.0 |
| **PPW** | **Mean (N)** | 58.3 (6) | 64.5 (7) | 65.5 (5) | - | 65.5 (1) | 61.8 (1) | 63.84 (5) | - | 38 (1) | - | 34.1 (1) | - | 73.8 (20) |
| | **Min-Max** | 50.3-63.0 | 49.7-76.3 | 62.0-69.5 | - | - | - | 58-68.9 | - | - | - | - | - | 55.5-90.0 |
| **APW** | **Mean (N)** | 29.7 (6) | 39.8 (6) | 34.9 (5) | - | 42.5 (1) | 33.6 (1) | 34.68 (5) | - | - | - | - | - | 46.8 (17) |
| | **Min-Max** | 24.8-36.6 | 35.0-55.5 | 29.0-43.6 | - | - | - | 33.0-38.0 | - | - | - | - | - | 32.0-56.6 |

Table 6

**Table 6.** Comparative measurements (mm) of the metacarpal in selected *Leptobos* and *Bison* s.l. samples. Abbreviations as in Fig. S1 and Table S2. Data taken from: [a]Masini (1989); [b]Rodrigo (2011); [c]Garrido (2008); [d]Tong et al. (2016); [e]Bukshianidze (2005); [f]this work; [g]Maniakas and Kostopoulos (2017); [h]Kostopoulos et al. (2018); [i]Sher (1997); [j]Brugal (1994); [k]Moullé (1992); [l]Brugal and Fosse (2005); [m]Schertz (1936); [n]Sala (1986); [o]Sorbelli et al. (2021a); [p]Breda et al. (2010); [q]Vercoutère and Guerin (2010); [r]Prat et al. (2003); [s]Drees (2005); [t]Castaños et al. (2012); [u]Empel and Roskoz (1963).

| Taxon | Site | Statistics | Lmax | PEW | PET | DW | DT | DEW | DETm |
|---|---|---|---|---|---|---|---|---|---|
| *Leptobos elatus* [a, b] | Les Étouaires, Villarroya | **Mean (N)** | 253.6 (25) | 57.5 (32) | 37.8 (27) | 33.9 (20) | 26.1 (18) | 55.1 (23) | 34.5 (23) |
| | (France, Spain) | **Min-Max** | 242.2-270 | 52.0-64.7 | 32.1-42.9 | 29.6-39.4 | 22.0-30.0 | 49.1-63.6 | 31.5-36.9 |
| | | **SD** | 8.1 | 3.7 | 2.9 | 3.0 | 2.2 | 3.8 | 1.6 |
| *Leptobos merlai* [a, b] | St. Vallier | **Mean (N)** | 245.5 (8) | 58.2 (13) | 39.2 (14) | 36.8 (7) | 27.1 (7) | 57.5 (14) | 33.8 (13) |
| | (France) | **Min-Max** | 231.6-255.8 | 51.1-62.5 | 34.5-46.4 | 32.5-40.0 | 23.4-29.1 | 51.9-62.9 | 30.3-37.4 |
| | | **SD** | 9.2 | 3.9 | 3.6 | 3.0 | 2.1 | 3.7 | 2.1 |
| *Leptobos etruscus* [a, c] | Senèze, Faella, Matassino, | **Mean (N)** | 248.3 (32) | 58.1 (40) | 45 (40) | 39.3 (37) | 28.5 (37) | 62.6 (49) | 35.7 (43) |
| | Olivola, Fonelas-1 | **Min-Max** | 234.5-265.5 | 36.2-67.9 | 36.7-65.6 | 31.8-43.7 | 25.0-31.5 | 50.4-68.6 | 32.0-41.1 |
| | (France, Italy, Spain) | **SD** | 6.9 | 9.5 | 9.2 | 3.0 | 1.6 | 3.9 | 1.7 |
| *B.* (*Eobison*) *palaeosinensis* [d] | Nihowan Basin | **Mean (N)** | 234.8 (4) | 68.4 (4) | 40.4 (3) | 39.4 (1) | 30.6 (1) | 63.5 (4) | 34.6 (3) |
| | (China) | **Min-Max** | 226.0-248.1 | 60.0-73.8 | 35.0-47.5 | - | - | 58.8-65.2 | 34.2-34.9 |
| | | **SD** | 9.4 | 6.1 | 6.4 | - | - | 3.1 | 0.4 |
| *B.* (*Eobison*) *georgicus* [e, f] | Dmanisi | **Mean (N)** | 237.0 (3) | 66.9 (4) | 42.4 (4) | 39.9 (3) | 29.2 (3) | 65.3 (4) | 35.4 (4) |
| | (Georgia) | **Min-Max** | 230.0-244.7 | 62.8-70.8 | 37.7-45.2 | 34.3-44.6 | 25.8-31.1 | 61.0-71.6 | 33.2-37.8 |
| | | **SD** | 7.3 | 3.6 | 3.3 | 5.2 | 3.0 | 4.5 | 2.0 |
| *B.* (*Eobison*) sp. [g] | Venta Micena | **Mean (N)** | 225.6 (30) | 58.5 (43) | 36.6 (44) | 35.3 (31) | 26.9 (30) | 60.1 (36) | 33.0 (35) |
| | (Spain) | **Min-Max** | 208.2-248.7 | 52.3-69.5 | 32.8-46.5 | 31.4-44.2 | 24.1-32.1 | 53.5-69.1 | 30-36.3 |
| | | **SD** | 10.2 | 4.6 | 3.4 | 3.7 | 2.1 | 4.7 | 1.6 |
| *B.* (*Eobison*) *degiulii* [e] | Pietrafitta | **Mean (N)** | 240.0 (8) | 67.1 (7) | 43.8 (7) | 42.3 (8) | 29.5 (7) | 65.0 (8) | 36.8 (8) |
| | (Italy) | **Min-Max** | 218.9-250.2 | 59.7-74.2 | 38.9-51.1 | 36.7-50.0 | 24.9-32.9 | 57.5-70 | 33.3-39.5 |
| | | **SD** | 12.8 | 5.7 | 3.9 | 4.4 | 2.9 | 5.2 | 2.6 |
| *B.* (*Eobison*) *degiulii* [a, e] | Pirro Nord | **Mean (N)** | 222.2 (3) | 62.1 (4) | 38.7 (4) | 38.5 (3) | 27.4 (3) | 64.8 (4) | 33.1 (5) |
| | (Italy) | **Min-Max** | 211.5-230.0 | 58.0-69.5 | 35.5-41.7 | 29.8-46.2 | 25-30.1 | 62.0-66.4 | 29.3-37.3 |
| | | **SD** | 9.6 | 5.3 | 3.2 | 8.3 | 2.6 | 1.9 | 3.2 |
| *B.* (*Eobison*) cf. *degiulii* [e] | Capena | **Mean (N)** | 222.5 (2) | 68.4 (2) | 43.1 (2) | 44.4 (2) | 29.7 (1) | 64.6 (2) | 35.4 (2) |

| | | | | | | | | | |
|---|---|---|---|---|---|---|---|---|---|
| | (Italy) | **Min-Max** | 220.0-225.0 | 68.1-68-7 | 42.0-44.0 | 44.3-44.4 | - | 64.1-65.0 | 34.1-36.7 |
| | | **SD** | 3.5 | 0.4 | 1.4 | 0.1 | - | 0.6 | 1.8 |
| *B.* (*Eobison*) *degiulii* [h] | Mygdonia Basin | **Mean (N)** | 238.5 (19) | 67.4 (24) | 40.1 (24) | 42.4 (23) | 29.4 (23) | 70.3 (22) | 39.3 (22) |
| | (Greece) | **Min-Max** | 220.7-258.1 | 57.7-78.3 | 32.9-48.4 | 31.8-51.2 | 23.5-35.2 | 59.5-88.8 | 34.4-48.2 |
| | | **SD** | 10.6 | 4.9 | 3.0 | 5.1 | 2.9 | 6.7 | 3.0 |
| *B.* (*Eobison*) cf. *degiulii* [e] | Capena | **Mean (N)** | 222.5 (2) | 68.4 (2) | 43.1 (2) | 44.4 (2) | 29.7 (1) | 64.6 (2) | 35.4 (2) |
| | (Italy) | **Min-Max** | 220.0-225.0 | 68.1-68-7 | 42.0-44.0 | 44.3-44.4 | - | 64.1-65.0 | 34.1-36.7 |
| | | **SD** | 3.5 | 0.4 | 1.4 | 0.1 | - | 0.6 | 1.8 |
| *B.* (*Poephagus*) *menneri* [f, i] | Untermassfeld | **Mean (N)** | 276.4 (37) | 77.0 (50) | 46.5 (48) | 44.8 (43) | 32.8 (40) | 75.6 (41) | 38.2 (38) |
| | (Germany) | **Min-Max** | 255.8-296.0 | 64.37-91.4 | 39.27-52.6 | 35.3-57.7 | 27.8-39.0 | 65.4-86.0 | 29.5-47.3 |
| | | **SD** | 10.2 | 5.6 | 3.2 | 4.7 | 3.0 | 6.3 | 5.8 |
| *B.* (*Bison*) *schoetensacki* [f, g, j, k, l, m, n, o, p] | Durfort, Le Vallonnet, Le Vassirie, Mauer, | **Mean (N)** | 252.2 (54) | 78.4 (68) | 46.8 (61) | 49.3 (49) | 33.9 (51) | 76.9 (67) | 42.1 (54) |
| | Süssenborn, Cesi, Vallparadís, Cromer Forest-bed | **Min-Max** | 225.0-277.0 | 46.9-93.0 | 37.6-56.0 | 36.3-64.0 | 27.9-46.6 | 65.9-88.5 | 35.3-52.4 |
| | (France, Germany, Italy, UK) | **SD** | 12.8 | 7.0 | 3.6 | 5.7 | 3.9 | 6.0 | 3.3 |
| *B.* (*Bison*) cf. *schoetensacki* [f, m] | Mosbach | **Mean (N)** | 256.0 (22) | 84.5 (22) | 48.9 (22) | 49.9 (22) | 32.6 (22) | 82.9 (22) | 42.8 (22) |
| | (Germany) | **Min-Max** | 241.1-277.8 | 72.0-97.3 | 43.4-56.4 | 43.3-55.1 | 30.2-35.1 | 73.0-97.1 | 40.1-46.0 |
| | | **SD** | 22.0 | 18.0 | 19.0 | 4.0 | 4.0 | 19.0 | 4.0 |
| *B.* (*Bison*) *priscus priscus* [e, g, q] | Chatillon-Saint-Jean, | **Mean (N)** | 254.5 (40) | 87.9 (39) | 53.1 (38) | 55.7 (38) | 36.3 (38) | 87.9 (23) | 46.1 (40) |
| | Romain-La-Roche, Taubach | **Min-Max** | 232.0-286.5 | 71.4-102.0 | 44.0-63.0 | 42.3-63.0 | 30.6-42.5 | 75.5-98.1 | 37.0-51.5 |
| | (France, Germany) | **SD** | 13.0 | 8.1 | 5.2 | 6.1 | 3.6 | 6.9 | 3.1 |
| *B.* (*Bison*) *priscus* [g, m, n, r, s, t] | Habarra, Roter Berg, Cava Filo, | **Mean (N)** | 234.5 (58) | 81.5 (66) | 48.2 (31) | 50.3 (40) | 33.4 (29) | 84.7 (56) | 42.6 (50) |
| | North Sea, Kiputz IX, Joint Mitnor Cave | **Min-Max** | 216.8-260.0 | 60.0-96.5 | 42.5-56.0 | 39.5-59.0 | 28.8-40.0 | 70.5-101.5 | 31.1-53.0 |
| | (France, Germany, Italy, North Sea, Spain, UK) | **SD** | 10 | 7.1 | 3.5 | 5.9 | 2.8 | 7.1 | 5.8 |
| *B.* (*Bison*) *bonasus* [u] | Białowieża | **Mean (N)** | 213.9 (32) | 73.5 (31) | 45.7 (30) | 42.9 (31) | 27.1 (32) | 69.9 (32) | 39.7 (30) |
| | (Poland) | **Min-Max** | 202.0-231.0 | 64.0-88.0 | 39.0-54.0 | 35.0-55.0 | 23.0-32.0 | 61.0-80.0 | 30.0-46.0 |
| | | **SD** | 7.6 | 6.6 | 3.8 | 5.7 | 2.5 | 5.5 | 3.3 |

Table 7

**Table 7.** Summary list of morphological characters that define the four main groups of *Leptobos* and *Bison* studied in this work.

| | ***Leptobos* gr. LSEM** | ***Leptobos* gr. LEV** | ***Bison* (*Eobison*)** | ***Bison* (*Bison*)** |
|---|---|---|---|---|
| **Horn-core shape** | Long with double bending and strong torsion. Markedly compressed dorsoventrally at the base. | Long with single bending and feeble torsion. Circular section at the base. | Short and stout with double bending and feeble torsion. Dorsoventrally compressed at the base. | From short and stout to very long. Single or double bending with feeble torsion. Circular to dorsoventrally compressed at the base. |
| **Horn-core position** | Emerging more laterally than posteriorly (i.e., forming a wide angle with the sagittal axis). Pedicle long. | Emerging more posteriorly than laterally (i.e., forming a small angle with the sagittal axis). Pedicle long. | Emerging more laterally than posteriorly (i.e., forming a wide angle with the sagittal axis). Pedicle long to short. | Emerging laterally (i.e., forming a very wide angle with the sagittal axis). Pedicle short. |
| **Occipital squama** | Small. Bell shaped, wide base and narrow top. | Trapezoidal to semicircular shaped, wide base and narrow top. | Trapezoidal to bell shaped, wide base and narrow top. | Trapezoidal to square shaped, wide base and top. Dorsoventrally compressed. |
| **Intertemporal bridge** | Well developed. High and narrow. | Poorly developed. Short and wide. | Poorly developed to absent. | Absent. |
| **Temporal fossae** | High, developing posteriorly. The distance between the two posterior ends is short. | High, developing posteriorly. The distance between the two posterior ends is relatively short. | Relatively low, developing posteriorly. The distance between the two posterior ends is relatively long. | High, developing posteriorly. The distance between the two posterior ends is very long. |
| **Frontals** | Relatively small, long and narrow. Concave, poorly pneumatized at the horn-core bases. | Relatively large, long and narrow. Concave, poorly pneumatized at the horn-core bases. | Relatively large, short and wide. Concave, poorly pneumatized at the horn-core bases. | Large, very short and wide. Concave to convex, strongly pneumatized at the horn-core bases. |
| **Ethmoidal fenestrae** | Present. | Present. | Absent. | Absent. |
| **Orbits** | Not tubular nor protruding. | Slightly protruding, not tubular. | Protruding and slightly tubular. | Extremely protruding and tubular. |
| **Nasals** | Short, ending anteriorly to the anterior margin of the orbits. | Short, ending anteriorly to the anterior margin of the orbits. | Long, ending at the anterior margin of the orbits or slightly posteriorly. | Long, ending posteriorly the anterior margin of the orbits. |
| **Premaxillae** | In contact with the nasals. | In contact with the nasals. | Not in contact with the nasals. | Not in contact with the nasals. |
| **Teeth** | Low degree of hypsodonty. | Medium degree of hypsodonty. | Medium degree of hypsodonty. | High degree of hypsodonty. |
| **Limbs** | Very slender. Radius short. Metatarsals slightly longer than metacarpals. | Slender. Radius relatively short. Metatarsals slightly longer than metacarpals. | Relatively robust. Radius relatively short. Metatarsals relatively longer than metacarpals. | To relatively to extremely robust. Radius long. Metatarsals from relatively to extremely longer than metacarpals. |
| **Body size** | Small. | Medium. | Medium to large. | Large to very large. |

| | | | | |
|---|---|---|---|---|
| **Sexual dimorphism** | Female hornless. Size difference between male and females reduced. | Female hornless. Size difference between males and females reduced. | Female horned. Size difference between male and females accentuated. | Female horned. Size difference between male and females extremely accentuated. |

**Declaration of interests**

☒ The authors declare that they have no known competing financial interests or personal relationships that could have appeared to influence the work reported in this paper.

☐The authors declare the following financial interests/personal relationships which may be considered as potential competing interests:

**Author contributions**

L.S, M.C and J.M.-M conceived the research and wrote the paper; L.S, performed the analyses; L.S, M.C, D.S.K., R.F., B.M., V.P., M.P.V., B.A., S.V.B. and J.M.-M. collected the data, revised all the manuscript versions and made improvements in the manuscript.

Supplementary figure 1

Click here to access/download

**e-Component/Supplementary data**

Fig.S1.tif

Supplementary figure 2

Click here to access/download

**e-Component/Supplementary data**

Fig.S2.tif

Supplementary figure 3

Click here to access/download

**e-Component/Supplementary data**

Fig.S3.tif

Supplementary figure 4

Click here to access/download

**e-Component/Supplementary data**

Fig.S4.tif

Supplementary figure 5

Click here to access/download

**e-Component/Supplementary data**

Fig.S5.tif

Supplementary figure 6

Click here to access/download

**e-Component/Supplementary data**

Fig.S6.tif